

MATERIALS ON GENETIC AND EXPERIMENTAL MINERALOGY

V. S. Sobolev

FACILITY FORM 602	N 66-11609	
	(ACCESSION NUMBER)	(THRU)
	(PAGES)	(CODE)
	(NASA CR OR TMX OR AD NUMBER)	(CATEGORY)

GPO PRICE \$ _____

CFSTI PRICE(S) \$ _____

Hard copy (HC) 4.00Microfiche (MF) 1.00

ff 653 July 65

Translation of "Materialy po geneticheskoy i
eksperimental'noy mineralogii."
Trudy Instituta Geologii i Geofiziki, Vol. 2, No. 30, 1964.

NATIONAL AERONAUTICS AND SPACE ADMINISTRATION
WASHINGTON
NOVEMBER 1965

ACADEMY OF SCIENCES OF USSR
SIBERIAN BRANCH

TRANSACTIONS OF THE INSTITUTE OF GEOLOGY AND GEOPHYSICS

Edition 30

MATERIALS
ON GENETIC
AND EXPERIMENTAL
MINERALOGY

VOLUME 2

Editor-in-chief
academician V. S. SOBOLEV

EDITORIAL AND PUBLISHING DEPARTMENT OF SIBERIAN
BRANCH ACADEMY OF SCIENCES OF USSR
NOVOSIBIRSK

1964

АКАДЕМИЯ НАУК СССР
СИБИРСКОЕ ОТДЕЛЕНИЕ

ТРУДЫ ИНСТИТУТА ГЕОЛОГИИ И ГЕОФИЗИКИ

Выпуск 30

МАТЕРИАЛЫ
ПО ГЕНЕТИЧЕСКОЙ
И ЭКСПЕРИМЕНТАЛЬНОЙ
МИНЕРАЛОГИИ

ТОМ II

Ответственный редактор
академик В. С. СОБОЛЕВ

РЕДАКЦИОННО-ИЗДАТЕЛЬСКИЙ ОТДЕЛ
СИБИРСКОГО ОТДЕЛЕНИЯ АН СССР
НОВОСИБИРСК

1964

METAMORPHISM IN CONTACTS OF THE ANAKIT TRAPPEAN
MASSIF ON THE LOWER TUNGUSKA RIVER

by

V. V. Reverdatto

The complex of unusual metamorphogenic calcium silicates formed in the replacement of carbonate rocks low in silica content in contact zones of intrusion was first described by F. E. Wright, who established the presence of spurrite in association with helenite and hillebrandite in calcite marbles of Velardena, Mexico [97]. During the half century that has passed since that time the list of minerals formed under such conditions has grown considerably, and the geography of their discovery has widened markedly. New discoveries of minerals of this association were made in Crestmore, California [76, 77, 80]; on Sky, Muck and Rhum Islands, Scotland [75, 91, 98]; in Scot Hill and Carlingford, Ireland [82-84, 88-90]; in the Iron Mountains and Tres Hermanas, New Mexico [68, 74]; in the Little Belt Mountains, Montana [86]; Christmas Mountains, Texas [64]; Tokatoka, New Zealand [78]; Malarajanahundi Nanjangud, Mysore State, India [81]; and in Coahuila, Mexico [87]. The first discovery of spurrite-merwinite marbles in the Soviet Union -- at the time it was the fourth such discovery in the world -- was made on the Lower Tunguska River in 1935 by V. S. Sobolev, who described the contact traps with carbonate rocks [48]. Recently, information in the press has appeared about the discovery of spurrite containing rocks at another point in the Siberian platform in the basin of the Podkamennaya Tunguska River [29].

An important characteristic of these metamorphic rocks, as established by a number of investigators [48, 62, 76, 77], is their capacity to form only

at shallow depths and under the influence of sufficiently high temperatures in exocontact basic sub-igneous intrusions. On the basis of the facts, and stressing the importance of small pressures in the process of metamorphic mineral formation in this group of rocks, D. S. Korzhinskiy, who used certain thermodynamic computations to obtain equilibrium curves, distinguished the larnite-merwinite abyssal facies; it included all the contact marbles known at the time containing larnite, merwinite, spurrite, tilleyite, and others [21]. The Abyssal facies, characterized by somewhat lower temperatures and higher pressures (hypabyssal conditions) was named the helenite-monticellite facies from the typical minerals which were stable in this condition. P. Eskola includes both groups of rocks in the sanidinite facies, thereby stressing their relationship with igneous formations and frequent associations with sanidinite, mullite, glass and other. Monticellite, spurrite, merwinite and larnite are regarded by him as critical minerals in the sanidinite facies [62, 66]. Later, F. J. Turner distinguished the following two sub-facies in the sanidinite facies for carbonaceous rocks poor in SiO_2 : 1) the high temperature facies, and 2) the relatively low temperature facies (at higher pressures), identified respectively as larnite-merwinite and helenite-monticellite metamorphic abyssal facies of Korzhinskiy [55]. This division into sub-facies was preserved by Turner in a number of later studies described jointly by Fife and F. J. Verhoogen [67, 56]. In distinguishing the sub-facies these authors were guided in large measure by the studies of N. L. Bowen dealing with the progressive metamorphism of silica containing limestones and dolomites [63], using high temperature reactions for this purpose (8-13 degrees) of the Bowen series. At the present time they distinguish the following: 1) larnite-merwinite-spurrite sub-facies "corresponding to high temperatures and low pressures, and characterized by associations containing one of the following minerals: larnite, merwinite, rankinite, spurrite, tilleyite" [56, page 457], and 2)

monticellite-melilite sub-facies "corresponding to somewhat lower temperatures or higher pressures than sub-facies 1" [56, page 457].

In order to determine precisely the mineral composition and position of the larnite-merwinite-spurrite sub-facies (larnite-merwinite abyssal facies according to Korzhinskiy [22]) in the PT interval, and to determine the physical conditions of metamorphism and the kinetics of metamorphic processes in the stability field of this sub-facies, this author, with the guidance of Academician V. S. Sobolev, undertook in 1960-1962 to study the unique contact of the Anakit trappean intrusion with Paleozoic carbonate rocks. During the course of the study the list of minerals described in the rocks of this contact [48] was supplemented considerably by a number of new discoveries. The first, discovered in the USSR, was the extremely rare calcium silicate -- tilleyite; also discovered were tridymite, formed in the metamorphism of silicite concretions, and quartzitic calcareous sandstones, sanidine, andalusite, wollastonite, and others. The discovery of tridymite made it possible to define more accurately the question of the temperature of metamorphism and to confirm the accuracy of identifying the larnite-merwinite-spurrite sub-facies as the highest temperature metamorphogenetic mineral association. Special attention was paid to the petrological characteristic of the Anakit trappean differentiated intrusion and its structure, as well as to the study of the metasomatic rocks, ores, and products of hydrothermal activity. Among the latter, special interest is seen in the abyssophobe hydrosilicates of calcium (hillebrandite and others). This paper is devoted to a discussion of the results of studies made on the Anakit contacts.

1. HISTORY OF EXPLORATION OF THE AREA

The object of the exploration and study of the area is a trappean intrusion and its contacts located in the lower reaches of the Lower Tunguska River,

approximately 285 km from the mouth. It is disposed in the valley of the river somewhat above the point of confluence with the Anakit River; the immediate region is named after this river. Administratively this area is part of the Evenkis National Area (Okrug) of Krasnoyarsk Kray. It is close to the Novoginsk graphite mine ten kilometers up the Lower Tunguska River.

In the pre-revolutionary period the Anakit Region was visited only by A. A. Chekanovskiy who was the first to discover outcroppings of limestone in the valley of the Lower Tunguska River above the mouth of the Anakit River. This formed the basis for the study of the Anakit anticlinal structure [61]. After the revolution a great contribution to the study of the geology of the region was made by V. S. Sobolev, who made the first detailed description of a number of igneous and metamorphic rocks [48, 49]. The theoretical studies by Sobolev were included in the basic work "The Petrology of Traps of the Siberian Platform"; it was based, to a considerable degree, on the materials obtained from studies made of the Anakit trappean massif.

During the thirties the region was studied by a number of geologists of the West Siberian Geological Survey Trust of the Arctic Institute and others including: L. M. Shorokhov, S. L. Kushev [25], A. F. Mikhaylov, I. V. Moiseyev, V. P. Tebenkov, D. S. Gaytman, O. L. Eynor [32, 52-54], R. P. Radchenko and N. A. Shvedov [41]. In 1947 there was a search and survey party for iron ores led by V. N. Egorov [20]. From 1950 to the present time studies were made in this region by geologists of GIN [State Research Institute] USSR Academy of Sciences; VSEGEY [All Union Geological Scientific Research Institute]; All-Union Geodetic Trust [VAGT]; SNIIGGIMS [Northern Scientific Research Institute of Hydraulic Engineering and Soil Reclamation]; and others. The geologists included the following: Memner, Rasskazova, Ivanova, Vysotskiy, Dragunov [11]; Pavlov [38, 39]; Chaikovskaya, Bazhenova [3]; Petrakov Mikutskiy;

Staritskiy, Ykovlev, Malich, Polunina, Afanas'yeva [40]; Semenov [45, 46]; Sadovnikov, Markevich, Vokov, and others. The author worked in the Anakit region in 1960-1961. The purpose of the expedition, as we have already indicated, was to study the contact metamorphism and petrology of the Anakit massif.

It should be mentioned that the Anakit region consists of one of the most interesting sections of the earth's surface where, on a comparatively small area, there are grouped together some of the most interesting geological objects of study including: tectonics stratigraphy, lithology, trappean petrology, gas-bearing strata, metalogeny, coal and graphite formations, to say nothing about the unique manifestation of contact metamorphism of limestones. This may be an explanation of why the Anakit structure has attracted the attention of geologists of various specialities for over thirty years. However, it should be stated that the area still has not been thoroughly enough studied due to the paucity of outcroppings. This applies primarily to iron mineralization which has only been studied from the surface, and the possibilities of petroleum and gas deposits. Absolutely unclear is the problem of depth formation and composition of the lower upheaval horizons. These problems cannot be resolved without a vast amount of mining work and drilling which has practically been untouched in the Anakit region during the long history of its exploration.

II. GEOLOGY OF THE ANAKIT REGION

The region under survey is in the Anakit anticlinal upheaval which is in the Lower Tunguska Valley that emerged to the surface as a result of the intensive scouring of the over-lying rocks both by the river and its tributaries, the most important of which is the Anakit River. The relief of the terrain and the nature of the Lower Tunguska River valley are due to the geological

formation of this part of the Siberian platform and to the erosional activity of rivers. The peculiarity of the Lower Tunguska River valley is due to the abundance of intrusive strata of traps which perforate the subsident paleozoic rocks. More durable against erosion than the rocks mixed in with them are the traps which form "steps" in the sides of the river valley, fully justifying the idea embodied in the phrase by the Swedish geologists in the premicroscopic period [27].

The Anakit upheaval is within the limits of the Anakit rampart of the north-northwest strike, which, along with a number of other ramparts (trough-shaped) structures is found in the area of the western slope of the Tunguska syncline. These arch-like upheavals being structures of a second order with respect to a syncline are a characteristic peculiarity of its tectonic formation within the limits of the marginal parts. They follow along the boundary of the syncline, oriented parallel to its outer contours [5, 10, 16].

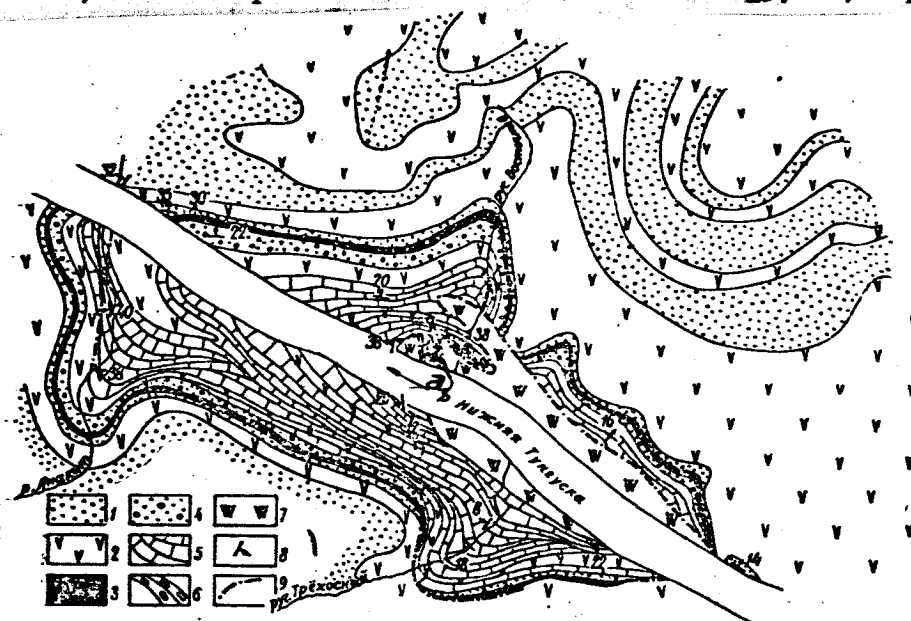


Fig. 1. Schematic geological chart of the Anakit dome-like upheaval region.

Markings: 1 - Lower Permian deposits (Burguklinskaya platform); 2 - non-differentiated traps; 3 - Carboniferous deposits (Katskaya platform); 4 - Devonian deposits; 5 - Kochumdekskaya platform of the Lower Silurian; 6 - Dolborskaya platform of the Upper Ordovician; 7 - Anakit Massif; 8 - Elements of stratification; 9 - Tectonic dislocations.
Legend: a) Lower Tunguska River.

It is obvious from the investigations made by N. S. Malich that the formation of most of the bars of the Podkamennaya Tunguska (lower reaches), the Bakhta River, and others in the Priyeniseysk Trough occurred over a long period of time. This is demonstrated by an analysis of the thickness and facial changes of deposits, embankment components, and troughs. The great stratigraphic resemblance of the deposits which form the Anakit structure to the deposits of a number of uplifts of the more southerly regions enables us to see a certain analogy in their tectonic development. Apparently, the Anakit embankment, like other positive structures of this portion of the Tunguska syncline, was established during the Lower Paleozoic and was in a continuous state of formation until the end of the Paleozoic. However, its growth was occasionally either temporarily interrupted or periodically intensified.

The Anakit upheaval is the largest upheaval in the Anakit embankment. It is brachy-anticlinally elongated in a northwesterly direction with an area of 6 x 12 kilometers. The angles of dip change from steep angles of up to 40° in the central portion of the anticline to about 8° on the flanks where the rocks of the Permian age are developed. The Anakit upheaval is broken up by a large number of tectonic disturbances, especially in the central portion. Intrusions of dolerites penetrated through the largest of them.

Rocks which form upheavals are characterized by the great variegation of their composition. The most ancient deposits are the rocks of the Ordovician Period which are found in the central portion of the brachy-anticline. The Ordovician rocks, just like the Silurian deposits upon them, are of great interest to us because they fall into the contact zone of the trappean massif which experiences high temperature metamorphism.

Ordovician outcroppings emerge on both sides of the Lower Tunguska River at the very edge of the stream, as well as in the lower reaches of Vostochnyy Stream (Fig. 1). The rocks are broken by numerous tectonic disturbances, crevices, metamorphosed dike apophyses of the Anakit trappean massif which cuts them up. The lower boundary of the Ordovician layer is not laid bare; the visible portion is about 60 meters thick.

The rocks of this age group are represented by sandstones and limestones or dolomitic sandstones gradually changing into sandy, slightly dolomitic limestones as well as calcareous (dolomitic) aleurolites, argillites and marls. Characteristic of this is the clearly expressed stratification and variety of color in the rocks, which ranges from gray to yellowish or brown-green.

The sandy faction is represented mainly by quartz which forms grains up to 0.1 cm in dimension. The structure is non-uniformly grainy. The fragments are semi-rounded or rounded. In the sandstones the cement is calcitic or calcite-dolomitic, basal or porous; in some sections the cement is essentially chloritic. The chorate is thinly squamous, greenish in color with an index of refraction at N_m of 1.603. With an increase in the amount of carbonate cement the sandstones change to sandy weakly dolomitic limestones and limestones consisting essentially of calcite (the amount of dolomite is not in excess of 5 - 10%), which forms aggregates of thinly crystalline grainy structure not infrequently with clear signs of cataclasm. Upon decreasing the cement down to the point of complete disappearance, there appear quartzite sandstones with quartzite structure containing an admixture of orthoclase and fragments of flinty rocks. Here and there we observe scarce and scattered impregnations of hard bitumens [3].

The sandstone rocks make up the main portion of the Ordovician layer. The marls, aleurolites and argillites, just like the limestones, form a

separate layer with a thickness of several centimeters to several meters; they are characterized by extreme non-persistence in thickness and often peter out along the strike.

The rock mass described contains a great abundance of faunistic residues of brachiopods, trilobites, and other. Many of the forms found here are very characteristic and we can reliably class the deposits in the central portion of the Anakit upheaval as part of the Dolborskaya formation [35], i.e., the upper Ordovician (O_3dl).

Rocks of the Dolborskaya formation with its non-evident disconformity are covered over with Lower Silurian carbonate deposits. The main volume of the Lower Silurian stratum is made up of striated marls. They have a gray or dark gray color and a fine to medium-grained structure. The striations of the rocks are emphasized by their color: the darker separations containing a considerable admixture of clayey and carbonaceous material (up to 50%) form irregular spots, bands, etc., on the common, lighter background of the essentially carbonate portion of the marl. It is interesting to note that the basic mass of clay particles is concentrated in the internal portions of the carbonate-clay separations. A similar tendency is noted also in a dolomite whose content is 10 to 15% (in this case the rock approaches a dolomite marl in composition). The peripheral portions of the separations usually contain no dolomite, but apparently they contain a certain admixture of thinly dispersed free silica in the form of chalcedony or opal recrystallized into quartz. The structure of the rocks for the most part is crystalline-granular in some places it is cataclastic or granoblastic.

In the upper parts of the profile of the Lower Silurian stratum the clay substances are less important; here, we find various stratified limestones, blue, green, or white in color with occasional interlayers of dark marls. In

the lower portions there are interlayers of dolomites, dolomitic marls, dolomitized limestones, etc. In the middle portion of the stratum, just as in the lower parts, we find well developed siliceous concretions forming thin horizons. The concretions are mainly chalcedony (or quartz) and carbonate in composition, i.e., calcareous silicates.

Table 1

Results of the Roentgenostructural Analysis of Clay Minerals in Marls of the Kochumdeks Formation of the Anakit Region*

Dolomitic marls				Dolomitic-like marl				Limestone			
Minerals of the hydro-mica group		Minerals of the kaolin group		Minerals of the hydro-mica group		Minerals of the kaolin group		Minerals of the hydro-mica group		Minerals of the kaolin group	
I	$\frac{d}{n}$	I	$\frac{d}{n}$	I	$\frac{d}{n}$	I	$\frac{d}{n}$	I	$\frac{d}{n}$	I	$\frac{d}{n}$
17	12,93— —10,19	38	7,16	20	12,98— —9,77	28	(8,01)	10	11,46	37	7,20
6	5,53	18	4,58	13	(4,99)	73	7,32	29	4,55	25	4,50
18	4,58	27	3,65	42	(4,54)	30	(4,47)	26	3,88	18	4,11
5	4,10	21	2,67	22	4,31	22	4,36	15	3,36	65	3,65
9	3,35	100	2,50	28	(4,05)	28	(4,05)	18	3,22	100	2,50
17	3,22	30	2,306	77	3,64	70	3,57	10	2,94	18	2,21
98	2,97	20	2,204	6	3,33	24	(2,76)	100	2,50	23	1,80
34	2,89	44	2,148	8	(2,86)	20	2,56	26	2,33	36	1,54
100	2,51	30	1,831	26	2,59	75	2,50	23	2,22	29	1,509
22	2,206	30	1,756	100	2,48	44	2,14	56	2,15	13	1,313
44	2,148	17	1,715	44	2,14	17	(1,97)	21	2,03		
38	2,025	47	1,622	17	(1,97)	13	(1,91)	44	1,531		
38	2,011	17	1,587	17	1,654	15	(1,82)	13	1,313		
27	1,969	32	1,527	55	1,531	24	1,788				
17	1,715	34	1,501	33	1,502	17	(1,736)				
23	1,653	19	1,328	8	(1,445)	28	(1,693)				
38	1,531	18	1,280	11	1,274	20	1,654				
22	1,423	10	1,259	8	1,249	10	1,578				
19	1,281	10	1,245	6	1,218	55	1,531				
10	1,245					11	1,459				
						5	1,451				
						24	1,304				

* Roentgenostructural analyses made in the roentgenostructural analysis laboratory of IG and G SO AN SSR [Institute of Mining and Geological Sciences, USSR Academy of Sciences].

Cu -- anti-cathode, $\lambda = 1.537\text{kX}$; U = 30 kV; I = 10mA; diffractometer URS-501. Radiation filtered. Intensity by the hundred point scale.

They are rounded or irregular shaped, with dimensions ranging from 1 to 10 cm along the longitudinal axis. Concretions usually coincide with the carbonaceous-clayey interlayers of limestones and are enveloped with a dark

Table 2

Results of Chemical Analyses of Carbonaceous Rocks in the Kochumdeks Formation

Type rock	SiO ₂	TiO ₂	Al ₂ O ₃	Fe ₂ O ₃	FeO	MnO	MgO	CaO	Na ₂ O	K ₂ O	H ₂ O	Misc.	Total
Limestone*	3.55	0.03	0.16	0.07	0.11	0.04	1.61	53.90	none	none	-	40.80	100.27
Dolomitic marl*	17.54	0.085	2.29	0.91	0.18	0.067	6.80	40.67	none	none	-	31.45	99.99
Dolomitic marl**	6.30	0.07	1.71	0.39	0.46	0.03	7.19	45.46	none	0.36	0.10	37.48	99.55
Dolomite*	2.80	0.025	0.53	0.29	0.14	0.056	21.45	37.17	none	none	-	38.09	100.55

* Chemical analysis made in the Central Chemical Laboratory of the Novosibirsk Territorial Geological Department.

** Chemical analysis made in the chemical-analytical laboratory of (IG and G SO) Academy of Sciences, USSR, Institute of Mining and Geology.

marly material containing insoluble particles amounting to from 40 to 50%. In the middle portions of the rock mass concretions are encountered in layers of siliceous limestones and marls containing sponge spicules.

The Lower Silurian deposits have a wide variety of organogenic limestones. Individual horizons of these are encountered along the entire section; they are characterized by a clearly developed detritus structure (crinoidal limestones and others).

The clayey fraction of limestones, marls, and dolomites of the Lower Silurian rock mass is represented by minerals from the hydromica and kaolin groups. They form aggregates of extremely small scales in associations with organogenic carbon substances. The indexes of refraction of the minerals are as follows. Minerals of the kaolin group: $n_g = 1.556$, $n_p = 1.549$ (all ± 0.003). Minerals of the hydromica group: $n_g = 1.568$, $n_p = 1.542$ (all ± 0.003). The interplanar distances of the minerals indicated are

given in Table 1.

The data on the study of the mineral composition of the rocks are confirmed by the results of chemical analyses given in Table 2. The presence of nickel, copper, and sodium (in amounts from 0.001 to 0.1%) in limestones was also confirmed by spectrographic tests. The spectral analysis was made in the spectral analysis room in the Institute of Mining and Geology, USSR Academy of Sciences. The age of the carbonaceous rock mass described is established rather reliably on the basis of occurrences of faunal remains like llandovery-venlok [sic]. Apparently, it is comparable to sedimentations of the Kochumdeks formation of the Lower Silurian which are developed in the basin of the Podkamennaya Tunguska River [28] (S₁ktch).

Occurring in the limestones of the Kochumdeks formation are various rocks of the Devonian age: motley-colored clayey-carbonaceous deposits of the Zubovsk and Tynepsk formation, organogenic limestones of the Yuktinsk formation and comparable to the Zhivetsk carbonaceous rocks [1], and sandstones of the Dzhalitulinsk formation of the Upper Devonian. The Devonian rocks with non-evident disconformities are covered with quartz sandstones, coaly shales and aleurolites of the Katsk Formation of the middle-upper Carboniferous Period [34]. The shales and aleurolites contain a large quantity of vegetative detritus which were described by a number of authors who have studied them [17, 60, 85]. Impressions of the flora described compare favorably with the floral complexes of the Alykaeyevsk and Mazurovsky horizons of the Lower Balakhensk formation of the Kuzbass [43]. Lower Permian terrigenous rocks are in conformable bedding with the Carboniferous deposits.

The region of the Anakit upheaval is rich in non-differentiated Noginsk complex traps of the third phase of trap magnetism in the Siberian platform [40]. The intrusive bodies usually are conformable with the enclosing rocks.

They are practically horizontal in the Permian deposits beyond the limits of the Anakit upheaval, and appear like the harpolites in the more ancient paleozoic rocks which make up the internal portions of the anticlinal structure (cf. Fig. 1).

The traps are represented by the gabbro-dolerites, allivalite gabbro-dolerites, pegmatoid gabbro-dolerites and microdolerites (dolerite aphanites). The gabbro-dolerites with frequent taxitic composition and allivalite gabbro-dolerites predominate in the central and lower portions of the trappean bodies; they frequently contain schlierens of pegmatoid varieties and are rather intensively amphibolized.

The mineral composition of the rocks is quite uniform. The plagioclase consists of from 40 to 60% of the total of the rock and is represented by andesine-labradorite. Monoclinial pyroxene has a composition consisting of $Wo_{32-42} En_{43-54} Fs_{20-25}$ (according to optical data) and is contained in rocks in the amount of 10 - 42%. Olivine is represented by hortonolite; its content varies from 0 to 27%.

Among the variable admixtures is magnetite (sometimes magnetite is present in noticeable amounts -- up to 15%), biotite and others. The content of micropegmatite mesostasis is also subject to great variations -- from 0 to 15%; pegmatoid gabbro-dolerites are characterized by an increased amount of mesostasis.

The intrusive bodies vary in thickness. The large strata bodies have thicknesses ranging to 300 meters. The basic mass of trappean bodies is of a thickness not exceeding 150 meters. Sills of 2 to 3 meters in thickness are also somewhat developed.

III. ANAKIT DIFFUSED TRAPPEAN MASSIF

The Anakit trappean massif occurs in the vaulted portion of the cupola-shaped upheaval and, being the youngest intrusive formation in the region,

breaks through the previously formed trappean bodies. According to L. A. Polunina and M. A. Afanas'yeva it belongs to the Kuz'movsk Complex of the 4th phase of trappean magmatism [40]. The intrusion is in the shape of an irregular phacolith, a fact due to the layer-by-layer invasion of magma into the strata of sedimentary rocks contorted into a double plunging anticline.

In the northeastern portion the phacolith changes to a thick (about 250 meters) dike-like body, cutting one of the wings of the elevation (Fig. 2). The northwestern tip of the massif is characterized by the invasion of magma to the tectonic dislocations which divides the sedimentary paleozoic rocks into separate blocks and is rich in numerous xenoliths.

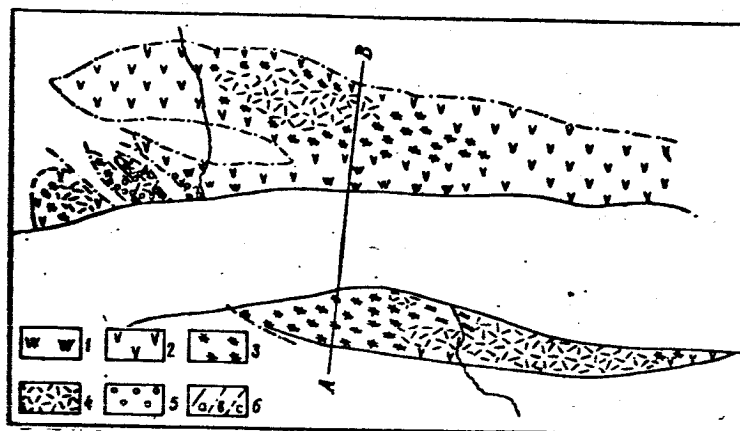


Fig. 2. Schematic geologic chart of the Anakit trappean massif. Conventional markings:

1 - troctolyte dolerites, olivine and olivine-hypersthenite gabbro-dolerites; 2 - gabbro-dolerites; 3 - ferrogabbro; 4 - granophyres and dolerite-pegmatites; 5 - hybrid rocks; 6 - a) conformable intrusive contacts; b) intersecting intrusive contacts; c) undetected contacts.

The visible thickness of the stratum-like portion of the intrusion is not under 100 meters. It is characterized by a marked differentiation: from troctolite dolerites to granophyres. The lower portion of the massif is made up of olivine and olivine-hypersthenic gabbro-dolerites with poorly expressed schlieren of troctolite dolerites. Higher up these rocks change and we find normal gabbro-dolerites consisting of plagioclase labrador and monoclinial

pyroxene with an admixture of hypersthene, olivine, titanomagnetite and others. Still higher on the section the gabbro-dolerites are replaced, in turn, by ferro-gabbro and quartzian gabbro-dolerite rocks which are tied together by mutual transitions.



Fig. 3. Section through chart of Anakit massif (cf. Fig. 2). Section shown in enlarged scale.

Legend: a) Section through AB; b) Lower Tunguska River.

In the uppermost portion of the massif the dolerite-pegmatites and granophyres (Figs. 2, 3) are extensively developed. In the endocontact portions the microdolerites and porphyry microdolerites are generally distributed.

The most striking feature of the trappean magma during the course of its crystallization is the absolute concentration of iron and alkalis in the later stages of the process. This phenomenon was discovered by V. S. Sobolev over 25 years ago [49], and it is clearly manifested in the Anakit differentiated massif; it is expressed as a successive crystallization of minerals of variable composition related together by definite paragenetic ratios of olivines, pyroxenes and plagioclases in which the content of iron and lye changes during the crystallization of the magma. The composition and distribution of minerals in the vertical section of the massif undoubtedly point to the presence of processes of differentiation in the crystallization of the trappean magma and to the non-simultaneous formation of separate differentiates. The mineralogical characteristic of rocks in the Anakit massif is given in Table 3.

The gravitational, crystallizational differentiation of the magma was affected during the process of movement (extrusion) of magmatic melt, a fact pointed to by the arrangement of crystals of plagioclase in all the differentiates of the massif with the exception of dolerite-pegmatites and granophyres.

Table 3

Changes in Composition of Dark-Colored Components and Plagioclase
Through the Vertical Section of the Anakit Massif

Differentiate	Mineral			
	Olivine	Rhombic pyroxene	Monoclinic pyroxene	Plagioclase % An
Troctolitic dolerite	Fa ₂₃₋₂₅	Fs ₄₅	Wo ₃₉₋₄₁ En ₄₄₋₄₅ Fs ₁₆₋₁₈	85-89
Olivine gabbro- dolerite	Fa ₂₅₋₄₅	Fs ₅₀	Wo ₃₉₋₄₂ En ₃₉₋₄₁ Fs ₁₈₋₂₂	80-85
Gabbro-dolerite	Fa ₄₈₋₅₀	Fs ₅₀	Wo ₃₉₋₄₄ En ₃₁₋₃₈ Fs ₂₂₋₃₀	60-78
Quartzian gabbro- dolerite	—	—	Wo ₄₀₋₄₃ En ₃₀₋₃₅ Fs ₂₀₋₃₀	48-59
Ferrogabbro	Fa ₅₀₋₇₀	—	Wo ₄₉₋₄₇ En ₂₅₋₃₂ Fs ₃₀₋₃₉	42-53
Dolerite-pegmatite	—	—	Wo ₃₉₋₄₈ En ₁₇₋₂₅ Fs ₃₂₋₄₂	31-44
Granophyre	—	—	Wo ₄₄ En ₄₋₅ Fs ₅₂₋₅₃	21-30

In analyzing the orientation of the plagioclase¹⁾ in the rocks of the Anakit massif we succeeded in establishing the presence of two incurrent canals through which the magma was conducted to the space presently occupied by the intrusion: 1) the dike-like intersecting body in the northeastern portion of the massif, 2) the group of apophyses in the northern and northwestern portion (the latter presumably are connected together in the depths). In general, the magma progressed in a southerly direction from both of the channels squeezing itself out into the rock mass which makes up the Anakit upheaval. The intrusive body formed hereby inherits the cupola-like form of the enveloping, double-plunging anticlinal fold acquiring the shape of a phacolith.

On the basis of the direction of differentiations, the composition of the rocks and their mutual distribution in the vertical section, the Anakit massif closely resembles the Skaergard massif in Greenland [79, 95] and the Alandzhakhsk trappean massif in the Vilyuya River basin [30]. A special article by author is devoted to a more detailed petrological description of the Anakit trappean massif.

1) In making the analysis of the structure of the massif we used micro-structure observations in the large scale processing of orientated schlieren using the method of V. V. Zolotukhin [18, 19].

IV. EXOCONTACTS OF THE ANAKIT MASSIF

The contact influence of the Anakit intrusion on the interfering rocks of the Ordovician and Lower Silurian was expressed in the high temperature metamorphosis as a result of which there was a formation of marbles, containing rare silicates of calcium, hornfels of larnite-merwinite-spurrite subfacies, and others. The next stage in the contact effect was the appearance of garnet-pyroxene skarns and magnesioferrite ores. The concluding stage is characterized by a rather abundant hydro-thermal activity which was manifested in the formation of a number of hydrosilicates of calcium, silicification, serpentinization, etc.

A. Metamorphic Stage

Under this heading it is appropriate separately to consider the products of metamorphism as a function of the original nonmetamorphosed rocks on the one hand, and the temperature of the contact effect from the trappean intrusion, on the other. Two groups of contact-metamorphic rocks are to be distinguished from their temperature characteristics:

- 1) high temperature marbles and hornfels of a larnite-merwinite-spurrite subfacies (sanidinite facies of contact metamorphism according to F. Turner and G. Ferry [56]);

- 2) the comparatively lower temperature marbles and hornfels of pyroxene-hornfels facies than in the preceding case [56]. These two groups of rocks clearly differ from one another in their mineral composition and position in the contact zone of the Anakit massif. Depending on the composition of the original rocks in each of the above mentioned groups we differentiated between several mineral associations formed:

- a) in the metamorphism of calcareous marls with a certain admixture of free silica and dolomite;

- b) in the metamorphism of dolomitic marls and silica dolomites;
- c) in the metamorphism of calcareous, calcareous-dolomitic, and dolomitic sandstones and aleurolites with interlayers of argillites.

High Temperature Contact Metamorphism

(Sanidinite Facies)

Metamorphism of Calcareous Marls

The highest temperature metamorphic rocks of the contact aureole of the Anakit differentiated trappean massif are located in the central portion of the cupola-shaped structure where the magma irrupted through numerous ruptured tectonic dislocations, i.e., in the immediate vicinity of the incurrent channel.

The area of distribution of these rocks is the right bank of the Lower Tunguska River, somewhat below the mouth of Vostochnyy Stream. The main portion of the original exit is found in the area of the river flood plains and is covered by the deep flood waters. The first description of the rocks was made by V. S. Sobolev [48].

Marbles, containing rare silicates of calcium of the larnite-merwinite-spurrite subfacies of contact metamorphism coincide with the contacts of the thick asymmetric apophysis of the Anakit massif (Fig. 4). In the western contact zone are to be found chiefly rocks formed from essentially dolomitic marls and consisting of calcite, monticellite, melilite, and others.

In the eastern contact zone of the apophysis there are marbles formed in the metamorphism of essentially calcareous marls (the content of dolomite is between 10 and 15%) and, in addition to calcite, they contain spurrite, merwinite, tilliite, and others.

The position of the enclosing rocks on both sides of the apophysis is varied. On the western side the apophysis is in contact with the non-dislocated carbonaceous stratum of the Silurian period; the contact bears a clear

concordant imprint. On the east it is bounded by a block of Silurian calcareous marls severed from the substratum and various Ordovician sandstones and aleurolites. This block is cut up by veins (apophyses) of traps and is metamorphosed. The eastern portion of the block comes in contact with still another thick apophysis of the Anakit massif. Made up of rocks of the Ordovician period, the eastern portion of the block is converted in metamorphism into various hornfels described below. The block of Silurian rocks is not like the xenolites although the latter are also encountered in the endocontact areas of the massif, but their dimension is usually not over several meters (along the larger axis). The block is isolated and somewhat turned as a result of disjunctive tectonic activity of the enveloping stratum bounded on all sides by ruptured dislocations into most of which the trappean magma intruded. Shown in the large-scale schematic chart (Fig. 4) of the right bank portion of the Lower Tunguska River in the area of the apophysis of the northwestern part of the Anakit massif is the interrelation of traps with enveloping rocks, including the previously mentioned blocks of metamorphosed Silurian-Ordovician rocks. One is struck by the distinctly intersecting character of the apophysis which irrupts into the internal portion of the block.

Despite the fact that all sedimentary deposits making up this block are rather strongly metamorphosed, nevertheless, the rocks immediately adjacent to the contact with traps are distinguished by the more intensive metamorphism. This zone of intensive contact metamorphism is 10 - 18 meters thick.

The marbles in the zone of intensive metamorphism are light gray to dark gray in color and broadly striated in texture. The nature of the coloration emphasizes the striated (or striated-mottled) texture of the rock. The darker portions, made up chiefly of silicates of calcium, are clearly seen on the overall light gray background of calcite marble and contain practically no

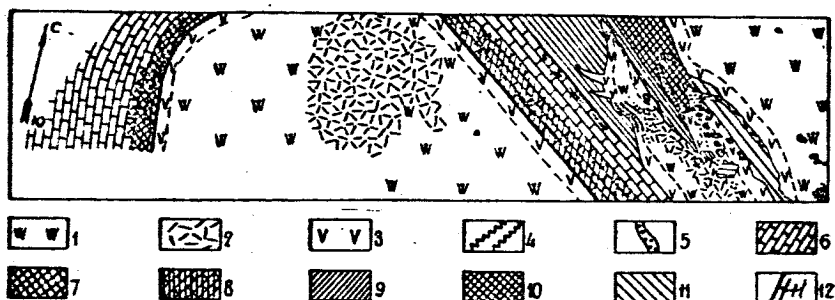


Fig. 4. Large-scale schematic geological chart of the right bank portion of the Lower Tunguska River in the area of the Anakit cupoloid elevation somewhat below the mouth of Vostochnyy Stream.

Legend: 1 - gabbro-dolerites and ferro-gabbro; 2 - granophyres and dolerite-pegmatites; 3 - microdolerites; 4 - hybrid pyroxene-feldspar rocks; 5 - hybrid shonkinites; 6 - Kochumdeks formation marls; 7 - contact zone with an extensive development of monticellite-melilite rocks; 8 - contact zone with a substantial development of spurrite-melilite-merwinite rocks; 9 - pyroxene-wollastonite, pyroxene-plagioclase, pyroxene and other hornfels; 10 - area of main development of phlogopite-and-sandine-containing rocks; 11 - quartz rocks; 12 - skarn veins.

silicate minerals. Isolations of silicate minerals are striated, irregularly lens-shaped, or streaky in appearance. The boundary between them and the marble is usually quite distinct. When exposed to the weather they are more durable than calcite and emerge as eminences on the surface of the marble. The structure within the bounds of the isolation and in the enclosing marble is characterized by heterogeneity, changing from fine to medium granular. The individual layers of calcite silicates in the marble do not exceed 7 - 10 cm, and the general thickness seems to be between 1 and 3 cm. The distance between adjacent lines, separated essentially by a calcite interlayer, also varies within these limits. Along the strike the bands made up of silicate minerals vary greatly in thickness and often taper out at a distance of 30 to 50 cm. In some places within the limits of thin, lens-shaped and striated isolations one encounters nodular "swellings" with a cross section length of 10 - 11 cm. Similar nodular isolations are sometimes found isolated in marble. Very often the larger isolations have thin, streaky ramifications, thin leaders, and the like which may connect with adjacent isolations.

All the numerous lens-shaped, banded, nodular and other kinds of isolations are usually grouped and oriented in the plane of a definite horizon (Fig. 5) and extend over a considerable distance. The isolations grouped within the bounds of this horizon make up the above mentioned coarse, streaky texture of metamorphic rocks.

The calcium silicates which make up the isolations in marble are represented by *merwinite*, *spurrite*, *melilite*, and *tilleyite*. In addition, usually present in this association are *pyrrhotite* and *chalcopyrite*. Here and there in the interior portions of the nodular swellings and in large nodular isolations one encounters concentric sections made up of *wollastonite* aggregate. Macroscopically, these *wollastonite* "nuclei" are white, rose, or light gray in color and have a fine grain structure. The boundaries of the "nucleus" are usually sharp and clean. Occasionally *tridymite* and *pyrrhotite* are found in association with *wollastonite*.

Given in the following are the characteristics of silicate minerals which are formed in the metamorphism of calcareous marls containing a certain admixture of dolomite and free silica.

Tridymite -- SiO_2 . The mineral is found in certain concentric isolations of fine grain *wollastonite* (in *wollastonite* "nuclei" from nodular swellings). It forms microcrystalline growths, consisting of irregular and coarsely laminated grains the dimensions of which rarely exceed a hundredth part of a millimeter. Ordinarily, one finds knotty, lens-shaped, and fusiform accumulations of grains of *tridymite* interspersing the *wollastonite* "nucleus" either in irregular fashion or oriented parallel to its edges. The grains of the mineral are rich in circular inclusions of *wollastonite* and graphite. The indexes of refraction of the mineral are: $N_g = 1.473 \pm 0.003$, $N_p = 1.469 \pm 0.003$. In the laminated crystals one clearly observes negative elongation and straight extinction. The optic axial angle is not great and is positive. Double

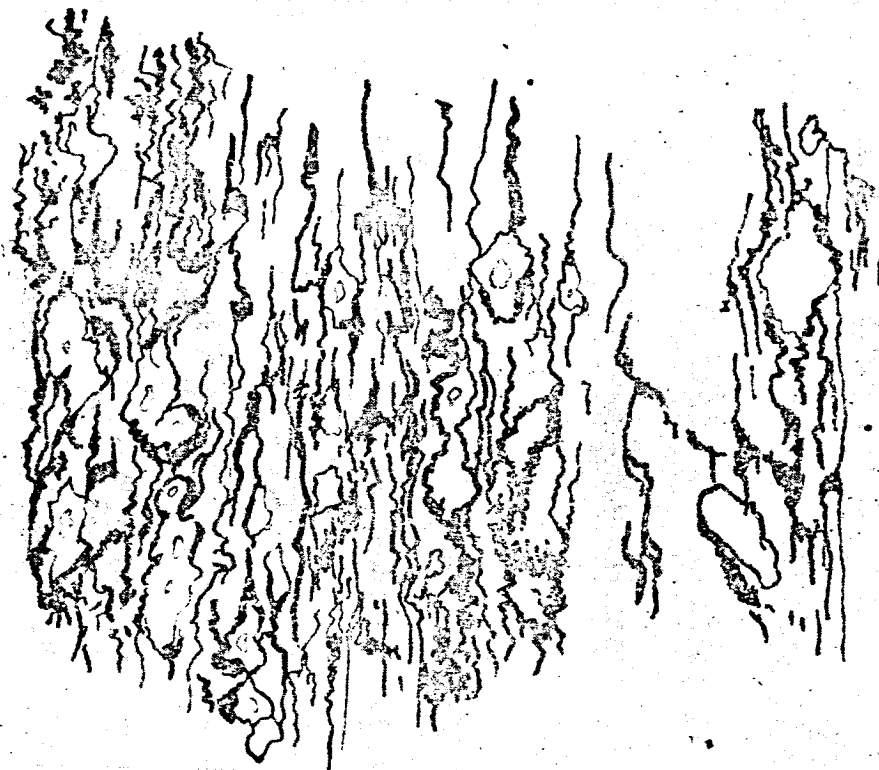


Fig. 5. Detail drawing of surface of contact metamorphic marble (schematic drawing of outcropping).
Scale: 1 cm - 0.07 m. White -- spurrite-melilite isolation with central "nuclei" of wollastonite. Black -- merwinite-melilite banded, streaky isolations. Gray -- marble.



Fig. 6. A large polysynthetic twin crystal grain of merwinite (at the top -- intersecting twin crystals are visible) in association with spurrite (upper left). Interlacing of nicol. Mag. 32.

refraction is low and of the order of 0.003 - 0.004. All of these data enable us to define the mineral as tridymite.

Merwinite -- $\text{Ca}_3\text{MgSi}_2\text{O}_8$. Triclinic system [50]. There is a statement in some literature to the effect that this mineral crystallizes into a monoclinic system [60], but the results of studies on the orientation of the optical indicatrix of merwinite contradict this.

The mineral forms brown or brown-gray small grains associated with melilite, spurrite, pyrrhotite and others. The grains are irregular, circular or coarsely tabular; usually, they contain inclusions of spurrite and melilite.

Individual mineral elements of merwinite are not over 1 mm in size, although one occasionally encounters rather large-sized grains tabular in shape up to 3-4 mm in size. The mineral is characterized by the presence of two systems of polysynthetic twinning, which intersect along the edges of the prism (110) and $(\overline{1}\overline{1}0)$ at an angle of 43° (Fig. 6). Quite often one notes a complete cleavage (possibly a separation), which divides the angle between the two systems of twin seams into approximately equal parts. Most likely this "cleavage" is complicated in nature and is manifested by a combination of systems of twin seams of polysynthetic twinning.

The twinned axis coincides with the rib [001]. The angle cNp is about 33° . Nm almost coincides with \perp to (010), a fact that can be established in well formed table-shaped crystals.

The orientation of the optical indicatrix of merwinite with respect to the twin axis, to the pole of the twin seam, and plane of imperfect cleavage is given in the following:

Twin Axis [001]	Twin Plane of Intergrowth (110)	Cleavage
$Ng=82^\circ$	$Ng=33^\circ$	$Ng=14^\circ$
$Nm=61^\circ$	$Nm=74^\circ$	$Nm=87^\circ$
$Np=33^\circ$	$Np=67^\circ$	$Np=74^\circ$

It should be mentioned that these data agree well with the results of study of the optical orientation of merwinite given by V. S. Sobolev [50].

The indexes of refraction of the mineral are: $N_g = 1.722 \pm 0.003$, $N_p = 1.705 \pm 0.003$, $N_g - N_p = 0.017$. The angle of optical axes is large and positive, $2V = 73^\circ$.

The specific gravity of this mineral is 3.2, Hardness 6, streak is black, the luster is glassy.

The interplanar distance of merwinite determined roentgenoscopically are given in Table 4.

Table 4

Results of Roentgenostructural Analysis of Merwinite*

I	$\frac{d}{n} \alpha$	I	$\frac{d}{n} \alpha$
6	2.94	4	1.753
.6	2.832	3	1.693
4	2.730	1	1.624
10	2.650	1	1.561
2	2.442	7	1.530
2	2.296	3	1.430
2	2.200	3	1.378
4	2.145	2	1.332
3	2.008	2	1.320
8	1.889	1	1.224
8	1.856	1	1.195

Photographing conditions: $D = 57.3$ mm; Co = anticathode; $\lambda = 1.78529$ Å; $I = 11$ mA; $U = 37$ kV. Radiation filtered. Corrections made in accordance with combined graph for KCl and chlorite. Exposure time 20 hours. Intensity on ten-point scale.

* Made in the roentgenostructural analysis laboratory of IG and G, SO AN SSSR.

Spurrite -- $\text{Ca}_5\text{Si}_2\text{O}_8(\text{CO}_3)$. Monoclinical system. The mineral forms large tabular colorless or light gray crystals with several systems of cleavage cracks. In nature, spurrite forms solid grainy masses resembling marble. The luster on the surfaces of cleavage is glassy, hardness 5 - 6, specific gravity 3.0, white streaks; mineral transparent or semi-transparent. Dimensions of

individual crystalline grains up to 5 mm. The mineral is characterized by the presence of perfect cleavage along (100) (accepting the orientation of spurrite according to S. E. Tilley [88, 91]) and imperfect along (001). Both cleavages intersect at an angle of 79° - 80° . The optic axial is perpendicular to (010) and is inclined at an angle of 58° to the plane of perfect cleavage; the axis N_m forms an angle of 32° with the rib [001].

The mineral shows two systems of polysynthetic twins. The most common and usual are twins with a plane of perfect coalescence (100). They are expressed beautifully and remind one of plagioclase twins. Characteristic of polysynthetic twins of spurrite is a special phenomenon expressed in the regular alternation of broad twin plates with relatively narrower ones, the width of the narrow and wide alternating plates persists rather clearly. Twinning in spurrite is just about as widely distributed as in the plagioclases, and it is a very characteristic diagnostic feature; however, totally non-twinned grains are also encountered. The latter feature is most typical of the large crystalline mineral aggregates. Very uncommon is simple twinning.

Less prevalent is twinning along the plane (101). Twins with this plane of coalescence not infrequently intersect with the previously mentioned twins with the plane of coalescence (100)¹⁾. The angle between the two twin surfaces is about 120° here. This peculiarity in the Anakit spurrite was first noted by V. S. Sobolev [48].

The sections perpendicular to the peak of the bisectrix show a symmetrical extinction of the adjacent twin plates; the crystal is frequently extended in the direction of twinning and perfect cleavage (Fig. 7). The section perpendicular to the plane (010), shows a highly interferential coloring.

1) It is possible that in this case there is twinning along (101) and (101); however, this cannot be proved definitively due to the closeness of the coordinates of the twin surfaces (101) and (100).

The orientation of the optical indicatrix of spurrite with respect to the poles of twin surfaces of coalescence (edge twinning law) after making a determination on the Fedorov universal stage is as follows:

Twin Plan of Coalescence
Perfect Cleavage along (100)

$$Ng = 32^\circ$$

$$Nm = 58^\circ$$

$$Np = 90^\circ$$

Twin Plane of
Coalescence (101)

$$Ng = 25^\circ$$

$$Nm = 65^\circ$$

$$Np = 90^\circ$$

The indexes of refraction of the mineral are as follows: $Ng = 1.679 \pm 0.003$, $Np = 1.640 \pm 0.003$, $Ng-Np = 0.039$. $2V = -39^\circ$, $r > v$. These data agree well with the determinations of other investigators who studied spurrite. Specifically, according to F. E. Wright: $Ng = 1.679 \pm 0.002$, $Np = 1.640 \pm 0.002$, $Ng-Np = 0.039$ (in Na light), $2V = -39.5^\circ$ [97]; according to S. E. Tilley: $Ng = 1.680$, $Np = 1.640$, $Ng-Np = 0.040$, $2V = -40^\circ$ [88]; according to O. F. Tuttle and R. I. Harker: $Ng = 1.679 \pm 0.002$, $Np = 1.640 \pm 0.002$, $Ng-Np = 0.039$, $2V = -40^\circ (\pm 5^\circ)$ [92], etc.

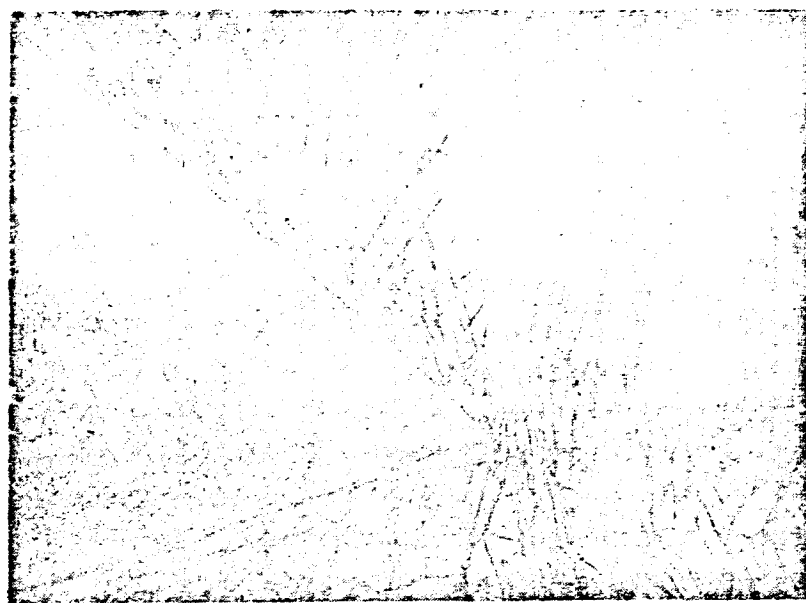


Fig. 7. Spurrite rock. The large grain of spurrite (on the left) apparently forms as a result of smaller tablet-shaped spurrite grains in re-crystallization. The nicols are twisted. Magnification 32.

In the rock spurrite associates with calcite, merwinite, melilite, tilleyite, pyrrhotite, wollastonite, and others. Disintegrates readily and is replaced by a number of later minerals, specifically garnets, calcium hydrosilicates, etc.

The interplanal distances in spurrite, roentgenoscopically determined, are given in Table 5.

Table 5

Results of Roentgenostructural Analysis of Spurrite*

<i>h</i>	$\frac{d}{a}$	<i>h</i>	$\frac{d}{a}$
1,5	3.779	3	1.976
4	3.480	10	1.882
4	3.152	1	1.821
6	3.020	1	1.811
10	2.698	1	1.792
5	2.674	2	1.766
2	2.650	5	1.709
10	2.620	1	1.657
2	2.531	3	1.607
3	2.418	3	1.537
2	2.230	1	1.473
6	2.185	3	1.432
6	2.174	8	1.413
1	2.130	1	1.273
2	2.086	1	1.257
4	2.011	1	1.197

Photo conditions: Co - anticathode; D = 57.3 mm; $\lambda = 1.78529 \text{ \AA}$; I = 11 mA; U = 37 kV. Correction made according to combined graph of KCl and chlorite. Exposure time 25 hours. Intensity on the ten-point scale.

* The roentgenostructural analysis was made in the roentgenostructural analysis laboratory of IG and G SO AN SSSR.

Tilleyite -- $\text{Ca}_5\text{Si}_2\text{O}_7 \cdot (\text{SO}_3)_2$. Mono-

clinical system. Mineral first found in the Soviet Union [44].

In addition to the contact zones of the Anakit massif, tilleyite was established in a few other points around the world, to wit, Crestmore, California, by Larsen and Dunham [76]; Iron Mountains, New Mexico by Glass, Jahns, and Stevens [68]; Carlingford, Ireland by Nockolds [82]; and in Camas Mor, the Island of Muck, Scotland, by Prof. Tilley [91].

Tilleyite grains are not over 1 - 2 mm in size, but they occasionally reach 8-9 mm. For the most part the grains are irregular or coarsely isometric with a glassy luster on excellently expressed cleavage planes.

The mineral is transparent in thin fragments and reacts violently to muriatic acid. It has a specific gravity of 2.9 (this figure is probably high because tilleyite had a

slight admixture of spurrite), and a hardness of 5. The tilleyite content is usually quite small (0.5 - 1%), but in some instances it reaches 50 - 60% by volume.

It should be mentioned that macroscopically tilleyite is difficult to distinguish from the other silicates which accompany it, such as spurrite, merwinite, and melilite. Characteristic of it is the presence of several directions of well expressed cleavages.

In its optical properties tilleyite is similar to the mineral described by Nickolds [82] and Tilley [91]. It has three systems of cleavage cracks. The first distinctive cleavage (perfect cleavage according to Nickolds [82]) is parallel to (100) if we accept the orientation of tilleyite by Larsen and Dunham [76]. It forms an angle of 12° with the Ng axis and an angle of 54° with the other clearly expressed cleavage ("clear" cleavage [82]). This second cleavage is also a twin plane of coalescence.

The twins are laminated, simple, and rarely polysynthetic; the twinning is along the edge and axis. The nature of the polysynthetic twinning is different than in spurrite, the twins are not repeated as frequently and not with the strict regularity as in spurrite. The twin plane is parallel (101) and perpendicular (010) to the visual axis plane. In the section normal to Nm and parallel to (010) symmetrical extinction equal to 24° (angle between the axis Np and twin seam) is characteristic of a twinned crystal. The third cleavage is less clear. It is parallel to (010) (the "poor" cleavage according to Nickolds [82]). The fourth cleavage ("very poor" [82]), is perpendicular (010) was manifested in Anakit tilleyite. The Ng and Np axes lie in the (010) plane, and the Nm axis coincides with the second crystallographic axis.

The direction of the optical indicatrix of tilleyite with respect to the poles of the cleavage plane after determination on the Fedor universal stage was as follows:

Cleavage along (100) ("perfect")	Cleavage along (101) ("clear"), twin plane of coalescence	Cleavage along (010) ("poor")
$N_g=78^\circ$ $N_m=90^\circ$ $N_p=12^\circ$	$N_g=24^\circ$ $N_m=90^\circ$ $N_p=66^\circ$	$N_g=90^\circ$ $N_m=0^\circ$ $N_p=90^\circ$



Fig. 8. Spurrite-tilleyite aggregate. Relict poikilitic ingrowths of spurrite included in large irregular grains of tilleyite (light). Nicolite intertwined. Mag. 32.

The angle of optical axes of the mineral are very large, positive; $2V = 88^\circ$, $r < v$. Indexes of refraction: $N_g = 1.653 \pm 0.002$, $N_m = 1.634 \pm 0.002$; $N_p = 1.611 \pm 0.002$; $N_g - N_p = 0.042$. These data agree well with the determinations made by all investigators studying this rare silicate of calcium. According to Larsen and Dunham $N_g = 1.652$, $N_m = 1.635$; $N_p = 1.617$ (all ± 0.003); $2V = 90^\circ$ [76]. According to Glass, Jahns and Stevens $N_g = 1.651$; $N_m = 1.635$; $N_p = 1.616$; $r < v$ [68]. According to Nickolds $N_g = 1.653$; $N_m = 1.632$; $N_p = 1.612$ (all ± 0.003); $2V = +87^\circ$ [91]. Harker's determination who cited the research data on tilleyite from Carlingford ($N_g = 1.656$, $N_m = 1.632$, $N_p = 1.599$) raises doubt [71].

Tilleyite ordinarily develops from spurrite and is a later mineral phase. Oftentimes it forms borders and margins around the spurrite grain, appearing on the boundary between the spurrite and calcite. The resorbed crystals of spurrite not infrequently are included in this as nuclei in circular fused grains of tilleyite (Fig. 8). The large crystals of tilleyite (8-9 mm in cross section) may contain a multiplicity of poikilitic inclusions of spurrite, and in that case tilleyite plays an important part as a cementing tissue for spurrite grains. Oftentimes in tilleyite one can observe irregular relict inclusions of calcite and melilite.

Tilleyite disintegrates rather easily and is replaced by a number of later, lower temperature minerals, particularly columnar, hydrothermal wollastonite, as well as hillebrandite and other hydrosilicates of calcium.

The presence of tilleyite in the Anakit contact zone could be expected, on the basis of the analysis made here, under conditions of low pressures and high temperatures of a mineral association of larnite-merwinite-spurrite subspecies of contact metamorphism. Harker, in an article devoted to the problem of the formation of tilleyite, expressed the idea that in the Lower Tunguska River area tilleyite should be present not only on the strength of the appearance here of spurrite-merwinite rocks, but also as a consequence of the presence in the association observed of silica and fluorine-containing minerals, cuspidine and melilite [71, 72]. He confirms his own conclusions by data from a paragenetic analysis of natural associations of minerals and an artificial synthesis of tilleyite in the presence of traces of Al_2O_3 and CaF_2 . It should be noted, however, that cuspidine very clearly develops, in our instance, after tilleyite, replacing it. Hence, fluorine along with certain other components is added to the contact marbles after the formation of tilleyite. Our attention is invited to the following peculiarity: tilleyite in its formation

distinctly gravitates to the boundaries between spurrite and calcium (Fig. 9), and is the product of the reaction between them (or between spurrite and CO_2) with a drop in temperature.

Given in Table 6 are the interplanar distances of tilleyite determined roentgenoscopically.

Wollastonite -- CaSiO_3 . As we remarked previously, wollastonite forms thin, crystalline, dense concentration of isolations (wollastonite "nuclei") in the spurrite-merwinite-melilite sections of contact-metamorphic marl rocks (Figs. 10, 11).

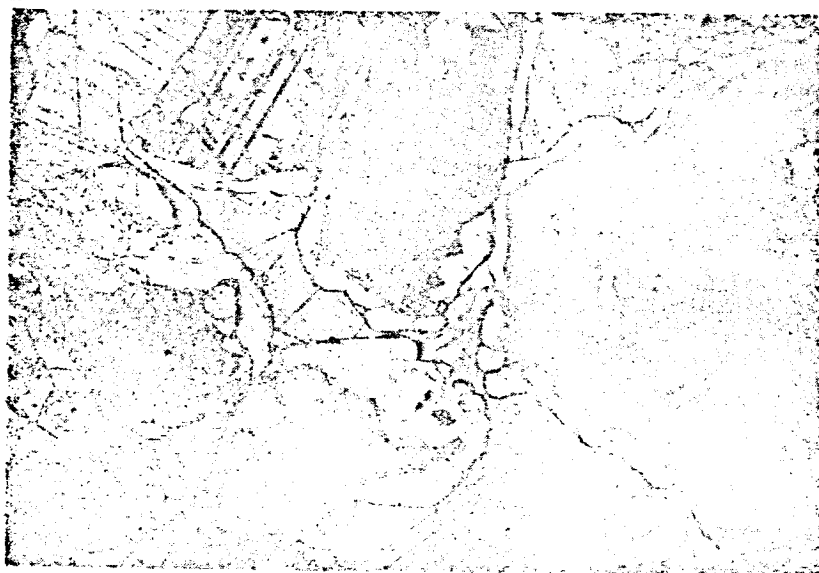


Fig. 9. Borders of tilleyite (light) about polysynthetic twinned grains of spurrite. Main background is calcite (gray). Nicoli inter-twined. Mag. 32.

The dimension of individual grains of wollastonite is not over 2-3 mm. Color: white, rose, or light gray with yellowish tint. Grain prismatic or more often tablet-shaped along (100), usually somewhat elongated. Glassy luster, hardness 5, specific gravity 2.8.

Two cleavages distinctly manifested in the mineral: the perfect cleavage along (100) and median cleavage along (001).

Table 6
Results of Roentgenostructural Analysis of Tilleyite

l	$\frac{d}{n}$	l	$\frac{d}{n}$
2	7.474	2	1.825
1	5.988	1	1.800
2	3.448	2	1.752
3	3.328	1	1.710
5	3.172	1	1.664
6	3.091	7	1.614
10	2.999	2	1.537
6	2.789	1	1.509
2	2.528	2	1.432
6	2.488	2	1.376
1	2.334	2	1.361
1	2.254	3	1.257
5	2.086	2	1.212
3	1.926	2	1.175
2	1.906	2	1.150
5	1.892	4	1.107

Photo conditions: Co = anticathode; D = 57.3 mm; λ = 1.78529 kX; I = 11 mA; U = 37 kV. Correction made according to combined graph of KCl and chlorite. Exposure time 25 hours. Intensity according to the ten-point scale.

* Roentgenostructural analysis made in the Institute of Geology and Geography, USSR Academy of Sciences.

planes of coalescence is as follows:

Cleavage along (100) Twinned Plane of Coalescence

$Ng=32^\circ$

$Nm=90^\circ$

$Np=58^\circ$

Cleavage along (001) Twinned Plane of Coalescence

$Ng=52^\circ$

$Nm=90^\circ$

$Np=38^\circ$

The indexes of refraction of the mineral are: $Ng = 1.635 \pm 0.003$, $Np = 1.623 \pm 0.003$. $2V = -39^\circ$, $r > v$.

The results of a chemical analysis of a monomineral fraction of wollastonite are as follows: $SiO_2 = 49.12\%$, $TiO = 0.07\%$, $Al_2O_3 = 0.04\%$, $FeO = \text{none}$, $Fe_2O_3 = 0.13\%$, $MnO = 0.04\%$, $MgO = 0.37\%$, $CaO = 48.31\%$, $Na_2O = \text{none}$, $K_2O = 0.06\%$, $H_2O = 0.06\%$, other = 1.07%. Total -- 99.63% (in percentile weight)¹; in

1) The chemical analysis was made in the chemical-analytical laboratory at the Institute of Geology and Geophysics, Academy of Sciences, USSR.

Polysynthetic twinning parallel to elongation widely distributed. The number of twinning lamellae does not exceed 3 or 4. The first pinacoid serves as the intergrowth plane. In individual, comparatively rare cases twinning occurs along (001). The twinning is on the facets. The plane of optical axes forms an angle of 4° with the second crystallographic axis and lies in the (010) plane. The Np axis forms an angle of 32° with the third crystallographic axis.

The orientation of the optical indicatrix of wollastonite relative to the cleavage poles and twinned

general this corresponds rather closely to the theoretical formula for the mineral CaSiO_3 .

Wollastonite from concentric isolations is usually quite pure and forms virtually monomineral aggregates. Sometimes admixtures of tridymite and graphite (cf. above) as well as small flakes of hematite in amounts under one percent are observed.

Given in Table 7 are the interplanar distances of wollastonite.

Melilite -- $(\text{Ca}, \text{Na})_2(\text{Mg}, \text{Al})(\text{Si}, \text{Al})_2\text{O}_7$. Tetragonal system. Mineral forms round or short prismatic, fine crystals (up to 1 mm), associated with merwinite, spurrite and tilleyite. It is ordinarily found as an inclusion in merwinite and in spurrite. Rarely forms independent accumulations. Colorless mineral with an unclear cleavage along third pinacoid. Glassy luster, hardness 5, specific gravity 2.9-3.0.

Insofar as its optical properties are concerned, the mineral is essentially an akermanite-melilite. The indexes of refraction are: N_m (high index of refraction) = $1.650-1.645 \pm 0.003$, N_p (lower index of refraction) = $1.647-1.641 \pm 0.003$. $N_m - N_p = 0.001 - 0.005$. Single axis. Sign of elongation positive or negative. Characteristic of the mineral grains is a blue-violet or blue anomalous interferential color.

From these data it follows that the optical properties of melilite are characterized by a high order of variation. Irregularity in properties occurs even within the limits of the individual grain and is expressed most clearly in the case of zonal crystals of melilite. Usually in this case the central portion of the grain is practically isotropic and has the following indexes of refraction: $N_m = 1.648-1.647 \pm 0.003$, $N_p = 1.647-1.646 \pm 0.003$. The border portions have double refraction of the order of $0.004 - 0.005$ and the following indexes of refraction: $N_m = 1.646-1.645 \pm 0.003$, $N_p = 1.643-1.641 \pm 0.003$.

Making use of data by I. R. Goldschmidt [9] and Trager [58] to obtain information about the chemical composition of melilite we can conclude that the central portions of such zonal grains of melilite are richer in molecular helenite (up to 40% of helenite) than the border grains, which contain up to 80% and more of akermanite.

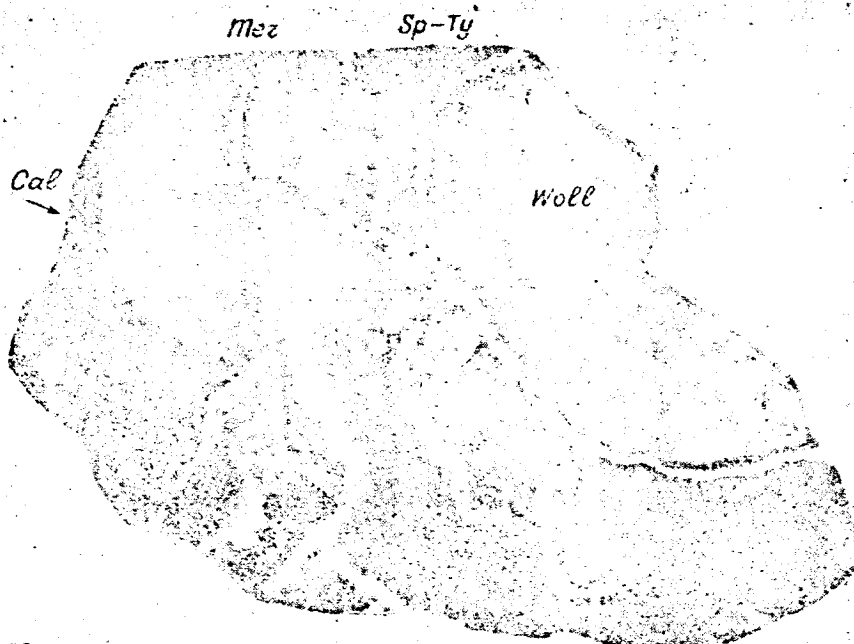


Fig. 10. Wollastonite pseudomorphosis (Woll.) through a silicillite concentration (central light nucleus) surrounded by concentric borders of cuspidine and garnets (thin fringes around the wollastonite nucleus; cuspidine - white, garnet-dark), tilleyite and spurrite (Ty. - Sp.) and merwinite (Mer.) in fine grained marble (Cal.). Polished lump of ore. Natural size.

Variations in the optical properties of various crystals of melilite are explained by the same reason, i.e., a considerable change in the chemical properties of the minerals. These variations occur even in comparatively small volumes of the rock (within the limits of one section) and are a characteristic feature of Anakit melilite. One other characteristic feature should be mentioned: in association with spurrite, melilite usually contains somewhat more helenite (compared with median composition).

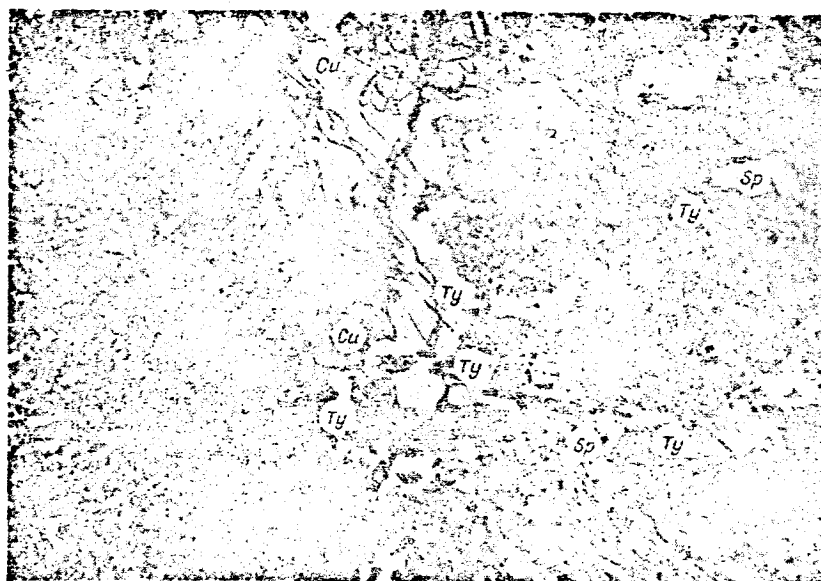


Fig. 11. Details of wollastonite pseudomorphosis along silicilite concretion. Fine grained material on left of microphotograph -- wollastonite aggregate surrounded by a margin of cuspidine (Cu). Ty - Tilleyite, Sp - spurrite. Nicoli crossed. Mag. 32.

Table 7

Results of Roentgenostructural Analysis of Wollastonite*

I	$\frac{d}{n}$	I	$\frac{d}{n}$
5	3.83	4	1.749
5	3.51	7	1.709
8	3.30	7	1.595
4	3.08	3	1.527
10	2.96	6	1.472
1	2.79	6	1.456
3	2.70	6	1.355
3	2.53	2	1.340
3	2.46	4	1.262
5	2.32	2	1.237
5	2.28	2	1.209
6	2.16	5	1.172
3	2.008	2	1.142
3	1.974	2	1.104
2	1.874	4	1.089
3	1.823	4	1.030

Photo conditions: Co - anticathode; D = 75.3 mm; λ = 1.78529 kX; I = 11 mA; U = 37 kV. Exposure time 25 hours. Radiation filtered. Correction made according to combined KCl and chlorite graph. Intensity by the ten-point scale.

* Roentgenostructural analysis made in roentgenostructural analysis laboratory of the IG and G SO AN SSSR.

Table 8

Results of Roentgenostructural Analysis of Melilite*

I	$\frac{d}{n}$	I	$\frac{d}{n}$
2	4.22	3	2.040
4	3.72	3	1.967
2	3.42	4	1.856
5	3.09	2	1.812
10	2.832	9	1.753
2	2.442	2	1.670
6	2.398	3	1.510
6	2.296	3	1.472
2	2.195	6	1.430
4	2.145	3	1.405
		5	1.378

Photo conditions: Cu - anticathode; D = 57.3 mm; λ = 1.53739 kX; I = 16 mA; U = 37 kV. Exposure time 20 hours. Radiation filtered. Correction made according to combined KCl and chlorite graph. Intensity according to the ten-point scale.

* Roentgenostructural analysis made in roentgenostructural analysis laboratory of the IG and G SO AN SSSR.

The interplanar distances of melillite, containing about 70% akermanite, are given in Table 8.

Table 9

Results of Roentgenostructural Analysis of Pyrrhotite*

Hexagonal Modification		Monoclinic Modification	
<i>I</i>	$\frac{d}{n}^{\circ}$	<i>I</i>	$\frac{d}{n}^{\circ}$
6	2,97	—	—
9	2,63	—	—
1	2,50	—	—
1	2,26	—	—
10	2,07 m	10	2,07 m
—	—	4	2,05
9	1,70 —	9	1,70 m
6	1,62	—	—
—	—	4	1,59 m
—	—	3	1,48
—	—	4	1,45
4	1,43 m	4	1,43 m
—	—	2	1,41
6	1,32 m	6	1,32 m
—	—	6	1,31
—	—	2	1,29 m
4	1,179 m	4	1,179 m

Photo conditions: Co - anticathode; $d = 57.3$ mm; $\lambda = 1.78529$ kX; $I = 11$ mA; $U = 37$ kV. Exposure time, 13 hours. Radiation filtered. Correction according to combine graph of KCl and chlorite. Intensity according to ten-point scale.

* Roentgenostructural analysis made in the roentgenostructural analysis laboratory of the IG and G SO AN SSSR.

merwinite, tilleyite, calcite and others. Dimensions of grains vary from 2 to 3 mm and less. Color is bronze-yellow, black streaks, metallic luster, hardness 4, specific gravity 3.6. Discloses imperfect cleavage. In the polished

Usually encountered in small amounts among the above-described silicate minerals are sulphides of copper and iron -- pyrrhotite, chalcopyrite and graphite. These minerals are rather broadly distributed, especially pyrrhotite. However, as small impregnations in the silicates and in calcite, they constitute a small part of the total volume of the rock (not over 3% by volume).

Graphite - C. The mineral forms a thin, flaky aggregate in association with tridymite (cf. above). The size of these mineral associations rarely exceeds several hundredths of a millimeter. Color of graphite is steely-black, dull luster, hardness 1, has pronounced double reflection and distinct anisotrophy.

Pyrrhotite - Fe_{1-x}S . In the contact zone of the Anakit massif the mineral is a mixture of two modifications: hexagonal and monoclinic. Pyrrhotite does not form separate crystals; it is observed in the form of fine impregnations of grains of irregular form or aggregates of several grains. It is associated with spurrite,

sections it has strong anisotropy and yellow-rose coloration. When scoured in HF vapors weakly expressed, sharply-angular laminations are exposed in individual grains or in portions of grains; this is developed in two mutually perpendicular directions.

The interplanar distances of pyrrhotite, represented by a combination of monoclinic and hexagonal modifications, are given in Table 9.

The interplanar distances of the monoclinic modification agree rather well with the data quoted by E. N. Yeliseyev on the monoclinic pyrrhotites of the USSR. Likewise very characteristic is the cleavage of lines on debayegrams of Anakit pyrrhotites, a fact which might indicate the presence of monoclinic modifications (8 - pyrrhotite) [12].

Spectral analysis shows the presence in pyrrhotite of Ni, Co, Cu, Ga in the amount of 0.3 - 0.001%¹⁾.

Chalcopyrite - CuFeS_2 . The mineral forms small, irregular growths or aggregates of individual grains whose dimension rarely exceeds 1 mm. The color is brass yellow, black and green streaks, metallic luster, hardness 3, very brittle. The presence of chalcopyrite in marbles of the contact zone of the massif is supported by data obtained from spectral analysis²⁾ of the monomineral fractions of this mineral; it showed the presence of large amounts of copper, iron, and sulphur. Also present, but in small quantities, were Co, Ni, V and other elements. Chalcopyrite is extensively associated with the same minerals as pyrrhotite. Occurs very commonly.

Structural Relationships of Minerals

The internal structure of calcium silicate isolations in marbles is very interesting. Two groups of such isolations stand out rather clearly insofar as structural peculiarities are concerned: with the central wollastonite "nucleus" and without the wollastonite "nucleus".

1) Spectral analysis made in the spectral analysis room of IG and G SO AN SSSR.

2) Spectral analysis made in the spectral analysis room of IG and G SO AN SSSR.

Isolations without the central wollastonite nucleus having, as we already mentioned, laminated, irregular lens-shaped, nodular or veined appearance are usually made up, in the interior portions, of merwinite, which forms coarsely isometric, tablet-shaped or irregular polysynthetic twinned grains, not infrequently with sinuous boundaries. Merwinite always contains numerous poikilitic ingrowths of prismatic and circular grains of melilite. The peripheral parts of the isolations consist of elongated tablet-like or irregular polysynthetic twinned grains of spurrite, which also contain inclusions of melilite but in smaller quantity. Merwinite apparently forms somewhat later than does spurrite and melilite because the latter are sometimes attacked by merwinite with partial replacement and form resorbed poikilitic ingrowths in it. Worthy of attention is the fact that the content of melilite increases from the edge portions of the isolations toward the center, i.e., the amount of it increases in associations with merwinite. Another characteristic is that in associations with merwinite melilite contains a large amount of akermanite molecules (cf. above). Sometimes, melilite forms virtually a monomineral accumulation inside the essentially merwinite section of the rock (cf. Fig. 12). All of the above listed minerals contain ingrowths of pyrrhotite [and chalcopyrite], which are more or less uniformly scattered throughout the rock, and they are encountered also in isolations of calcic silicates and in marble.

Here and there spurrite is replaced by tilleyite which forms large porphyroblasts or reactional borders appearing on the boundary between spurrite and calcite (cf. Fig. 9).

Isolations with a central wollastonite nucleus have quite a different structure. Thin-crystalline wollastonite nuclei are surrounded by concentric rims of tablet-like grains of spurrite, radially orientated to the boundaries of the nuclei. The peripheral part of the rim is made up of tablet-like small

grains of merwinite. Tied in spatially with spurrite and merwinite is melilite which forms poikilitic inclusions; its amount in this case is also not a constant quantity; it increases in associations with merwinite. Pyrrhotite is also universally present. In the internal portions of the rims and directly in contact with the wollastonite nuclei, spurrite not infrequently is intensively replaced by tilleyite which forms comparatively large (up to 1 cm in cross section) coarsely isometric porphyroblasts rich in relict, resorbed grains of spurrite (cf. Fig. 8).

The details of the internal structure of the isolations are clearly revealed on the exposed surface of marble. On exposure, calcite, spurrite, and tilleyite disintegrate more readily than merwinite and wollastonite, and in their place there are formed pits in the marble. The spurrite and tilleyite are covered over with a white, floury deposit and they stand out clearly against the background of gray, medium grained marble. The merwinite forms dark protrusions, borders and rims, while wollastonite portions -- of the nucleus -- form white or rose colored concentric projections inside the spurrite (cf. Fig. 5).

Table 10

Results of Chemical Analysis of Contact-Metamorphic Rocks
(percentile weight)*

	SiO ₂	TiO ₂	Al ₂ O ₃	FeO	Fe ₂ O ₃	MnO	MgO	CaO	Na ₂ O	K ₂ O	H ₂ O	Other	Total
Spurrite rock	25.55	0.07	0.8	0.68	1.44	0.02	2.60	57.56	Her	Her	0.14	10.19	99.05
Spurrite rock	25.08	0.05	1.27	0.79	0.42	0.03	2.59	56.33	Her	Her	0.16	12.71	99.43
Merwinite-mel- itite rock	28.70	0.25	5.08	1.02	0.94	0.08	5.84	50.10	Her	0.06	0.14	7.55	99.76

[HET = None]

* Chemical analysis made in the chemical-analytical laboratory of IG and G SO AN USSR.

The chemical composition of certain types of contact-metamorphic rocks is illustrated in Table 10. In all of the analyzed rocks there was a certain admixture of melilite, calcite, tilleyite, cuspidine, pyrrhotite and other.

Metamorphism of Dolomitic Marls

In the western contact zone of the asymmetric apophysis of the Anakit intrusion there is an extensive development -- as is the case also in the eastern contact zone -- of marbles containing spurrite, merwinite, tilleyite, melilite and other. They have approximately the same structural-textural peculiarities as the previously described metamorphic rocks. However, in the marbles of the western zone there are layers, lentils, and thin horizons of monticellite-melilite and monticellite rocks, in which monticellite and melilite or monticellite alone are the basic components of marble apart from calcite (Fig. 12). Apparently, these rocks were formed in the contact metamorphism of dolomitic marls or silicious dolomites forming thin layers in the part of the Kochumdeks formation.

Rocks of the western contact zone have a mottled appearance due to the dark gray to black color of silicate isolations on a light gray background of medium to fine grained calcite marble. Silicate isolations (spurrite-merwinite-tilleyite-melilite) that are striated, lens-shaped, nodular or veined in appearance are grouped together in a definite horizon, forming a coarsely striated texture similar to the one described in the previous chapter. Monticellite-melilite and monticellite marbles are light gray in appearance and differ little macroscopically from pure calcite marble. They form layers 20 - 50 cm in thickness in the coarsely striated, essentially spurrite-melilite-merwinite rocks. The overall trend of layers coincides with the strike of unchanged marls beyond the limits of the aureole of contact metamorphism of the trappean massif. The thickness of the western contact zone is 12-13 m.

Given in the following are the characteristics of monticellite and melilite -- the main silicate minerals of marble formed from the metamorphism of dolomite marls and siliceous dolomites.

Monticellite -- CaMgSiO_4 . This mineral forms fine, scattered irregular grains or coarse prismatic crystals (Fig. 13). The grains are colorless or dull gray colored and are rarely larger in size than 0.5 mm. The mineral has a glassy luster, hardness 5. Imperfect cleavage is observed along (010). The plane of the optical axes is parallel to (001), axis N_p coincides with [010]. Orientation of pole of cleavage of monticellite relative to optical indicatrix following determination on the Fedorov universal stage proved to be as follows:

Cleavage along (010)

$$\begin{aligned} N_g &= 90^\circ \\ N_m &= 90^\circ \\ N_p &= 0^\circ \end{aligned}$$

The angle of optical axes of the mineral is 75° , negative. Indexes of refraction are as follows: $N_g = 1.661 \pm 0.003$, $N_p = 1.649 \pm 0.003$, $N_g - N_p = 0.012$.



Fig. 12. Melilite-monticellite rock. The melilite forms short, prismatic crystals in the calcite. Monticellite (Mont) in the shape of irregular grains. Crossed nicoli. Mag. 32.

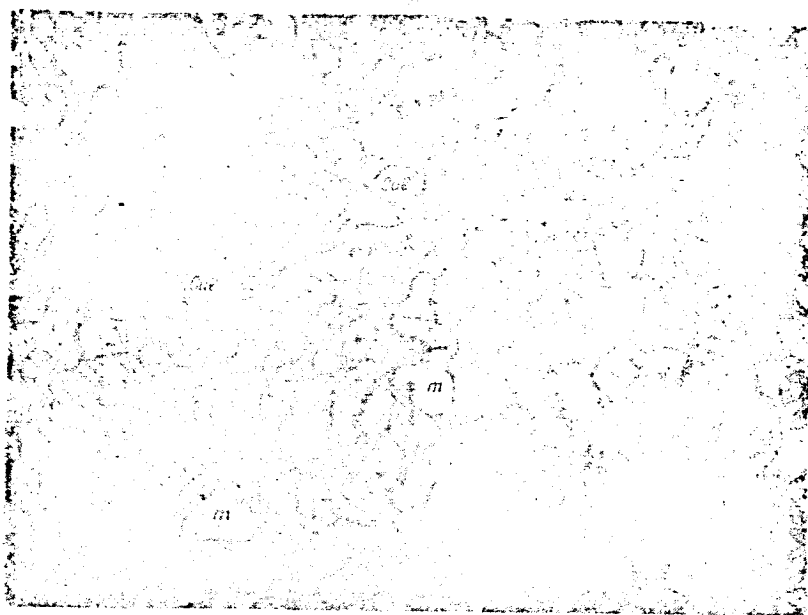


Fig. 13. Irregular grains of monticellite (M) in associations with melilite (dark short prismatic crystals) and calcite (Cal). Nicoli crossed. Mag. 32.

The amount of monticellite in monticellite marble is usually not great and does not exceed 25 - 30%, more often - 10-15%. It associates spatially with melilite (almost pure akermanite) and occasionally mostly irregular shaped grains of merwinite. Monticellite is partially replaced (and sometimes entirely) by irregular or tablet shaped, polysynthetic twinned grains of merwinite. Sometimes, one can observe resorbed grains of monticellite included as poikilitic ingrowths in the irregular grains of merwinite. Tilleyite, pyrrhotite and other grains occur at random in this association.

The interplanar distances of monticellite, reontgenoscopically determined, are given in Table 11.

Melilite (mineral closely related to akermanite) -- $(Ca, Na)_2(Mg, Al)_2(Si, Al)_2O_7$. Tetragonal system. Mineral forms short-columnar, isometric or irregular grains (cf. Figs. 12, 13), usually closely associated with monticellite and merwinite if the latter is present. Dimension of individual grains 2-3 mm in cross-section. Color of mineral gray-white, dull gray. Mineral

semi-transparent, glassy luster, Hardness 5.

Cleavage manifested clearly along (001). This mineral differs from the previously described melilite observed in associations with spurrite, merwinite, tilleyite and others by a somewhat lower index of refraction and somewhat higher double refraction: Nm (greater index of refraction) = 1.643 ± 0.003 , Np (lesser index of refraction) = 1.638 ± 0.003 , Nm-Np = 0.005. Sign of elongation negative.

The mineral is usually characterized by a uniform structure. Zoning absent. If present, merwinite sometimes partially disintegrates the melilite grains. In its optical properties, the mineral is classed as melilite with a high content of akermanite molecules [58], containing helenite, not exceeding 15%. Thus, in associations with monticellite, melilite contains somewhat less helenite molecules than in associations with spurrite, merwinite, tilleyite and other minerals formed in the metamorphism of essentially calcareous marls.

Pyrrhotites are encountered as insignificant admixtures in monticellite and monticellite-melilite marbles.

Structural Relationships of Minerals

In composition, as in its structural characteristics, isolations of calcium silicates (spurrite, merwinite, tilleyite and others) found in the marbles of the western contact zone near the asymmetrical apophysis of the Anakit massif are very similar to the same kind of isolations found in the marbles of the eastern zone. The obvious difference in these isolations (of the western exocontact apophysis) is the absence of wollastonite "nuclei" surrounded by radially-orientated, tablet-shaped grains of spurrite which are rather commonly distributed in the marbles of the eastern contact zone (cf. above). Another peculiarity is the somewhat more widespread development, compared with the eastern contact, of tilleyite which forms large porphyroblasts

or reactional rims. We should also note the abundance of varied secondary minerals, mainly products of hydrothermal activity, which replace the mineral complexes of the metamorphic stage. A detailed account of the relationships of monticellite and melilite to other minerals was given previously in discussing their characteristics. Calcite, monticellite, and merwinite are not encountered together with spurrite.

Table 11

Results of Roentgenostructural Analysis of Monticellite*

<i>h</i>	$\frac{d}{a}$	<i>h</i>	$\frac{d}{a}$
3	4.16	1	1.539
4	3.62	3	1.498
2	3.14	2	1.425
3	3.08	5	1.386
6	2.88	2	1.350
10	2.65	1	1.222
5	2.57	1	1.270
4	2.38	3	1.204
8	1.810	3	1.157
3	1.761	1	1.123
3	1.714	1	1.112
6	1.590		

Photo conditions: Mo - anticathode; D = 57.3 mm; $\lambda = 1.542$ kX; I = 6 mA; U = 30 kV. Radiation filtered. Exposure time 5 hours. Intensity according to the 10-point scale.

* Roentgenostructural analysis made in the roentgenostructural laboratory of Tomsk State University.

Metamorphism from Calcareous, Limestone-

Dolomitic, and Dolomitic Aleurolites and

Sandstones

The sandstones and calcareous, limestone-dolomite or dolomitic sandstones gradually changing over to sandstone, sub-dolomitic limestones, as well as calcareous, limestone-dolomitic and dolomitic aleurolites, argillites and marls with thin layers of practically pure argillites, containing virtually no admixtures of carbonates occur in the central portion of the Anakit cupola upheaval; it is of the upper Ordovician period (O_3 dl). Such sandstones and aleurolites with layers of argillites make up the eastern portion of the bloc of Silurian and Ordovician rocks, separated from the remaining sedimentary layers by a number of tectonic disturbances through which the traps in-

truded later on (cf. above). The western part of this block, as we have already indicated, is made up of striated marls of the Kochumdeks formation (S_1 ktch) (cf. Fig. 4). The rocks in this block were metamorphosed in the

contact zone of the Anakit massif which were converted into varied striated hornfels. Although the visible thickness of Ordovician deposits, which make up the eastern portion of the block, vary from 60 to 65 meters (the overall thickness-width of the block amounts to 100 meters), nevertheless all these rock are deeply metamorphosed and ordinarily do not contain relict minerals. This is apparently explained by the abundance of trappean (dike-like) apophyses which contact the block not only on the eastern and western tips but also penetrate into the internal portion intruding as varied veined and irregular bodies mutually ties in with one another and with the Anakit massif. One of the peculiarities of the traps which penetrated into the block is the abundance of various kinds of xenolites of enclosing hornfels. Their dimensions vary within broad limits: from parts of a centimeter to several meters. Usually associated with them are hybrid formations represented by shonkinite, pyroxene-feldspar rocks and various hybrid dolerites. These rocks, closely tied in spatially with the dolerite-pegmatites, ferrogabbros, dolerites and granophyres, are formed in accumulations of hornfels magma which appeared as a result of metamorphism of deposits of the Dolborskaya formation. The composition of the hybrid rocks is somewhat related to that of the assimilated hornfels. For example, the assimilation of potassium from hornfels containing phlogopyte and sandinite exerted an influence on the formation of hybrid shonkinites, although the main portion of K_2O is probably of magmatic origin. The increased content of CaO in hybrid shonkinites and pyroxene-feldspar hybrid rocks with which the shonkinites are tied by mutual transitions is explained by the assimilation of the magma of wollastonite, wollastonite-pyroxenite, pyroxenite-plagioclase and other hornfels.

Hornfels rocks making up the eastern part of the block of the Paleozoic rock mass are observed in the form of numerous platform bedrocks on the right bank of the Lower Tunguska River about 100 meters below the mouth of Vostochnyy

Creek (cf. Fig. 4). The total area taken up by the hornfels is $3,500 \text{ m}^2$. A large portion of the bedrock hornfels, as is true of the spurrite-merwinite marbles, is located in the flood plain of the Lower Tunguska River, and are therefore completely flooded during high water.

Hornfels are very typical rocks and can be seen some distance away because of the beautifully expressed striated texture manifested in a contrasted combination of alternating light and dark bands. Hornfels, as a rule, are broken up by several (3-4) systems of parting joints which, incidentally, have the same elements of occurrence or bedding as the parting joints of traps. Because of the well expressed horizontal and vertical systems of cleavage the outcroppings of hornfels are step-like in character, a fact which makes it possible to expose in all its details the textural peculiarities of these rocks.

The hornfels in the main mass are dense, fine-grained and brittle rocks with striated formation. The colors vary, changing from white, whitish-gray or yellowish to dark gray, black or brownish-red. The nature of the coloration is governed by the mineral composition of the rocks. The plagioclase, wollastonite, wollastonite-plagioclase, plagioclase-diopside and other hornfels are usually of a whitish color, whereas rocks in which the pyroxene contains a considerable admixture of hedenbergite are usually darker or black in color. Hornfels containing phlogopyte are characterized by a brownish-red or a brownish-cherry red coloration.

Striation in the rock is very clearly expressed and conforms with the strike and pitch of the metamorphosed Silurian-Ordovician deposits within this enclosing rock mass block (separated from the substratum by disjunctions). The striations stand out clearly because of the nature and intensity of colorations which have marked boundaries. The structure within the limits of the different bands does not change substantially, remaining fine grained (down to

micrograined). The striated structure of hornfels rocks is due to the clearly expressed, sometimes rhythmic, alternation of thin horizons, layers, lenses, irregular linearly extended isolations, spots and the like, varying in composition. The thickness of individual bands changes from fractions of a centimeter to one or more meters, although the predominating width of the bands is within the interval of 10 - 30 cm (Fig. 14). Sometimes within the band one can observe very fine lenses (2-4 mm) and chains of small lenses, as well as thin layers of some other composition than the hornfels which inclose them, and these are oriented in strict conformance with the strike of the overall striation of metamorphic rocks. Mottled textures are extensively developed among the phlogopite-containing rocks.



Fig. 14. Surface erosion of striated hornfels. Right bank of the Lower Tunguska River.

Two types of hornfels stand out rather clearly insofar as mineral composition is concerned. The first of these are the hornfels containing sanidine, phlogopite, quartz (or tridymite), diopside with an admixture of basic plagioclase, andalusite, pyrrhotite and others. Included among the second type are

hornfels containing pyroxene (a number of diopside-hedenbergites), wollastonite, plagioclase, quartz (or tridymite), with an admixture of calcite, pyrrhotite and magnetite. The first kind of hornfels are distributed, mainly, in the eastern part of the block of the Paleozoic deposit, whereas the hornfels of the second type make up the central part of the block, and are directly on the boundary with the metamorphosed marls (cf. Fig. 4). Among the hornfels of the first type we find interbeds of the second type of hornfels and vice versa; however, the tendency noted above is expressed rather distinctly.

In the following we present the characteristics of the basic silicate minerals that make up the hornfels.

Quartz, tridymite -- SiO_2 . Quartz in hornfels is encountered in the form of individual, irregular grains or aggregates of grains whose dimensions change from fractions of an inch to 2-3 mm. The grains are usually chunklike in appearance, being angular, semiangular or rounded forms; they are relict, terrigenous materials of primary sedimentary rocks. Quartz has a glassy luster and is transparent. Cleavages absent, hardness 7. Optical properties: optically positive, single axis; indexes of refraction: $N_g = 1.553 \pm 0.003$, $N_m = 1.544 \pm 0.003$. Roentgenostructural analysis of the mineral showed a Debayegram identical to a - quartz¹⁾.

In the process of metamorphism, quartz usually undergoes a number of changes. It is characterized by a wavy extinction or disintegrates into blocks having a varied optical orientation. The boundaries of such blocks inside the grain of quartz are uneven, sinuous, and often serrate. Aggregates of quartz grains are converted into a microgranoblastic mass in which the primary fragments lose their contours, acquiring dentate boundaries at

1) The roentgenostructural analysis was made in the roentgenostructural analysis laboratory of the IG and G SO AN SSSR.

junctions with one another. In direct contact with the intrusive traps the grains undergo partial rheomorphic fusion, becoming altered into a glass-like, amorphous material. In this, apparently there is simultaneous fusion of the clayey materials in the sandstones and aleurolites containing quartz fragments.

It should be mentioned that the small (less than 0.1 mm) quartz grains in hornfels are encountered rather rarely. Those individual grains or their aggregates, which are preserved in the metamorphosed rocks, appear varied to the unaided eye. This is apparently explained by the fact that the smaller grains of quartz cannot exist in hornfels as relict mineral phases reacting with the surrounding carbonate-clay substances in the process of metamorphism.

In the most common instance the aggregates of quartz grains form small lens-shaped isolations arranged in conformance with the banding of the hornfels and are concentrated into chains. The dimension of the lens is up to 1 cm in length and 1-3 mm in width. Sometimes one finds larger sections of irregular or lens-shaped forms with dimensions up to 3-4 cm. Ordinarily, quartz in such isolations has a granoblast-dentate structure, although now and then fragmented forms of the grain are clearly preserved. In associations with quartz, we find wollastonite, diopside, plagioclase, phlogopite, sanidine, andalusite and others. Sometimes relict calcite is observed together with wollastonite and quartz; it serves as the cementing material for the terrigenous fraction in the non-metamorphosed rocks.

Tridymite in hornfels is found very rarely in the form of a thin, scaly fringe on the fragmentary grains of quartz or in independent microcrystalline aggregates in associations with wollastonite. Tridymite is easily distinguished by its optical properties -- low double refraction and its indexes of refraction: $N_g = 1.475 \pm 0.003$; $N_p = 1.471 \pm 0.003$; $N_g - N_p = 0.004$. The mineral has a straight extinction in tabular grains and negative elongation. The dimension

of individual scale-platelets of tridymite is not great and never exceeds a few hundredths of a millimeter. In the platelets one can sometimes observe circular inclusions of wollastonite. In general, laminated crystals of tridymite are found rather infrequently; more often the mineral forms growths of fine, coarsely isometric and irregular grains with sinuous outlines.

Andalusite -- Al_2SiO_5 . The mineral is found very rarely in associations with quartz, basic plagioclase and phlogopyte in mottled micro-grained hornfels consisting of sanidine, phlogopyte, plagioclase, and pyrrhotite. The presence of andalusite in these rocks by no means testifies to the existence of lower temperature than those which occur under conditions of a sanidinite facies of metamorphism, because here, apparently it is a relict, metastable mineral phase (cf. below).

Andalusite forms very small needle-like or coarsely prismatic elongated crystals whose long dimension is not over 0.1 mm. Characteristic of the latter are sinuous, not infrequently "laced" boundaries. The mineral is colorless or has a weak pleochroism from colorless (Ng) to rose colored (Np). Characteristic is an intersecting perfect cleavage in two directions, the plane of optical axes is perpendicular $[010]$, axis of Np coincides with $[001]$. Elongation is negative, straight extinction, angle $2V = -79^\circ$, $r < v$. Indexes of refraction: $\text{Ng} = 1.644 \pm 0.003$, $\text{Np} = 1.634 \pm 0.003$, $\text{Ng} - \text{Np} = .010-.011$.

Orientation of optical indicatrix of andalusite with respect to the cleavage pole (110) after determination on the Fedorov universal stage was as follows:

cleavage with respect to (110)

$$\begin{aligned}\text{Ng} &= 45^\circ \\ \text{Nm} &= 45^\circ \\ \text{Np} &= 90^\circ\end{aligned}$$

The mineral is not stable in the process of subsequent hydrothermal action and is replaced by thin-scaly sericite.

Wollastonite - CaSiO_3 . Wollastonite is found chiefly in diopside-wollastonite, diopside-wollastonite-plagioclase, and plagioclase-wollastonite hornfels. Sometimes it forms thin, almost monomineral -- wollastonite intercalations in the above indicated rocks in thicknesses from 1 to 3 mm.

The mineral forms tabular, well formed crystals 1 to 2 mm long, elongated to the second crystallographic axis, or aggregates of several grains. In solid masses we find coarsely tabular, irregular and isometric grains of smaller dimensions.

Color white, yellowish. Glassy luster, hardness 4 - 5, Specific gravity 2.8 - 2.9.

The mineral has perfect cleavage along (100) and good cleavage along (001). Twins, usually straight along (100), are encountered rather rarely.

The optical characteristic of wollastonite from hornfels is similar to that of wollastonite described in the previous chapter. The roentgenogram of this wollastonite is almost completely identical to that given in Table 7. There is some difference only in the indexes of refraction of the mineral: $N_g = 1.632 \pm 0.003$; $N_p = 1.620 \pm 0.003$; $N_g - N_p = 0.012$; $2V = -39^\circ$, $r > v$. In associations with pyroxene in which there is about 60% hedenbergite, the wollastonite has the following indexes of refraction: $N_g = 1.639 \pm 0.003$; $N_p = 1.626 \pm 0.003$; $N_g - N_p = 0.013$; $2V = -39^\circ$, $r > v$. The somewhat higher indexes of refraction in this case are apparently explained by the entry into wollastonite of a small amount of ferrosilicate.

In micrograined hornfels with pyroxene and plagioclase wollastonite is more or less uniformly scattered through the rock, having a microgranoblastic structure. In some, essentially diopsidal, hornfels wollastonite forms separate, well-defined tabular grains having larger dimensions than the basic diopsidal, granoblastic mass (Fig. 15). These grains can be regarded as porphyroblasts. Along with this, wollastonite forms small growths of grains

appearing like circular isolations or spots, which causes the glomeroporphyritic structure of the rock. These spots are sometimes extended in shape and are confined to definite horizons in the hornfels that are oriented according to the striations (Fig. 16).

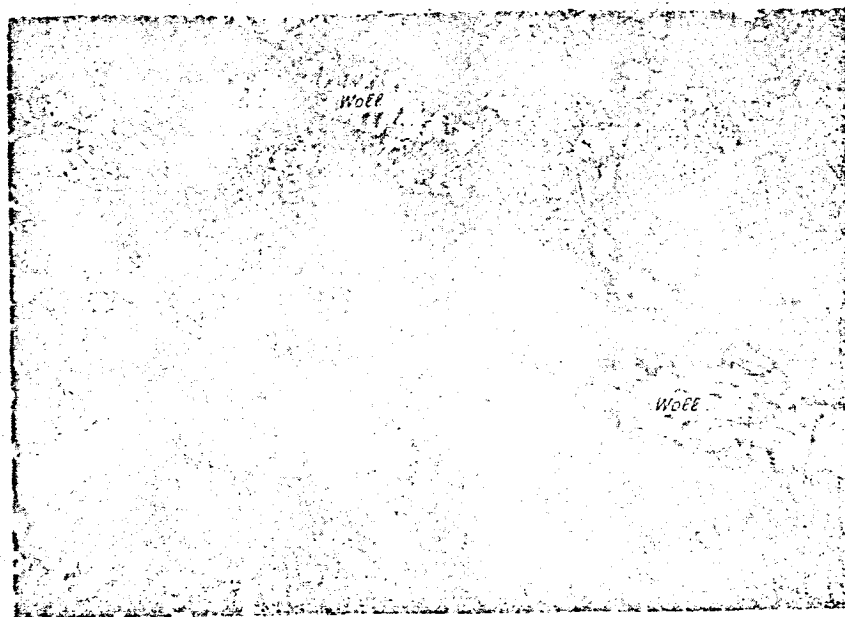


Fig. 15. Wollastonite lens-shaped isolations (Woll) in pyroxene-plagioclase rock. Nicoli crossed. Mag. 32.



Fig. 16. Isolations of wollastonite (white) in pyroxene-plagioclase hornfels. On the left the section is essentially sanidinite rock (gray). Polished lump of ore. Natural size.

In hornfels the wollastonite associates with pyroxenes of the diopside-hedenberg series, plagioclase of variable composition, pyrrhotite and magnetite. Sometimes, it is found with large, corroded grains of quartz and

calcite (this association, no doubt, is unstable in the conditions of the facies under consideration and is preserved only in consequence of the fact that the metamorphic reaction is not complete enough (cf. below).

Pyroxenes of the diopside-hedenbergite series -- $\text{CaMgSi}_2\text{O}_6$ - $\text{CaFeSi}_2\text{O}_6$.

The mineral of this series is the most common constituent of hornfels rocks. Diopside and hedenbergite mix together in all proportions, forming virtually pure terminal members of the isomorphic series, as well as various transitional forms of sahlite and ferrosahlite compositions.

Well-formed crystals are not encountered at all: ordinarily, one observes micrograined aggregates formed together with certain other minerals in rocks of granoblastic structure (cf. Fig. 15). The size of the pyroxene grains does not exceed 0.1 - 0.4 mm. The color changes from gray or white (for diopside varieties) to dark green and black. Glassy luster, hardness 5-6. Brittle. Perfect cleavage along prism (110) is characteristic. Twins rare and are encountered only in comparatively large grains.

The first pinacoid usually serves as the twinning composition face.

The optical constants for diopside are the following. Indexes of refraction: $N_g = 1.695 \pm 0.003$; $N_p = 1.667 \pm 0.003$; $N_g - N_p = 0.028$; $2V = +57^\circ$, $r > v$; angle $cNg = 38^\circ$. Plane of optical axes parallel to plane of second pinacoid. Optical properties of hedenbergite are: $N_g = 1.750 \pm 0.003$; $N_p = 1.723 \pm 0.003$; $N_g - N_p = 0.027$; $2V = +63^\circ$, $r > v$; angle $cNg = 46^\circ$. These data indicate that the content of diopside in hedenbergite [9, page 407] is not in excess of 5 - 8%.

The orientation of the optical indicatrix of hedenbergite with respect to the cleavage pole after determination on the Fedorov stage is as follows:

Cleavage along (110)
perfect

$N_g = 60^\circ$
 $N_m = 44^\circ$
 $N_p = 61^\circ$

Cleavage along (010)

$N_g = 90^\circ$
 $N_m = 0^\circ$
 $N_p = 90^\circ$

Sahlite and ferrosahlite pyroxenes have intermediate optical properties between the two extremes of the series described. The interplanar distances of diopside and hedenbergite are given in Table 12.

The pyroxenes are usually found in associations with plagioclases of variable composition, wollastonite, quartz, and pyrrhotite. Diopside sometimes associates with phlogpyte and sanidinite and is never found together with pyrrhotite. Magnetite is not infrequently encountered together with sahlite varieties. In the skarn stage and in the process of hydrothermal activity the pyroxenes are partially or completely displaced by magnetic ore, hornblende, prehnite, chlorite, and others.

Table 12

Results of Roentgenostructural Analysis of Pyroxene*

Diopside				Hedenbergite			
l	$\frac{d}{n^2}$	l	$\frac{d}{n^2}$	l	$\frac{d}{n^2}$	l	$\frac{d}{n^2}$
1	4.15	1	4.10	1	1.681	2	1.686
1	3.38	—	—	10	1.606	7	1.639
6	3.25	5	3.26	2	1.560	2	1.579
10	3.01	10	3.03	2	1.530	1	1.532
3	2.91	3	2.94	5	1.494	1	1.502
1	2.79	4	2.71	4	1.412	2	1.419
2	2.58	8	2.58	8	1.334	5	1.320
10	2.54	8	2.54	7	1.286	9	1.286
1	2.39	1	2.47	6	1.265	4	1.264
3	2.32	2	2.32	6	1.252	4	1.257
2	2.22	2	2.23	3	1.217	—	—
5	2.12	3	2.15	4	1.176	—	—
3	2.054	3	2.050	5	1.150	1	1.158
3	2.024	2	2.020	10	1.074		
4	1.845	1	1.819	6	1.052		
4	1.760	2	1.758	5	1.042		
4	1.733	1	1.736				

Photo conditions: Cu - anticathode; $\lambda = 1.537$ kX;
 $I = 10$ mA; $U = 35$ kV. Radiation filtered. Survey made
on diffractometer URS-501. Intensity according to the
ten-point scale

* Roentgenostructural analysis performed in
the laboratory of Roentgenostructural analysis IG
and G SO AN SSSR.

Phlogopite -- $\text{KMg}_3\text{Si}_3\text{AlO}_{10}(\text{F}, \text{OH})_2$. This mineral is encountered in individual, rather small flakes or flaky aggregates in associations with sanidine, diopside, plagioclase, and others. The dimension of individual flakes rarely attains 0.5 - 0.7 mm and more often it is 0.01 - 0.1 mm. The color is reddish brown to red. Glassy luster, perfect cleavage along (001) is characteristic.

The optic axial plane is parallel to (010). Optically, slightly biaxial. Index of refraction: $n_g = n_m = 1.593 \pm 0.003$; $n_p = 1.557 \pm 0.003$; $n_g - n_p = 0.036$. Some varieties have the following indexes of refraction: $n_g = 1.602 \pm 0.003$; $n_p = 1.564 \pm 0.003$; $n_g - n_p = 0.038$. This is probably explained by a certain isomorphic admixture of iron in the phlogopite. The Debayegram¹⁾ of Anakit phlogopite is absolutely identical with the standard phlogopite cited in the manual by V. I. Mikheyev [31, page 776].

We have already indicated that phlogopites containing hornfels are usually characterized by a mottled texture (Fig. 17). The boundaries of such spots are rather clearly expressed. The mottled texture is due to the large concentration of phlogopite in individual portions of the rock, whereas in concentrated sections of the mineral there is considerably less. The amount of phlogopite in such spots can be as much as 50% of the total. The dimensions of the spots are varied and can be measured in meters (in cross section). They are circular, lens-shaped, or irregular in outline and extended according to the striations in the hornfels.

The mineral is quite stable, but under some circumstances it is replaced intensively by a yellow-green chlorite.

The plagioclases. $\text{NaAlSi}_3\text{O}_8$ - $\text{CaAl}_2\text{Si}_2\text{O}_8$ series. Among the hornfels the composition of the plagioclases is quite varied. Found as the basic

1) Roentgenostructural analysis performed in the laboratory of Roentgenostructural analysis IG and G SO AN SSSR.

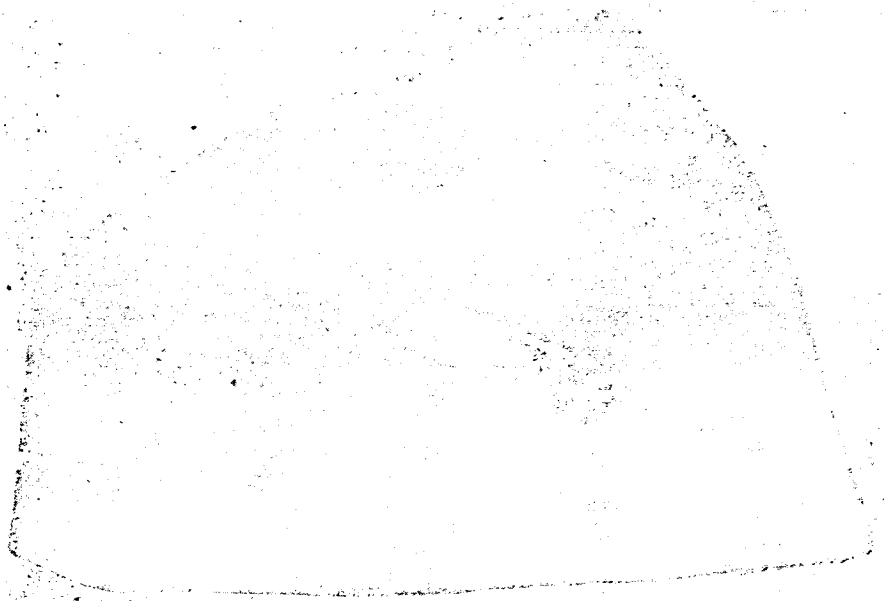


Fig. 17. Isolation of phlogopite (dark) in sanidine-plagioclase-diopside hornfels. Preinitization is clearly manifested (white spots). Polished piece of ore. Natural size.

representatives of this series are anorthite, as well as the median representatives -- andesine-labradorite. Plagioclase is one of the most widely distributed mineral components of hornfels. Usually forms very small, circular or irregular grains with sinuous edges, which form a microgranoblastic structure. Sometimes encountered are small, coarsely tabular grains. Polysynthetic twinning is a characteristic of the mineral. Plagioclase has a distinctly expressed high temperature characteristic which is demonstrated by projecting the poles of the twinned composition plane on the diagram of crystallographic feldspar directions referred to the optical indicatrix axes. It appears that the preponderant mass of the composition plane poles drops in the vicinity of the high temperature curves according to Zavaritskiy, Sobolev, and others [14] or Van der Kaaden [94].

The mineral is colored white or pale yellow. Glassy luster. Cleavage is good in two directions: along (001) and (010). Grains not over 1 - 1.5 mm in size.

In the hornfels rocks plagioclase associates mainly with pyroxene, wollastonite, quartz, and phlogopite. It is rarely found with sanidine, andalusite, pyrrhotite, and others. Characteristically, in association with wollastonite and andalusite plagioclase is represented, for the most part, by the basic varieties, although in some instances medio-plagioclase is found together with wollastonite. In phlogopite-sanidine rocks the plagioclase is represented by andesine-labradorite No 45 - 55, but here we also find the richer anortite varieties.

Texturally, plagioclase hornfels are characterized by a clearly expressed striation, and massive textures are rarely observed. The texture is emphasized, in places, by a vaguely expressed micro-striated structure of plagioclase-diopside, plagioclase-diopside-phlogopite-sanidine and other types of hornfels.

Sanidine -- $(K, Na) AlSi_3O_8$. The mineral forms irregular or tablet-shaped grains along (010), the dimensions of which vary greatly -- from fractions of a millimeter to 4 - 5 mm. The mineral is colorless or white; may be pale yellow or light brown. Luster glassy to dull. Hardness 6. Perfect cleavage along (001) and (010). Specific gravity 2.55.

The optical axial plane of sanidine and the Ng axis are perpendicular to (010). The Np axis forms with the third pinacoid plane an angle of 7 - 8°. Optical sign negative. Small optical axis angle, less than 40°, $r > v$. Indexes of refraction: $N_g = 1.525 \pm 0.003$; $N_p = 1.5.9 \pm 0.003$; $N_g - N_p = 0.006$. Not infrequent one finds simple twinning according to the Carlsbad law. Interplanar distances of sanidine are given in Table 13. The mineral contains insignificant amounts of sodium -- this is confirmed by spectroscopic analysis¹⁾.

Sanidine is usually found with phlogopite, diopside, plagioclase, and other minerals. In rocks it often forms large porphyroblasts of rather uniform

1) Roentgenostructural analysis made in the roentgenostructural analysis laboratory of IG and G SO AN SSSR.

Table 13

Results of Roentgenostructural Analysis of Sanidine*

	$\frac{d}{n}$	l	$\frac{d}{n}$	l	$\frac{d}{n}$		$\frac{d}{n}$
2	4,82	1	2,87	1	2,08	1	1,596
3	4,29	1	2,79	3	2,03	1	1,573
0,5	4,03	1	2,71	3	1,983	2	1,538
6	3,86	6	2,61	1	1,937	3	1,510
1	3,69	6	2,56	2	1,855	5	1,454
3	3,52	1	2,41	4	1,810	4	1,434
9	3,34	1	2,34	2	1,777	2	1,416
10	3,28	2	2,18	2	1,726	2	1,373
9	3,03	3	2,15	1	1,676		
5	2,96			4	1,635		

Photo conditions: Cu -- anticathode; $\lambda = 1.537$ kX;
 I = 10 mA; U = 35 kV. Radiation filtered. Survey
 made on diffractometer URS-501. Intensity according
 to the ten-point scale.

* Roentgenostructural analysis performed in the
 laboratory of Roentgenostructural analysis IG and G
 SO AN SSSR.

crystallographic profile with numerous inclusions of rounded grains of diopside and phlogopite (Fig. 18). Also forms solid granular masses with up to 80-90% of sanidine (volume percent). These areas enriched with sanidine form bands, lenses or irregular isolations in hornfels. In rocks sanidine is quite stable; it is usually water transparent. In the process of subsequent changes it may be replaced by prehnite.

Apart from the silicate minerals, as we have already mentioned, pyrrhotite and magnetite are found in hornfels. The pyrrhotite is similar in properties to the mineral described in the chapter dealing with the metamorphism of marls. It is represented in two modifications: hexagonal and monoclinic. The mineral forms a shallow impregnation or small lenses (5 x 2 mm) which are oriented along the striations in the hornfels. The magnetite also forms shallow impregnations of cubical or octahedral crystals, mainly in the pyroxene-containing hornfels. Both these minerals are replaced in separated parts of the rock with hematite and ferric hydroxide.

Metamorphism of Pyroxene-Hornfels Facies

Metamorphism of Marls

As we previously indicated, the contact metamorphic complex of marbles and hornfels of sanidine facies was formed in the immediate vicinity of an incurrent canal of a trappean intrusion; testimony of this comes from the data on the internal structure of the Anakit massif and the discovery of spurrite-merwinite-melilite marbles and hornfels rocks with intersecting, dike-type apophyses of the massif.

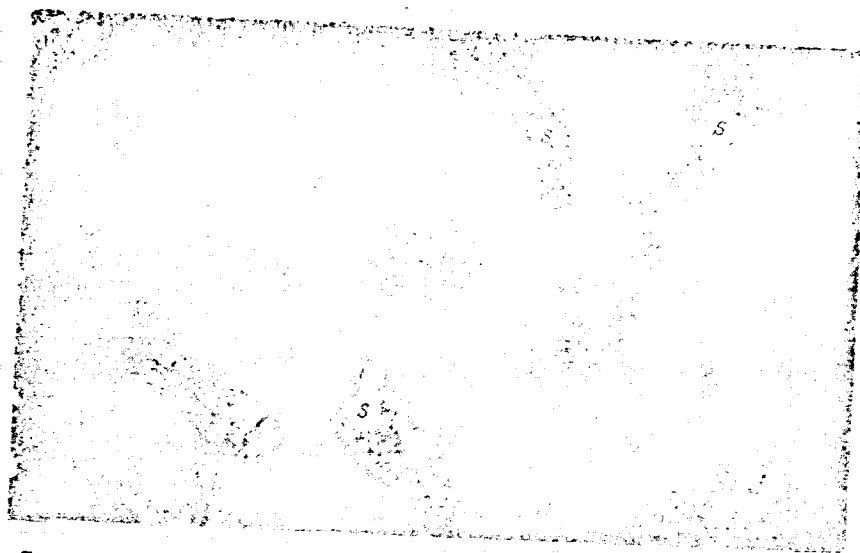


Fig. 18. Crystals of sanidine (light - S) in plagioclase-diopside-phlogopite hornfels. Nicoli crossed. Mag. 32.

Somewhat farther away from the incurrent canal, in contact with the stratum portion of the Anakit massif, there is formed a mineral association which points to the lower temperatures of the contact metamorphism, and corresponding in its composition to pyroxene hornfels facies [55, 56]. This mineral association is represented by the forsterite marbles containing as admixtures diopside, wollastonite, phlogopite and others. The most typical manifestations of this associations are found on the left bank of the Lower Tunguska River on the strike of the horizon of Silurian dolomitic marls which, under the action of the higher temperature metamorphism, are converted into the previously described

monticellite-melilite marbles. The distance between these two mineral associations, which are disposed within the same western contact zone of the Anakit massif but on differing banks of the Lower Tunguska River, is about 500 - 700 meters (cf. Fig. 1). Linearly associating with the forsterite calciphyres are the banded hornfels consisting of diopside, plagioclase, wollastonite and grossular, with a sparse admixture of relict (fragmented) quartz, calcite, and others. It is here that we find virtually pure layers of calcite marbles.

The zone of contact metamorphism in the left bank portion of the Anakit massif is from 3 to 5 meters thick. The main part of the contact is concealed under the present day deposits, hence the study of the exocontact calciphyres, hornfels, and marbles called for a certain amount of prospect holes and ditches. The basic mass of the bedrock of the exocontact is found in the flood plain of the river. Some outcroppings were found in the vicinity of the mouth of Trekhosnyy Creek. The eastern contact of the Anakit massif, especially the near contact rocks exposed on the left bank of the Lower Tunguska River is not interesting from the mineralogical standpoint, because the contact-metamorphic rocks developed here are represented by various calcite and dolomitic marbles with thin margins and veins superimposed by serpentinization.

The forsterite marbles are white or greenish fine-grained rocks of solid or striated texture. It forms thin layers and lenses in a stratum of non-forsterite marbles. The thickness of such layers is not over several tens of centimeters.

Forsterite -- Mg_2SiO_4 . The mineral forms colorless or light green grains, ranging in size from fractions of a millimeter to 1 - 2 mm. The grains are rounded or irregular with imperfect cleavage along (100) and (010). Glassy luster, specific gravity 3.2.

The optical axial plane is parallel to (001); axis Ng coincides with [100], axis of Np coincides with [010]. Optically positive, $2V = 87^\circ$, $R > v$. Indexes

of refraction of forsterite are the following: $N_g = 1.670 \pm 0.002$; $N_p = 1.636 \pm 0.002$; $N_g - N_p = 0.034$.

The mineral is readily disintegrated and is replaced by laminated grains of serpentine, chlorite, and others. Associating with forsterite are diopside, which forms small irregular or rounded grains; in its optical properties it corresponds to pure veinless members of the diopside-hedenbergite series: $2V = +58^\circ$; $N_g = 1.693 \pm 0.003$; $N_p = 1.667 \pm 0.003$; angle $cNg = 39^\circ$. Found in small quantities are fine flaky, reddish brown phlogopites, wollastonite, and pyrrhotites. Wollastonite forms white, fine tabular grains whose dimension is under 1 - 2 mm. The amount of wollastonite is under 1 or 2% (volumetric percent). Pyrrhotite forms a rare, fine impregnation.

The stable forsterite calciphyres are encountered relatively rarely. For the most part, they are subjected to the action of subsequent processes and are replaced by serpentine, magnetite (magnesioferrite), chlorite, iron hydroxide, and such. In many cases, especially in areas where skarns are developed, the presence of forsterite in the original rocks can be judged from the relicts of this mineral and by other symptoms (pseudomorphism of serpentine, etc).

Metamorphism of Calcareous and Dolomitic Aleurolites and Sandstones

In the metamorphism of various carbonates containing aleurolites and sandstones of the Upper Ordovician (the Dolborskaya series) in the contact zone of the Anakit massif there are formed on the left bank of the Lower Tunguska River diopside, diopside-plagioclase, diopside-wollastonite, and other hornfels rocks characterized by a clearly expressed banded texture. On the upper side these rocks are covered over with metamorphosed marls and limestones of the Kochumdeks series (Lower Silurian); the previously described forsterite calciphyres, as well as non-forsterite marbles, belong to this period.

The diopside hornfels are probably the most common rocks in the exocontact

zone on the left bank. They are characterized by a striated formation and a granoblastic, irregular grained structure. Standing out are striations and lenses 3 to 5 mm wide made up of relatively larger grained aggregates of grains (0.1 - 0.5 mm in cross section) among the micrograined basic mass. The hornfels of this type are usually mono-mineral rocks and contain almost pure diopside with a small amount of hedenbergite molecules (2-15%). Encountered in the form of an admixture are corroded, relicts of quartz and, rarely, plagioclase.

In the diopside-plagioclase hornfels which form the thin layers among the diopside hornfels, one finds scattered grains of grossular which appear like a porphyroblast (dimensions up to 2 mm in cross section), or, together with diopside and plagioclase, they make up the microgranoblast basic rock tissue. Grossular grains are rounded or irregular, color yellow-brown, glassy luster, specific gravity 3.5, index of refraction $N = 1.739 - 1.742$. Isotropic in thin section, and weakly polarized at the edges. Ordinarily in those sections where grossular is commonly developed we find in increased amounts plagioclase with the following basic composition bytownite and anorthite. Plagioclase forms fine isometric or irregular, polysynthetic twinned grains with albite-karlsbad or karlsbad twinning usually; the twinned streaks are relatively wide (in grains they are up to 1 mm). Here and there we encounter relict, re-crystallized calcite.

Hornfels change greatly and are subject to skarning processes and hydrothermal action. In the direct contacts with the massif, they are often completely replaced by garnet-andradite or andradite-grossular, diopside-hedenbergite, magnetite (magnesio-ferrite), chlorite, epidotite, actinolite, and others.

Metamorphism of Limestones

In the metamorphism of pure limestones of the Kochumdeks series there

are formed in the contacts of the massif various colored fine- to medium-grained marbles. Their color varies from white, bluish or greenish to gray-brown, sometimes with a wine-red tinge due to the presence of mineral admixtures of chlorite, iron hydroxides, etc. Occasionally, one finds in the marbles dolomite, small flaky phlogopite, graphite, pyrrhotite, wollastonite.

Marbles have very irregular-shaped grains and are streaky. Occasionally one finds coarse-grained varieties. The structure is usually granoblastic, not infrequently with clear symptoms of cataclasm. The latter peculiarity is most clearly manifested in the vicinity of the immediate contact of marbles and traps where sections of granulation and brecciation and the like are common.

Textural and Structural Peculiarities of Contact-Metamorphic Rocks

The composition and distribution of metamorphic minerals in exocontact rocks are explained fully by the primary distribution of substances and composition of original carbonate-siliceous-argillaceous fractions in the non-metamorphosed original sedimentary rocks. The re-distribution of substances in metamorphism, apparently, is brought about only in micro-volumes at distances not over several millimeters. This is demonstrated by the following: by the inheritance of streakiness in marls, sandstones and aleurolites; the inheritance of external contours of silicilite (quartz - chalcidony - carbonate) concretions and carbonate-clayey isolations, bands, nodules, etc., which are a constituent part of the marls converted into a complex of varied silicates of calcium; by the inheritance with respect to the distribution and composition of substances before and after metamorphism, etc. Associations of high temperature minerals studied like the larnite-merwinite-spurrite subfacies in the contact zones of the massif were formed as a result of a series of successive reactions, chiefly in the hard phases, with components of clay, free silica, calcite, and dolomite

(stages of progressive metamorphism). Special emphasis should be placed on the fact that the composition and structure of metamorphogenic calcium silicate isolations from exocontact marbles is determined by the original composition and distribution of components in the original sedimentary rocks (the addition of substances from the intrusion in the magmatic stage is virtually absent). (Fig. 19). The previously described zonality in the structure of calcium silicate isolations, which is expressed by the enrichment of their central parts with melilite and merwinite, was caused by a concentration of clayey (kaolin - hydromica clays) particles and dolomite (up to 10%) in the internal portions of the carbonate-clayey layers and nodules of marls, while the edge portions are essentially calcitic in composition and probably contain a certain admixture of thinly-dispersed free silica in the form of chalcedony or opal recrystallized into quartz; spurrite is formed in these sections in metamorphism. Zonality of another type, recorded around metamorphosed silicious concretions and forming horizons in the limestones of the Kochumdeks series, is also due to the primary distribution of components in sedimentary rock.



Fig. 19. Noduled and veined merwinite-melilite-spurrite isolation in marble (light gray). Polished rock. Natural size.

Silicillite concretions in metamorphism are replaced by micro-grained aggregates of wollastonite (similar to the displacement of concretions in contacts with dolerites in Scot Hill [88]). In this instance there appear wollastonite pseudomorphs of concretions with components preserving their internal contours. The silicious material is, in some instances, not completely replaced by wollastonite; it is converted into a thinly crystalline tridymite aggregate. With zonality of the second type, the free silica is often concentrated, during the process of sedimentation, inside the clay-carbonate isolations of marls, forming chalcedony concretions; it is replaced in the metamorphism of wollastonite. Spurrite rims about wollastonite "nuclei" are formed during the reaction of calcite with silica (both of free and clay minerals); characteristically, the carbonate material around the lithogenic silicillite concretion always contains increased amounts of thinly dispersed quartz (or even chalcedony) compared with sections more removed from concretions, although the boundaries of the concretions, just like the boundaries of the wollastonite "nucleus" which incloses it, always remain sufficiently sharp. The merwinite-melilite external fringes around the spurrite rims are formed in the replacement of clay-calcite-dolomite materials which encase those isolations in marls containing within them silicillite concretions.

The banded texture of hornfels is also a splendid illustration of the inheritance of structure of the original Ordovician sandstones, aleurolites and argillites. The thin, oftentimes rhythmic, alternation of layers of hornfels rocks, the analysis of mineral associations pointing to the inheritance of a chemical composition of the original rocks, and finally, the direct transition of streaky hornfels into non-metamorphosed, layered rocks of the Dolborsk series -- all these things indicate there was metamorphism without a considerable re-distribution of substances in rocks of the contact zones of the Anakit massif.

The peculiarities in the formation of metamorphic rocks was established both on the basis of a study of the original deposits outside the contact aureole of the intrusion and on contact-transformed rocks associated with the first mutual transitions.

Spurrite-merwinite and monticellite-melilite marbles are the highest temperature products of a series of progressive metamorphic conversions of mineral phases. Tilleyite is formed in the regressive lowering of the temperature from the spurrite in a union with CO_2 . The appearance of a tilleyite reaction rim around the wollastonite pseudomorphosis between the wollastonite "nucleus" and the spurrite fringe (this was previously mentioned) is explained by the increased micro-jointing of this zone which formed the conditions for the free penetration thither of CO_2 . This also explains the formation here of garnet and cuspidine rims (cf. Fig. 10) which are formed somewhat later. Sometimes the absence of rims of tilleyite, cuspidine and garnet, which usually appear together, can be tied in with the poor penetrance of gases and hydrothermal fluids of a given region if it is without a system of well developed micro-jointing.

B. Metasomatic Stage

During the metasomatic stage of contact action (on the enveloping trappean massif rock) garnet-pyroxene skarns and magnetite (ferro-magnetite) ores are formed. In this stage we have the formation of cuspidine; this, however, is preceded by the skarns and the very unusual metasomatic diopside-serpentine rocks which develop as veins in the carbonate-containing Ordovician rocks.

Metasomatic rocks are superimposed on the hornfels and contact metamorphic marbles, forming veined or lens-shaped bodies or impregnations of metasomatic minerals. Cuspidine is dimensionally confined to those contacts of

the Anakit massif where we find developed marbles containing spurrite, merwinite and other minerals. Garnet-pyroxene skarns form 40-50 cm veins on both sides of the asymmetric apophysis of the massif (cf. Fig. 4), or they form lenses cutting through the veins and veinlets which coincide positionally with the same marbles. Moreover, garnets also form metasomatic impregnations in marble both the right and left bank contact zones of the massif.

Diopside-serpentine veins are found along Vostochnyy Creek 10 meters from the contact with the traps. The bodies of iron metasomatic ores correspond to those in the southern contact of the Anakit intrusion.

Cuspidine

This mineral forms a scattered impregnation in the spurrite-merwinite marbles. The thickness of the contact zones in which it is encountered is 10 - 15 meters.

The composition of cuspidine is $\text{Ca}_4\text{Si}_2\text{O}_7(\text{F}, \text{OH})_2$. It crystallizes into monoclinic systems. Forms small (1-3 mm in cross section) or fine (0.01-1 mm) irregular or rounded grains which, for the most part, replace the previously formed silicates of calcium: spurrite, tilleyite, and others. In some instances, as we have already indicated, cuspidine forms thin metasomatic projections around the wollastonite pseudomorphoses according to the silicilate concretions (cf. Figs. 10, 11). In those cases cuspidine is represented in the form of irregular grains under 2 mm in size.

Color white, glassy luster, hardness 5, specific gravity 2.9, perfect cleavage along (001), plane of visual axes parallel to (010), axis Nm coincides with [010], angle $cNg = 6^\circ$. Mineral bi-axial, positive, $2V = 68^\circ$, $r > v$. Index of refraction of mineral is as follows: $N_g = 1.606 \pm 0.003$; $N_p = 1.594 \pm 0.003$; $N_g - N_p = 0.012$. Twinning is not very characteristic of the mineral. Simple twinning; edge and axial twinning; plane of intergrowth (001).

The orientation of the optical indicatrix with respect to the pole of cleavage (001) and the twinning axis, after measurement on the universal Fedorov stage, was as follows:

Cleavage along (001),
twinning plane of intergrowth,
twinning axis (in the case of
the face law)

$Ng = 6^\circ$
 $Nm = 90^\circ$
 $Np = 84^\circ$

Twinning axis [100]

$Ng = 84^\circ$
 $Nm = 90^\circ$
 $Np = 6^\circ$

The interplanar distances of cuspidine determined roentgenoscopically are given in Table 14.

In rocks cuspidine is formed after the metamorphic silicates of calcium, replacing them. In the microphotograph given (cf. Fig. 11) it is clearly evident that tilleyite is replaced by cuspidine, forming a concentric fringe around the wollastonite "nucleus". In other cases, when replacing the earlier minerals there are preserved in cuspidine relict inclusions of spurrite, merwinite and others. In later processes cuspidine is usually replaced completely or partially with garnet, partially by clear andradite, as well as by aqueous silicates of calcium, e.g., hillebrandite.

Skarns

Very characteristic and splendidly expressed metasomatic garnet, garnet-pyroxene and pyroxene veins and lenses, in part clearly intersecting, partly concordant with the deposit which includes metamorphic rocks, are formed in the western part of the block of Silurian-Ordovician rocks in contact with the asymmetric apophysis of the Anakit massif (cf. Fig. 4). The thickness of the veins and lenses is under 50 cm. They frequently have distinct zonal structure and dark brown greenish coloration. The texture is banded, less often solid. The structure is uniformly grained, medium or fine grained. Garnet is the main mineral of skarns. Ordinarily it is represented by a grossular-andradite variable composition, but almost clear andradite varieties of garnet

are also encountered.

Table 14

Results of Roentgenostructural Analysis of Cuspidine*

h	$\frac{d}{n}$	h	$\frac{d}{n}$
6	3.328	4	1.992
4	3.210	3	1.924
10	2.083	8	1.889
6	2.895	8	1.842
2	2.806	8	1.735
2	2.734	2	1.576
3	2.568	3	1.541
3	2.493	6	1.461
2	2.357	2	1.215
4	2.323	8	1.152
5	2.098	4	1.111
4	2.020	2	1.048

Photo conditions: Co - anticathode; $D = 57.3$ mm; $\lambda = 1.78529$ kX; $I = 11$ mA; $U = 37$ kV. Radiation filtered. Correction made in accordance with combined graph of KCl and chlorite. Exposure time 20 hours. Intensity by the ten-point scale.

* Roentgenostructural analysis made in the roentgenostructural analysis laboratory of the IG and G SO AN SSSR.

The mineral is observed in compact, mixed masses or forms impregnations of well-rounded small crystals (3-4 mm in cross section) of rhombo-decahedral appearance or aggregates of such crystals. The predominating coloration of garnets is brownish to yellow brown. Andradite is ordinarily colored dark brown.

The mineral has a glassy luster, hardness 7, separation rarely occurs along (110). Specific gravity varies from 4.0 (andradite) to 3.8 (grossular-andradite). The mineral is isotropic in most cases, but sometimes (very rarely) there are anisotropic areas in the edge portions of isotropic grains. Garnet often discloses a zonal structure. The indexes of refraction are as follows: $N = 1.88$ (andradite up to .76-1.79 (grossular-andradite)).

Roentgenostructural studies of andradite garnets confirmed their relationship with the

group of minerals in question: the parameter

a in the andradites was equal to $12,040 \text{ \AA} - 12,034 \text{ \AA}$.¹⁾

The following admixtures of elements were found in the garnets: Ni, Co, Ti, Ge, Ga, B; they were found to exist in the amount of $0.007 - 0.0001\%$.²⁾

Pyroxene was second greatest in distribution (after garnet) of the minerals in the skarn. Pyroxene often associates with garnet, but no less frequently it

1) The roentgenostructural research was made in the roentgenostructural analysis laboratory of the IG and G SO AN SSSR.

2) The analysis was carried out in the spectral analysis room of the IG and G SO AN SSSR.

forms independent mineral accumulations which contain virtually no admixtures of garnet. Pyroxene and pyroxene garnet skarns are found mainly in the casings of garnet metasomatic veins. Solid masses of pyroxene are colored yellowish-brown with varying intensities and shades, depending on the amount of pyroxene. The more ferruginous varieties are darker in color. The color in the skarns is zonally distributed, and this is also governed by changes in the composition of the pyroxene in the various zones. The clearest changes in coloring are manifested in the veined metasomatic formations in the marbles. These metasomatic veins have a symmetrically-striated structure with a rather strict orientation of striation parallel to the vein boundaries. The central portions are darker than the edge portions.

The structure of the pyroxene skarns is medium to fine irregularly grained. In observations of thin sections, it appears that the skarns are parallel-prismatic and sheath-shaped or radially-prismatic in structure due to the orientation of the prismatic and columnar individual crystals of pyroxene and its aggregates. The mineral composition is not consistent: the pyroxene of skarns is an intermediate variety of diopside-hedenbergite series (sahlites). The content of hedenbergite changes from 20-25% to 60-65%.

Some of the later products among the skarns are magnetite, serpentine, chlorite, actinolite, epidote, hematite, quartz, sulphides of copper and iron, calcite, iron hydroxide and others. The veinlets of epidote or actinolite-epidote composition sometimes occupy the central portion of the metasomatic skarn lenses or veinlets associating with the hydrothermal calcite, zeolites and quartz.

Individual isolated spots of garnet or garnet pyroxene skarns and skarned limestones are found rather far from the contact with the trappean massif. Such spots or thin veined deposits and lenses with a garnet composition are

found 200-250 meters and farther from the western contact of the Anakit massif in the shore outcroppings of Silurian carbonaceous rocks. Along with garnet one finds here epidote, hematite, chlorite, quartz, chalcopryrite and other hydrothermal minerals. Diopside-serpentine metasomatic veins, as we have already indicated, are found in rocky indigenous outcroppings in the valley of Vostochnyy Creek, approximately 150 meters from the point where it falls into the Lower Tunguska River. The veins occur in a deposit of dolomitic marls with layers of calcareous dolomite and calcareous aleurolites 10 meters from the thick intersecting dike body - the apophyses of the Anakit massif.

The veins are 5 - 15 cm in thickness. They have indistinct, gradual contacts with inclosing rocks and stand out mainly through their darker brownish color. The texture is compact or indefinitely striated. The structure is fine grained and the grains are not uniform. Composition: pyroxene (diopside), serpentine, calcite.

Table 15

Chemical Composition of Diopside-Serpentine Rock

	SiO ₂	TiO ₂	Al ₂ O ₃	Fe ₂ O ₃	FeO	MnO	MgO	CaO	Na ₂ O	K ₂ O	H ₂ O	Other	Total
Diopside-serpentine rock with admixture of calcite	47,11	0,05	0,88	2,68	0,98	0,24	19,47	20,33	none	0,05	—	8,25	100,05

Pyroxene is the main mineral component of the rock, making up 80 - 100% of its total volume. It forms small grains in aggregates of xenomorphic-granular structure or larger (up to 3 mm) idiomorphic, well bounded prismatic crystals associating with fibrous serpentine. In its properties diopside is similar to diopside of the skarns; its Debayegram is practically identical with that of standard diopside [31]¹⁾. The chemical composition of diopside-serpentine rocks is given in Table 15. The sample described, apparently, is

1) The roentgenostructural analysis was made in the roentgenostructural analysis laboratory of the IG and G SO AN SSSR.

formed in the selective displacement of thin dolomitic horizons of sedimentary strata.

Iron Mineralization

Iron mineralization in the Anakit River region has been known since 1931 when the L. M. Shorokhov expedition established three outcroppings of magnetic ores along the shore exposures of the Lower Tunguska River several kilometers above the mouth of the Anakit River.

The bodies of magnetic ores exposed on the surface in this area are spatially confined to the southern contact of the Anakit trappean massif (left bank of the Lower Tunguska).

The mineralization is localized in contact with the traps among the enclosing metamorphosed and skarned limestones and dolomitic marls, limestones, aleurolites and sandstones of the Silurian and Ordovician Periods. The ore bodies are disposed parallelly to the contact and are vein-like in appearance; they are not over 2 meters in thickness.

The zone of contact metamorphism in the points of localization of ore bodies encompasses the exocontact zone that is 3 to 5 meters wide. The enclosing rocks are the forsterite calciphyres, hornfels, and marbles. The skarning in places of ferro-mineralization is not very significant, consisting of thin lenses, patches and scattered mineralizations of garnet. Garnet-brown andradite (index of refraction 1.88) is found as single grains or aggregates of fine weakly zonal grains. The size of individual crystals of the mineral (and grains) is under a tenth of a millimeter.

Soon after the formation of garnet, there is formed a magnetite (magnesian-ferriting) mineralization of iron. The general spatial confinement of ore bodies to the contact of traps with the carbonate rocks, the presence of textures and structures pointing to the process of replacement leads us to conclude

that it is a contact-metasomatic method of ore formation. The ores are patchy with sections of massive texture. The patchy texture is formed by the replacement of magnetite of carbonate minerals and small grains of forsterite in forsterite marbles. Large grains of forsterite are preserved, in the replacement process, and somewhat later, during serpentization, they are converted into a lamelliform aggregate of serpentinite. The massive ores appear on the replacement of non-forsterite marbles and hornfels. Impregnated ores are characteristic of marginal portions of ore bodies and are spatially associated with the veined, lens-shaped magnetite isolations. The frequently observed textural non-uniformity of ores is probably related to the displacement by magnetite of the tectonically deformed and disintegrated rocks.

This conclusion is supported by the presence of pre-ore zones of disintegration beyond the limits of the ore bodies and by the cementation of the ore mass of fragments of enclosing hornfels with the formation of brecciaform textures.

In massive and patchy ores there are dispersed, irregularly grained structures. The mineral grains vary in size from hundredth of a millimeter to 2 mm or more. Morphologically the magnetite is usually seen as irregular isometric grains, forming aggregates of xenomorphic granular structure. Hypidiomorphic granular structures are less frequently observed. The impregnated grains are idiomorphic in appearance. Microzonality is not characteristic of magnetite: in all the samples studied its grains were characterized by uniformity. On the boundary with the rounded grains of the non-replaced (relict) forsterite the magnetite is usually microgranular, intruding here and there into the peripheral portions of its grains through very fine cracks. Among ores which metasomatically replaced the carbonate rocks we find in places micrograined (including cryptocrystalline) aggregates of magnetite with indefinitely expressed colloform structure.

Iron mineralization took place during one stage of mineralization because only one generation of magnetite is generally present. This circumstance was clearly demonstrated in field investigations and was ultimately confirmed in a microscopic study of slides and polished sections.

It is obvious from Table 16 that, insofar as the chemical composition is concerned, the mineral is a magnesioferrite. This conclusion is convincingly supported by the results of a roentgenostructural analysis of magnesioferrite powders calcined at 800-850°C. As a result of the calcination the mineral breaks down into two phases: magnesioferrite and hematite which makes it possible to classify it with complete unambiguity. The first such study of the Anakit magnomagnetite was carried out by N. V. Pavlov and M. T. Yanchenko [39] and repeated by us¹⁾.

Table 16

Chemical Composition of Anakit Magnesioferrite (percentile weight)

	SiO ₂	Al ₂ O ₃	Fe ₂ O ₃	FeO	TiO ₂	CaO	MgO	MnO	TOTAL
Magnomagnetite*	—	—	75,05	17,89	0,11	—	6,25	0,32	99,63
Magnomagnetite**	0,10	1,79	68,11	23,49	0,38	1,00	5,30	0,26	100,42

* Analysis made in the chemical analysis laboratory of IG and G SO AN SSSR.

** Analysis derived from study [39] by N. V. Pavlov and M. T. Yanchenko.

The presence in the chemical analyses (cf. Table 16) of TiO₂, MnO and, in part, Al₂O₃ is apparently tied in with the isomorphic entry of the given components into the makeup of magnesioferrite.

The somewhat increased content of Fe₂O₃ in analysis 1 is explained by the admixture of hematite, whereas the admixture of CaO in analysis 2 can be

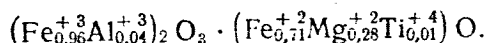
1) The roentgenostructural analysis was carried out in the roentgenostructural analysis laboratory of IG and G AN SSSR.

explained by the presence in the analyzed material of an insignificant admixture of non-metalliferous minerals.

The spectral analysis¹⁾ indicates the presence in the mineral of vanadium and barium in the amounts of 0.003 - 0.007%. All of these elements, like zinc, whose content according to spectroscopical data is equal to 0.1 - 0.2%, are also isomorphic admixtures.

The content of Al_2O_3 in the Anakit magnesioferrites varies greatly (cf. Table 16). This circumstance cannot be explained entirely by the presence of mineral mechanical admixtures: the only alumina-containing mineral in the ores is serpentine-serpophyte in which the content of Al_2O_3 is 2.5% (in percentile weight), but the assumption about the presence in the samples of serpentine analyzed is contradicted by the insignificant content of SiO_2 (analysis 2). Thus, a great portion of the alumina goes into the crystalline structure of the magnesioferrites as an isomorphic admixture as in other magnesioferrite deposits of the Siberian platform [2.38].

The crystallochemical formula of the Anakit magnesioferrite computed in accordance with analysis data 2 (without CaO) is as follows:



Serpentine is the second most abundant mineral component in the ores. It varies in amount from 5 to 20%, and in the marginal portions of ore bodies it is as much as 85%. Serpentine develops after the formation of magnesioferrite. Serpentine develops intensively due to forsterite, oftentimes replacing it wholly. Magnesioferrite is practically not replaceable by serpentine; in only exceptional cases do we find thin serpentine veins in the grains of the ore mineral. Outside the limits of the ore bodies and in contacts with traps there is strong serpentinization of marbles and marmorized limestones and dolomites. Replacement of carbonate minerals also occurs in the selvages of serpentine veins

1) The analyses were carried out in the spectral analysis laboratory of IG and G CO AN SSSR.

intersecting the enclosing the carbonate rocks. Diopside hornfels are not greatly subject to serpentinization.

Serpentine, in turn, is rather actively replaced by very fine-grained, imbricated diverse or radiate fibrous aggregate of white chlorite, which forms powdery or wooly accumulations.

Hematite is widely distributed in ores and appears simultaneously with magnetite (magnesio-ferrite). Also encountered in the ores are impregnations of apatite, pyrite, and chalcopyrite. The percentile content of sulfides of copper and iron in the ores is very small (under 0.5% by volume). Bornite, chalcocite, and covellite are developed through chalcopyrite. Among other products of hydrothermal activity deserving notice are ferric epidote, actinolite, zeolite, calcite, and others.

A special article by the author is devoted to a more detailed description of mineralization.

C. Post-Skarn Hydrothermal Stage

Minerals formed as a result of hydrothermal activity are formed after the minerals of the metasomatic stage, a fact that is supported through studies of structure and texture. The deposits of hydrothermal products are subjected, in most cases, to a definite structural control, forming veins, veinlets, small lenses or impregnations within limits sections. The minerals of this stage are deposited both in exocontact and endocontact rocks, but the main portion of hydrothermal products is formed in the skarned portions of the rock. The area of distribution of hydrothermal activity is quite large: individual hydrothermal veins were found in the enclosing rocks at distances of up to 300 meters from the contact of the trappean massif. The intensity of hydrothermal action varies. The rocks subjected to the greatest hydrothermal processing are those of the exo- and endocontacts of the left bank portion of the Anakit

massif in which the processes of actinolitization, chloritization, serpentinization and others are most intensively manifested. The processes of actinolitization are also strongly manifested in erupted rocks, especially in those sections where we find developed the dolerite-pegmatites and granophyres. Farther down we offer a brief description of minerals in the hydrothermal stage, particularly in the zone of exocontacts.

Sulphide hydrothermal minerals are represented by chalcopyrite and pyrite which are most often encountered in associations with iron ores and skarns. Ordinarily, they form irregular grains in the form of impregnations of veined outcroppings. In aggregates the xenomorphic-granular structures are typical; in the calcites or calcite-epidotic veins we find rather large (1-5 mm in cross section) idiomorphic grains. In drusy cavities we observed together with the calcite octahedric grains of chalcopyrite with dimensions of up to 1 cm. Pyrite is also encountered in drusy voids and in limestones, forming idiomorphic cubic crystals. In those cases, however, where the pyrite and chalcopyrite are encountered together it can be established that the pyrite is an earlier mineral and is replaced by chalcopyrite.

Hematite is virtually not encountered as a product of hydrothermal change of magnetite (martite). Ordinarily, it is formed almost simultaneously with magnetite (magnesioferrite) as indicated by the absence of signs of replacement and corrosion between the minerals as well as by the approximately similar degree of idiomorphism.

Hydrothermal hematite forms fine-grained or powdery masses of reddish color in associations with epidote and calcite; these masses, which are small zoned (20-30 cm), are distributed in marmorized and skarned limestones, conforming with the over-all strike of enveloping sedimentary strata. Hematite is encountered in the form of small tablets or radiate-fibrous microscopic aggregates.

Its amount in rocks of these zones is rather considerable and reaches 40-60% in volume. Within these zones there are sections that are more or less rich in hematite, right down to those that are without hematite, consisting of recrystallized, hydrothermal calcite.

Hematite is encountered in relatively small amounts in the actinolitized sections of rocks and in amphibolized gabbro-dolerites in the form of small scaly aggregates and individual microscopic platelets.

Quartz, as we have already mentioned, is present in exocontact rocks in the form of relict fragmented grains of the terrigenous fraction of sandstones, etc. With it is hydrothermal quartz, which forms veins, veinlets, pocketed-streaked isolations or impregnations in various rocks: skarns, hornfels, marbles, and others. The mineral usually associates with chlorite, calcite, epidote, prehnite, actinolite.

The very uniquely thick horizon of grainy gray quartz is disposed in contact with the trappean apophyse on the right bank of the Lower Tunguska River, not far from the sanidinite-phlogopyte hornfels (cf. Fig. 4). This quartz horizon is about 12 meters thick. It occupies the extreme eastern position in the block of Silurian-Ordovician metamorphic rocks in the region of the incurrent canal of the Anakit intrusion.

The horizon is streaky in formation and conforms with the mode of occurrence of the adjacent striated hornfels. The quartz is fine- to medium-grained and forms irregular or coarsely prismatic grains. Also encountered are portions contained granoblastic structures. Quartz associates with finely squamosed chlorite which often forms radiate fibrous and spherulitic aggregates and is rich in many solid, fluid and gaseous inclusions.

The formation of this quartz horizon apparently occurred due to the layer of quartz sandstones in the Ordovician stratum as a result of intensive

hydrothermal processes which led to the re-deposition of the silicate mineral. The formation of the quartz occurred within a broad interval of temperatures from 600 to 150° (determined from curves for the visual determination of temperatures of homogenization according to the correlation of phases [13]). The main mass of the quartz has a high temperature characteristic, judging from the abundance of gaseous envelopments, but its deposition occurred at lower temperatures also. Also characteristic is the fact that in redeposition the siliceous substance reacted strongly on the surrounding hornfels rocks; this is indicated by the replacement by the hydrothermal grainy quartz of the plagioclase-diopside hornfels, and by signs of corrosion and disintegration.

Calcite as a hydrothermal mineral is very widely developed and is a product of the mobilization and redeposition by hydrothermal solutions of the soluble substances of sedimentary carbonaceous rocks. It forms thin sections of veins in associations with hydrosilicates of calcium, quartz, hydrothermal wollastonite, serpentine, hematite and other minerals. It is also encountered in skarns, ores and hornfels, in the form of carbonization sections, or small lens-shaped isolations of a coarse grained structure together with sulphides, chlorite, and epidote.

Encountered as a scarce, scattered impregnation in magnesio ferrite ores is apatite, which forms short, prismatic or long prismatic, white, rose or gray idiomorphic crystals, which are 1 - 2 mm long. The indexes of refraction of the mineral are: $N_m = 1.636 \pm 0.003$; $N_p = 1.632 \pm 0.003$; $N_m - N_p = 0.004$. It corresponds to fluor-apatite.

Hillebrandite -- $\text{Ca}_2\text{SiO}_4 \cdot \text{H}_2\text{O}$. The mineral was first found in the Soviet Union. It forms fibrous aggregates or sparse, thin intersecting veins in spurrite-merwinite marbles, or it replaces wollastonite. Very often it forms radiate fibrous aggregates (Fig. 20), or it is encountered in elongated fibrous grains



Fig. 20. Radiate aggregates of hillebrandite enveloping calcite and wollastonite.

up to 3 mm in dimension. The color is white or light yellow. In solid aggregates the mineral forms porcelainous masses. Specific gravity 2.8 (with a small admixture of wollastonite).

The optic axial plane coincides with (010), N_g coincides with [001] (the mineral crystallizes in a rhombic system (9.97). $2V = -55^\circ$, $r < v$. The indexes of refraction are $N_g = 1.616 \pm 0.003$; $N_p = 1.608 \pm 0.003$; $N_g - N_p = 0.008$. Customary are blue anomalous interferential colors. Elongation positive.

The interplanar distances of hillebrandite are given in Table 17. Spectrophotometrical measurements in the infrared region gave a spectrum of absorption similar to the spectrum of standard hillebrandite. The presence of hydrogen association in the region of $3,600 \text{ cm}^{-1}$ supports the presence of water entering in the crystalline grid of the mineral¹⁾. The mineral associates with hydrothermal calcite, wollastonite and axinite. Hillebrandite is a product of

1) Studies made in the IG and G SO AN SSSR.

the disintegration of spurrite, tilleyite or wollastonite. In some instances it completely replaces wollastonite pseudomorphs through silicilite concretions (wollastonite "nuclei"), forming thereby "secondary" pseudomorphisms which are characterized by a whitish color and dense structure.

In some intersecting veins (1-2 mm thick) in marbles the larnite-merwinite-spurrite subfacies is found in associations with hydrothermal calcite mineral similar to hillebrandite but differing from it in its indexes of refraction, double refraction, and other respects. This mineral forms parallel fibrous or matted fibrous aggregates, as well as radiate fibrous and sheaf-like growths. Individual fibres are not over 0.3 mm in size. The veins of this mineral were also found in non-metamorphosed limestones rather far from the contact of the Anakit massif (110-150 meters) where it forms monomineral streaky accumulations (without admixtures of calcite).

Table 17

Results of Roentgenostructural Analysis of Hillebrandite¹⁾

<i>I</i>	$\frac{d}{n}$	<i>I</i>	$\frac{d}{n}$
3	3,488	1	1,868
3	3,286	5	1,815
2	3,229	6	1,750
10	3,030	1	1,680
1	2,823	1	1,651
3	2,720	1	1,620
4	2,466	6	1,598
4	2,284	3	1,526
5	2,160	4	1,467
1	2,010	3	1,456
1	1,966	6	1,360
		3	1,210

Conditions exposure: Co - anticathode; D = 57.3 mm; λ = 1.78529 kX; I = 11mA; U = 37 kV. Radiation filtered. Corrections made according to combined graph of KCl and chlorite. Exposure time 19 hours. Intensity according to 10-point scale.

¹⁾ Results were obtained by a roentgenostructural analysis laboratory of IG and G, SO AN SSR.

Table 18

Results of Roentgenostructural Analysis of Hillebrandite¹⁾

<i>I</i>	$\frac{d}{n}$	<i>I</i>	$\frac{d}{n}$
33	3,42	44	1,631
23	3,29	9	1,572
34	2,92	21	1,535
54	2,73	48	1,508
67	2,55	36	1,431
15	2,38	17	1,413
21	2,15	13	1,354
19	2,05	19	1,321
30	1,983	11	1,265
23	1,684		

Conditions exposure: CU - anticathode; λ = 1.537 kX; I = 10 mA; U = 35 kV. Radiation filtered. Exposure made on URS-50 i diffractometer.

¹⁾ Results were obtained by a roentgenostructural analysis laboratory of IG and G, SO AN SSR.

The indexes of refraction of the mineral are: $N_g = 1.538 \pm .003$; $N_p = 1.528 \pm .003$; $N_g - N_p = .009 - .012$. Direct extinction (pryamoye-ugasaniye) is a characteristic feature. Elongation coincides with N_g , axis N_p is perpendicular to cleavage (perfect cleavage). Specific gravity 2.4. Possibly the mineral is a gyrolite with the mixture: $Ca_4(OH)_2Si_6O_{15} \cdot 3H_2O$ [9].

Sphene is a rather widely distributed mineral, especially in hornfels rocks in the contact zones of the Anakit massif. It sometimes forms rather large (up to 1 cm in length) lengthy prismatic crystals; however, more frequently it is encountered as irregular or coarsely isometric grains not over 2 mm in size. The grains are often sinuous or have circular boundaries. Color brown or reddish. Ordinarily shows marked pleochroisms from reddish (N_g) to colorless (N_p). The mineral forms scattered impregnations in hornfels, associating with hydrothermal quartz, prehnite, epidote and chlorite.

Sphene is found also in erupted rocks: granophyres, dolerite-pegmatites, and hybrid rocks, together with actinolite, quartz, and others.

Axenite forms flat, wedge-shaped crystals or plate-like aggregates in hydrothermal veins together with calcite, hillebrandite, zeolite, and others.

The mineral is white, light gray, or yellowish in color and has a glassy luster. Hardness 7. Has perfect cleavage along (100) and imperfect along (001). Specific gravity 3.3; mineral optically negative. $2V = 70^\circ$, $r < v$. Indexes of refraction: $N_g = 1.685 \pm 0.003$; $N_p = 1.668 \pm .003$; $N_g - N_p = .015 - .018$. Wavy extinction is characteristic.

The interplanar distances of axinite are given in Table 18. Hydrothermal wollastonite has limited distribution forming columnar and tablet formed grains in association with hillebrandite and calcite.

Actinolite is a rather widely distributed mineral encountered in considerable quantities both in eruptions and in contact-metamorphosed hydrothermal

changes of rocks. It forms dense masses or together with other minerals it is found in veins and veinlets, as well as in pockety segregations.

Ordinarily dark green in color. The grains are long prismatic, needle-like, hairlike, as well as radiate, columnar or felt-like accumulations. The indexes of refraction are variable: $N_g = 1.66 - 1.68$; $N_p = 1.64 - 1.66$. (Sometimes we encounter minerals with higher indexes of refraction: $N_g = 1.706 \pm .003$; $N_p = 1.682 \pm .003$; $N_g - N_p = 0.024$). The angle $cNg = 14 - 18^\circ$, $2V = - 72^\circ$. The varieties with high indexes of refraction are transitional to ferroactinolite ($2V = - 80^\circ$) and radiate hornfels. Pleochroism with blueish-green coloring along N_g and light yellow along N_p is characteristic.

In some skarns we find sections which are made up of prismatic grains of radiate hornfels of the hastingsite variety ($N_g = 1.72$, $N_p = 1.70$). Amphiboles of the hydrothermal stage associate with various minerals: epidote, prehnite, chlorite, hematite, quartz, zeolites, etc. Here and there, along with them earlier minerals of the skarn stage are found including garnets, pyroxenes, and magnetite.

Epidote usually forms veins and veinlets or impregnations of fine grains. Crystals of this mineral are columnar in appearance; in aggregates they are irregular, isometric grains. It is found in small druses with calcite and sulphides. The mineral associates with quartz, hematite, prehnite, calcite and sphene.

Color of epidote is green to dark green. Indexes of refraction are: $N_g = 1.771 \pm .003$; $N_p = 1.737 \pm .003$; $N_g - N_p = 0.034$. $2V = - 72^\circ$. Characteristic is a strong pleochroism from yellowish green to colorless. In its optical properties epidote is close to pistacite. However, there have been found less ferrous varieties of this mineral: $N_g = 1.750 \pm .003$; $N_p = 1.723 \pm .003$; $N_g - N_p = 0.027$. Less ferrous varieties of epidote associate with

quartz, calcite, prehnite, and the like whereas pistacite is found together with actinolite among hydrothermally changed pyroxene-garnet skarns.

Well developed in the rocks of the exocontacts is prehnite. This mineral forms veins or rather extensive sections of prehnitization. It is most often found in the hornfels and in erupted rocks, especially in hybrid shonkinites and dolerite-pegmatites. It replaces the feldspars intensively forming radiate fibrous aggregates or tabular irregular grains. In veins prehnite forms lamelliform aggregates. Color white or yellow. Clear cleavage along (001). Elongation negative. $2V = + 68^\circ$. Indexes of refraction: $N_g = 1.645 \pm .003$; $N_p = 1.617 \pm .003$; $N_g - N_p = 0.028$. Frequently found together with epidote, calcite, quartz, amphiboles, and sphene.

Several varieties of chlorites are formed as a result of hydrothermal activity. The chlorites are one of the latest mineral formations replacing the amphiboles, serpentines and others. They are encountered in finely squamate aggregates, radiate fibrous growths, spherulites, dense flaky masses, etc. The composition and optical properties of chlorites are subject to marked variations. The color changes from white to dark green, almost black. The indexes of refraction change from $N_m = 1.58$ to $N_m = 1.63$. Double refraction amounts to $0.007 - 0.010$.

The least ferruginous variety, apparently, is the white or light yellow chlorite which replaces serpentine and forms powdery or cotton-like tangled fibrous aggregates. From the optical properties and roentgenogram (Table 19, sample 1) it corresponds to the intermediate variety in the series of pennine clinochlores (similar to leichtenbergite): $N_g = 1.582 \pm .002$; $N_p = 1.575 \pm .002$; $N_g - N_p = 0.007$. Direct extinction in the mineral with negative elongation.

Magnesian-ferruginous chlorite, dark green in color is found in spherulitic aggregates with quartz within the confines of the previously mentioned hydrothermally processed horizon of quartz sandstones. Indexes of refraction

are: $N_g = 1.629 \pm .003$; $N_p = 1.624 \pm .003$; $N_g - N_p = 0.005 - 0.007$. The interplanar distances of this chlorite are given in Table 19, sample 2. Some varieties of chlorite with indexes of refraction on Nm from 1.610 to 1.590 were encountered in skarns, veins, pocketed veinlet formations in associations with actinolite, quartz, calcite, and epidote. Chlorite in fibrous aggregates often forms impregnations, recesses and veinlets in hornfels with quartz, sphene, epidote, and prehnite. Chlorite develops intensively in pyroxenes of erupted rocks (ferrogabbro, dolerite-pegmatites), as well as in the previously formed amphiboles.

Serpentine usually forms margins 5-10 cm thick (sometimes up to 2.5 m.) in contacts with traps. Sometimes it forms metasomatic veins together with diopside or without it. It is rather widely distributed in magnesioferrite ores and is formed during the replacement of forsterite.

Table 19

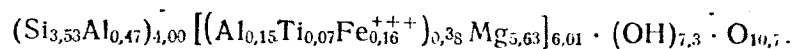
Results of the Roentgenostructural Analysis of Chlorites ¹⁾

Sample 1		Sample 2	
I	$\frac{d}{n} \alpha$	I	$\frac{d}{n} \alpha$
10	7.55	10	13.84
8	4.74	10 _{AB}	7.00
9	3.64	6	4.68
2	2.86	10	3.54
9	2.56	5	2.83
8	2.46	3	2.65
5	2.27	7	2.52
4	2.09	6	2.40
7	2.01	1	2.23
2	1.883	1	1.86
2	1.828	1	1.663
4	1.562	8	1.543
9	1.535	3	1.517
5	1.394	1	1.472
5	1.318	1p	1.413
4	1.286	1	1.320

Exposure conditions: Fe - anticathode; D = 57.3 mm; $\lambda = 1.9320$ kX; I = 11 mA; U = 37 kV. Radiation filtered. Corrections made using combined graph of KCl and chlorite. Exposure time 15 hours. Intensity according to ten-point scale.

1) Analysis made in the roentgenostructural laboratory of IG and G SO AN SSSR.

Serpentine is fibrous-laminated or fibrous in structure and is greenish-yellow or dark green in color. It always associates with calcite. An incomplete chemical analysis of the monomineral fraction of serpentine showed the presence of Al_2O_3 -- 2.5% and Fe_2O_3 (gross) up to 7.5% (percentile weight¹⁾). The indexes of refraction of the mineral are as follows: $N_g = 1.565 \pm 0.002$; $N_p = 1.561 \pm 0.002$; $N_g - N_p = 0.004$. This mineral may be referred to the ferruginous-aluminiferous serpophtes [24, 47]. Analysis of serpentines associating in magnesio-ferrite ores in the contact of the Anakit massif was given in a paper by N. V. Pavlov [38]. Conversion of the analysis into a crystallo-chemical formula gave the following results:



Hence, this mineral is classed with the serpentino-chlorites according to the classification of D. P. Serdyuchenko [47].

Serpentine is usually replaced by the chlorites.

Zeolites are the latest mineral formations in the hydrothermal stage. They are represented mainly by the calcium-sodium varieties: thomsonite and chabasite. These are distributed mainly in the traps (dolerite-pegmatites) subjected to hydrothermal changes. However, in individual instances they were found in small druse hollows not far from the contact of the massif with coarse-crystalline calcite. Thomsonite forms transparent lamelliform grains up to 1 mm in length with the following indexes of refraction: $N_g = 1.522 \pm .003$; $N_p = 1.510 \pm .003$; $N_g - N_p = 0.020$. Optically positive; $2V = 53^\circ$. Visual plane axis perpendicular to elongation. Chabasite forms white, cubic shaped crystals. Their dimension does not exceed 2 mm. The indexes of refraction are: $N_g = 1.490 \pm .003$; $N_m = 1.487 \pm .003$; $N_g - N_m = .003 - .004$.

1) Analysis made in the chemical-analytical laboratory of IG and G SO AN SSSR.

Minerals of the Hypergene stage are extremely limited in distribution. They are represented by chalcocite, covellite, and bornite which replace chalcopyrite as veinlets. Likewise associating with them are malachite and azurite which form thin sinter incrustations and earthy aggregates along cracks in the limestones. In the magnesioferrite ores and in hornfels rocks one finds earthy accumulations of limonite. Limonite also replaces pyrite and pyrrhotite, forming pseudomorphs in these minerals.

V. CONDITIONS FOR THE FORMATION OF EXOCONTACT ZONE ROCKS IN THE ANAKIT MASSIF

The complex of contact metamorphogenic minerals formed near the incurrent canal of the Anakit trappean intrusion is typical and a very characteristic example of high temperature mineral associations of larnite-merwinite-spurrite subfacies of the sanidinite facies of metamorphism. The minerals in this subfacies show up at very high temperatures (maximum for contact metamorphism) and low pressures (ordinarily minimal).

Tridymite, as we know, can form outside the limits of its stability field in the recrystallization of glass, but in contact-metamorphic processes the formation of this mineral occurs within the region of its stability, i.e., at temperatures in excess of 870° which gives, thus, a lower limit of temperature of metamorphism for atmospheric conditions. This limit should be increased to 950°C (Fig.21) for pressures of the order of 350 atmospheres (according to Ostrovskiy, Mishina, and Povilaytis [37]), which corresponds approximately to a depth of about 1300 meters (established by the addition of the thicknesses of Paleozoic deposits and stratified intrusive bodies of older traps -- the Noginskiy intrusive complex -- of the area under study). Consequently, the lower limit of temperature of the contact metamorphism in the vicinity of the incurrent canal of the Anakit massif, determined by the equiponderant tridymite -- quartz curve, corresponds to $940-950^{\circ}\text{C}$.

Fig. 21. PT projection of the silica-water system [37].

Legend: a) Tridymite-crystobalite;
b) Tridymite-quartz;
c) crystobalite-quartz.

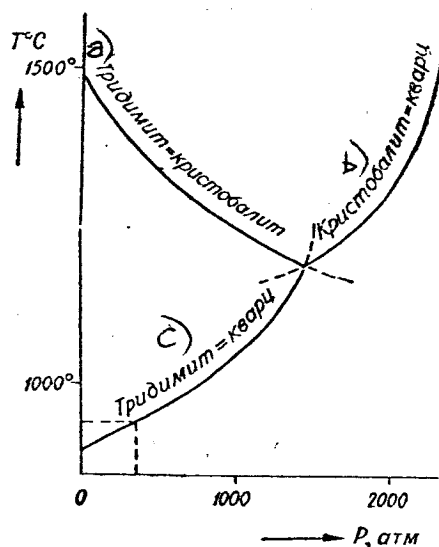
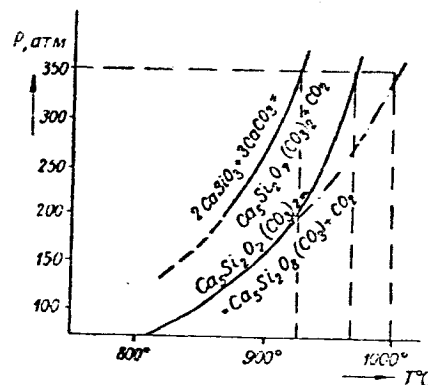


Fig. 22. Curves of monovariant equiponderance of spurrite and tilleyite: - - - equiponderant curve by Harker (1959); - - - - ditto according to Harker and Tuttle (1957).



Through the experimental work done by Tuttle and Harker in 1957, it was established that the reaction in the formation of spurrite



for a pressure of 350 atm may be carried out at temperature of not less than 1000-1020°C (Fig. 22) [92]. Sometime later, R. I. Harker expressed doubt in the accuracy of the limits of the spurrite (and tilleyite) fields of stability in the 200-350 atm region, and he lowered for these pressures the lower temperature limit for the synthesis of spurrite [71]. According to Harker, for a CO₂ pressure of 350 atm spurrite should appear at temperatures not under 970-980°C (cf. Fig. 22). Taking into account both figures, because in a final solution of the problem it is essential to set up additional experiments, we can state with conviction that the lower limit for the formation of spurrite at a pressure of 350 atm is in the interval of 970-1020°C.

The investigation of R. I. Harker conducted in 1959 showed that tilleyite is formed at somewhat lower temperatures than spurrite (cf. Fig. 22). At pressures of 350 atm the field of stability lies in the temperature interval from 930 to 1020°C [71]. Inasmuch as tilleyite is formed in the contacts of the Anakit massif from the spurrite in conformance with the reaction:

$\text{Ca}_3\text{Si}_2\text{O}_7(\text{CO}_3) + \text{CO}_2 \rightleftharpoons \text{Ca}_3\text{Si}_2\text{O}_7(\text{CO}_3)_2$, it can appear only if the temperature drops below the lower limits of the stability field of spurrite, i.e., 970-1020°C (at a pressure of 350 atm). Consequently, the maximum temperature of contact metamorphism somewhat exceeded these figures because in the exocontact massif not only tilleyite, but also spurrite were formed.

On the basis of these data, it can be concluded that the lower limit of temperature of metamorphism in the exocontacts of the Anakit trappean massif in the vicinity of the incurrent canal is approximately at 1000°C. The upper limit of the temperature of contact metamorphism in the immediate vicinity of the massif is determined by the temperature of the trappean magma (cf. below).

Characterized by somewhat lower temperatures are the lower limits of stability of monticellite and melilite. According to Tuttle and Harker, at a pressure of 350 atm, monticellite is formed in accordance with the reaction: $2\text{CaCO}_3 + \text{Mg}_2\text{SiO}_4 + \text{CaMgSi}_2\text{O}_6 \rightleftharpoons 3\text{CaMgSiO}_4 + 2\text{CO}_2$, at temperatures not below 800-820°C [73]. Akermanite, according to these authors appears as a result of the interaction of calcite and diopside: $\text{CaCO}_3 + \text{CaMgSi}_2\text{O}_6 \rightleftharpoons \text{Ca}_2\text{MgSi}_2\text{O}_7 + \text{CO}_2$ [73].

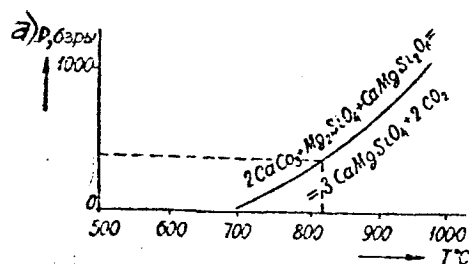


Fig. 23 - Legend: a) P, bars.

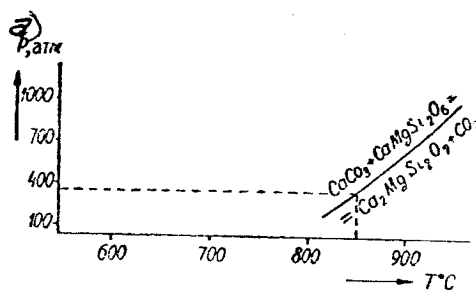


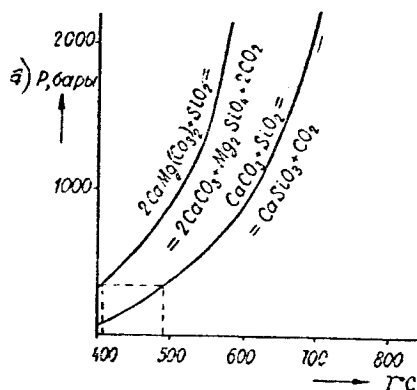
Fig. 24 - Legend: a) P, atm.

At a pressure of 350 atm, the latter reaction takes place at temperatures of not less than 850°C (Fig. 24). However, these figures cannot describe the maximum temperature of metamorphism because monticellite and tilleyite are stable in a broad temperature interval and could form at temperatures above their own lower limits of stability, i.e., at 1000°C. Their appearance in the contact marbles is due to the composition of the original sedimentary rocks and by no means can be regarded as a consequence of lower temperatures of contact metamorphism. In progressive metamorphism monticellite and melilite (akermanite) should appear sooner than spurrite and other high temperature minerals like merwinite, for example, which generally agrees with the results of observations: monticellite and melilite are somewhat eroded by later minerals (spurrite, merwinite, and others); this is not always observed, however.

From the associations of forsterite and wollastonite in the exocontact zone of the massif located 500-700 meters from the incurrent canal we can determine the temperature of metamorphism which exists in this portion of the contact at the moment of formation of forsterite calciphyres and hornfels rocks. The temperature of formation of wollastonite at a pressure of 350 atm is approximately equal to 480-500° (lower temperature limit) (according to Danielson [65]). The lower temperature limit of the formation of monticellite due to the interaction of forsterite and diopside, as we have already indicated, is 800-820°C at this same pressure. However, since monticellite is not formed and forsterite is quite stable in associations with diopside (forsterite is formed at pressures of 350 atm at temperatures not under 400°), we can conclude that the temperature of the exocontact interaction in this section did not exceed 800°C. The lower limit of temperature of metamorphism is determined from wollastonite: 480-500°C. Thus, at a distance of 500-700 meters from the incurrent canal the temperature in the contacts of the Anakit

trappean massif drops from 1000 to 500-800°C (we have direct contacts in mind).

It is interesting to note that the temperature in the contact of the massif near the incurrent canal is only slightly lower than the temperature of the trappean magma. The latter is determined by the temperature of formation of very extensively distributed eutectic intergrowths of monoclinical pyroxene and plagioclase. The temperature of the "dry" diopside-plagioclase eutecti containing 58% anorthite (plagioclase of such composition is usually found in micropegmatite intergrowths with pyroxene) is determined from the triple diagram of diopside-albite-anorthite [15] to be 1215°C. Introducing a correction for the pressure of water vapor at 350 atm, taking into account the data of Joder [99], we reduce the temperature to 1160-1170°C. Then, taking into account the content in pyroxene of 25-27% hedenbergite molecules



Legend: a) P, bars.

Fig. 25

and using the data of Fogt and Sobolev [49] regarding the linear relationship between the fusion temperature of pyroxene and the amount of iron in it, we again lower the eutectic temperature by 70°. In summary, the eutectic temperature of crystallization is 1100°. The crystallization temperature of earlier differentiates was somewhat above this figure, while the temperature

of crystallization of the later differentiates was lower. But as a whole, the temperature of the trappean magma near the incurrent canal was in the region of 1050-1150°C, and this determines the upper temperature limit of contact metamorphism. Intruding as layers inside the Paleozoic stratum, south of the incurrent canal, the magma quickly loses its heat, giving it off to the enclosing rocks. In consequence of the intensive loss of heat occurring during the process of movement (pressing out) of the magma in surface conditions, the metamorphic action on the exocontact rocks weakens, and this is expressed in the appearance at 700 meters from the incurrent canal of mineral complexes of a lower temperature facies of metamorphism; due to the profound cooling of the trappean magma in the process of intrusion there are two facies of contact metamorphism in the exocontact zones of the Anakit massif: the sanidinite and pyroxene-hornfels. These facies, which appear as a result of the same original rocks, reflect the temperature drop along the strike of the contact of the trappean massif. It is testimony, mainly, of the decreased amount of heat in it rather than a lowering of the magma temperature, even though the magma temperature is also lowered.

The more important mineral paragenetic associations of pyroxene-hornfels facies are the following. Associations with excess SiO_2 are not characteristic for this facies or the sanidinite facies. Quartz, if present, is usually a relict mineral and is not in equilibrium with other mineral phases, with rare exceptions. Associations with an insufficiency of SiO_2 are represented by the following derivatives: 1) dolomitic marls, and 2) calcareous and dolomitic aleurolites and sandstones. Metamorphic rocks formed from dolomitic marls are characterized by more important associations as: a) calcite-forsterite-diopside-phlogopite, and b) calcite-wollastonite-diopside. Metamorphic rocks formed from calcareous and dolomitic aleurolites and sandstones are characterized by the following associations: a) diopside-

plagioclase-glossular, and b) calcite-diopside-plagioclase.

The more important mineral paragenetic associations of the sanidinite facies are the following. In the case of hornfels rocks formed from calcareous and dolomitic aleurolites and sandstones: a) wollastonite-plagioclase-pyroxene (diopside-hedenbergite) - calcite; b) wollastonite-hedenbergite-pyrrhotite; c) diopside-phlogopyte-lusite-plagioclase-quartz - (sanidite-phlogopyte). For marbles of a larnite-merwinite-spurrite subfacies formed from calcareous marls with a certain admixture of free silica and dolomite: spurrite-merwinite-tilleyite-melilite (helenite-akermanite) - calcite-pyrrhotite. The following association is characteristic of this subfacies: wollastonite-tridymite; it is formed in the metamorphism of silicilate concretions.

Metamorphic rocks formed from dolomitic marls and siliceous dolomites under conditions of a larnite-merwinite-spurrite subfacies are characterized by an association of monticellite-melilite (akermanite) - merwinite-calcite. All these associations with the exception of the wollastonite-tridymite association are formed when there is an insufficiency of SiO_2 .

The main parageneses of high temperature hornfels rocks of a sanidinite facies are described in Fig. 26 as two tetrahedrals at the apex of which are the following components: $\text{CaO} - (\text{Mg, Fe})\text{O} - \text{SiO}_2 - \text{Al}_2\text{O}_3$ and $\text{MgO} - \text{K}_2\text{O} (+\text{Na}_2\text{O}) - \text{SiO}_2 - \text{Al}_2\text{O}_3$. In the first figure there are described mainly the paragenetic relationships with wollastonite, pyroxene, plagioclase, and others, while in the second we have associations with alkali-bearing minerals (containing potassium mainly). The bonding nodes between these two artificially segregated groups of parageneses are andalusite and the SiO_2 peak of the tetrahedron.

Critical minerals for hornfels rocks of sanidinite facies are tridymite and sanidine containing a certain amount of sodium. The temperature of

formation of sanidinite was, in any event, over 700°C [15, 56].¹⁾ A characteristic peculiarity of the facies is paragenesis of hedenbergite-iron-bearing wollastonite, which was first described by Professor Tilley in contaminated dolerite from Scot Hill, Ireland [88]. In hornfels from

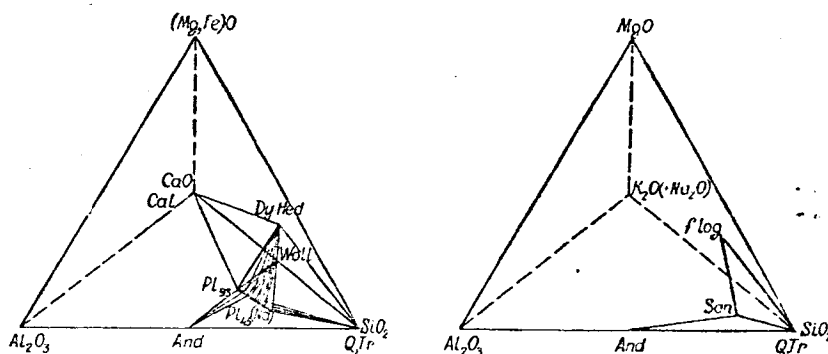


Fig. 26. Parageneses of hornfels of sanidinite facies for exocontacts of the Anakit massif.

contacts of the Anakit massif wollastonite, associating with hedenbergite, contains small amounts of ferrosilite (8-9% judging from the index of refraction), but in this case the thing that is important is the fact of such a paragenesis testifying to its high temperature character.

Extremely interesting is the problem of andalusite which is, as we all know, a relatively low temperature mineral, especially in conditions of lower pressures (up to 1500 atm), and it is encountered mainly when there is a pyroxene-hornfels facies. In the Anakit contacts it is encountered in the hornfels of sanidinite facies of metamorphism, i.e., in rocks which formed at somewhat higher temperatures. Ordinarily, in a sanidinite facies mullite is formed instead of andalusite, but the former was not detected in exocontact rocks, despite the meticulous search made. Incidentally, this discovery of

¹⁾ In the Anakit contacts, sanidine undoubtedly was formed at higher temperatures.

andalusite in contacts with traps is not the only one; Lebedev found this mineral in the basin of the Podkamennaya Tunguska River in associations with minerals of sandstone tuffs [26]. However, the conditions which existed at the time of formation of these andalusite-containing hornfels might have been not so high in temperature as in our case.

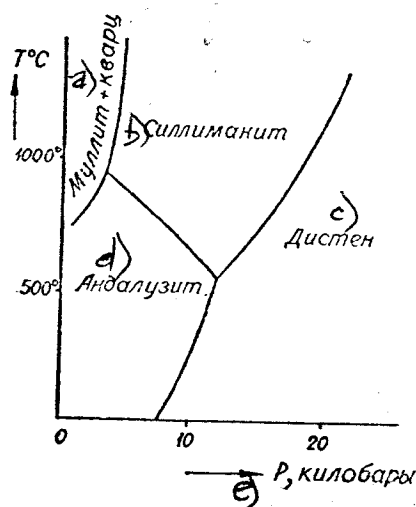


Fig. 27. PT-diagram of equilibrium in the $\text{Al}_2\text{O}_3 - \text{SiO}_2$ system [15].

Legend: a) mullite and quartz; b) sillimanite; c) disthene; d) andalusite; e) P, kilobars.

Taking into account the data on the stability of andalusite [15, 51], we can assume that this mineral is not stable in a sanidinite facies, particularly because thus far there is not enough data which might point to the contrary.¹⁾

Probably, in the Anakit exocontacts andalusite is preserved as a relict mineral phase which points to lower temperatures of progressive metamorphism

¹⁾ Indisputable evidence about the stability of andalusite in a sanidinite facies of metamorphism is the detection of interstratification of andalusite horizons with spurrite marbles or the direct paragenetic association of andalusite with tridymite.

in the earlier stages of conversion of sedimentary rocks (condition of pyroxene-hornfels facies) because not all the quartz is converted into tridymite. However, in this case, if andalusite is stable under conditions of contact zones in the Anakit massif, then its stability should probably be extended to 1000° at pressures of 350 atm. In this case, the PT diagram of equilibrium for the $\text{Al}_2\text{O}_3 - \text{SiO}_2$ system (Fig. 27), developed by Sobolov, the area of stability of mullite will approach the axis of temperature in the interval $700-1000^{\circ}\text{C}$.

The most important paragenetic associations of marble in sanidinite facies are shown in Figs. 28 & 29, in the lower left angles of triangles for the paragenesis composition $\text{CaO} - \text{SiO}_2 - \text{Al}_2\text{O}_3$ and $\text{CaO} - \text{SiO}_2 - \text{MgO}$. Shown in these triangles are certain associations of pyroxene hornfels facies.

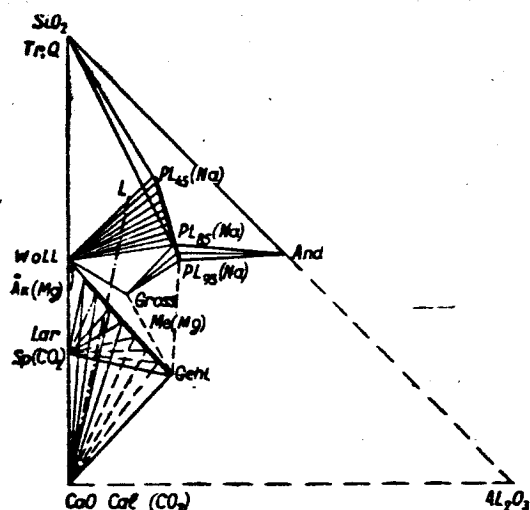


Fig. 28

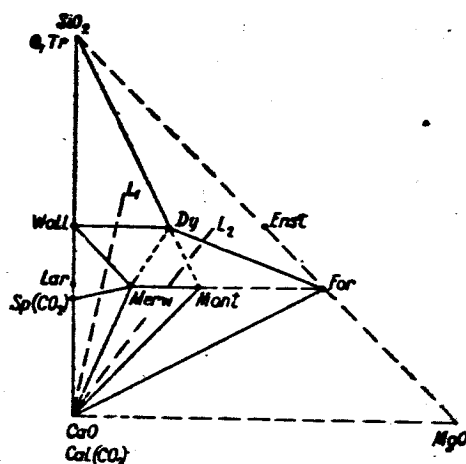


Fig. 29

Similar composite diagrams of paragenesis-composition were made in 1937-1940 by Korzhinskiy [21, 22]; they were based partially on data obtained from dry fusions [plavok] by Rankin and Wright [42] and others. Certain differences observed of concrete parageneses of Anakit contacts to the diagrams made by Korzhinskiy are expressed in the presence of CO_2 , at

least in associations described in the diagrams. The result of this is the appearance of parageneses with calcite instead of parageneses with corundum and calcium aluminate and periclase ([22], cf. Figs. 13 and 14).

The difference consists also in the presence of spurrite (and the absence of larnite) and in replacing the sillimanite node with andalusite in the $\text{CaO-SiO}_2\text{-Al}_2\text{O}_3$ triangle, and in replacing the associations of grossular-quartz with a paragenesis of wollastonite-plagioclase, which is quite common in hornfels rocks of exocontact zones.

The composition-paragenesis diagrams of $\text{CaO - Al}_2\text{O}_3 - \text{SiO}_2$ and CaO - MgO - SiO_2 were used by Korzhinskiy for the "theoretical determination of sequence in the decomposition of individual calcic compounds and minerals in the gradual increase of CO_2 pressure [22, page 41]. Moreover, the CO_2 pressure is regarded mainly as a function of the depth (overall hydrostatic pressure and load pressure) under relatively constant temperature conditions. According to Korzhinskiy, carbonization of associations in the $\text{CaO-Al}_2\text{O}_3\text{-SiO}_2$ and CaO - MgO - SiO_2 systems with increased depth (with an increased CO_2 pressure) should proceed in the direction of decreasing calcite content [22, page 41]. Apparently a similar effect should occur in these systems of composition and paragenesis not with an increase in the pressure (at constant temperature), but as a consequence of a decrease in the temperature (at relatively constant pressure). We reach this conclusion not only on the basis of analysis of natural parageneses, but also in considering curves of a monovariant equilibrium for decarbonization reactions [22, 70, 36] with a positive slope that inclines toward the lower pressures.

In decarbonization, reactions CO_2 can without difficulty be removed from the system, i.e., its mass is variable, but the chemical potential CO_2 is determined strictly for each of the selected values of P and t° (given fixed pressures the temperature will be determined and the reaction will

become stable) [36, page 100]. It means that at constant P the chemical potential μ_{CO_2} is determined entirely by a change in the temperature. Since μ_{CO_2} and t° are related inversely, the chemical potential CO_2 will generally increase with a decrease in temperature at a constant P (if the CO_2 concentration will not drop with unusual speed in the process). The pressure and chemical potential are generally tied in by a direct relationship (at relatively constant temperature). The sequence of reactions of carbonization will be determined by an increase (or decrease in the case of decarbonization) in the chemical potential μ_{CO_2} ; as a result of this there will be a decrease in CaO content in the products formed (an increase in the case of decarbonization). Thus, on the basis of a direct analysis of the functional relationship of the chemical potential of CO_2 to the intensive factors of equilibrium [23] one generally can note the change in mineral parageneses which is established when making observations of natural objects and in experiments.

To determine the sequence of decomposition of calcite minerals with an increase in CO_2 pressure, Korzhinskiy made use of "beams" emanating from the CaO angle of composition-paragenesis diagrams and which are characterized by a constant relationship of $\text{SiO}_2 : \text{Al}_2\text{O}_3$ or $\text{SiO}_2 : \text{MgO}$ correspondingly for each beam. This method may be applied in our case to establish the sequence of decomposition (or synthesis) of minerals in temperature drops (or increases) (at relatively constant pressures).

In Fig. 29 there are two rays -- L_1 and L_2 -- drawn from the vertex CaO. Following the ray from the vertex CaO we first run through the field of the highest temperature associations of Anakit exocontact spurrite-merwinite-calcite (original chemical potential of CO_2 at the point CaO is high enough to effect complete carbonization of lime with the formation of calcite). Approximately at these same temperature conditions of the contacts there is

a merwinite-spurrite-wollastonite association. With the increased chemical potential of μ_{CO_2} the beam intersects the line corresponding to the paragenesis of wollastonite-merwinite and hits the wollastonite-merwinite-diopside field. The association of wollastonite with diopside subsequently displaces the paragenesis of wollastonite-merwinite, an action due to the reaction of merwinite + $\text{CO}_2 \rightleftharpoons$ diopside + calcite; the correctness of this was established by a number of investigators [22,63]. The association of diopside-wollastonite-quartz is stable within a wide interval of temperatures and is encountered also in pyroxene-hornfels facies of contact metamorphism.

Further extending beam L_1 we reach the region of still lower temperature parageneses where it is impossible to form wollastonite: wollastonite + $\text{CO}_2 \rightleftharpoons$ calcite + quartz.

In considering beam L_2 we will establish that as we draw away from the CaO vertex the paragenesis of calcite-merwinite-monticellite of the sanidinite facies of metamorphism is replaced by the paragenesis of monticellite-diopside-(calcite), and then instead of the paragenesis of monticellite-diopside-(calcite), there appears the association of diopside-forsterite-(calcite) in conformance with the reaction of monticellite + $\text{CO}_2 \rightleftharpoons$ calcite+diopside+forsterite. The paragenesis of forsterite with diopside are typical of the pyroxene-hornfels facies and it is unstable at high temperatures.

We will now look at Fig. 28. In the composition-paragenesis triangle, there is drawn the beam L from the CaO vertex. Utilizing this beam we shall see that in moving from angle CaO we again come in contact with the higher temperature associations of spurrite-melilite-calcite which form under conditions of larnite-merwinite-spurrite subfacies of the sanidinite facies of metamorphism. Corresponding to this facies is the association with the lesser content of CaO: spurrite-melilite-wollastonite, which changes the preceding paragenesis. As we draw further down along the beam from the CaO

vertex we shall see that spurrite is unstable in all associations in conformance with the reaction $\text{spurrite} + \text{CO}_2 \rightleftharpoons \text{wollastonite} + \text{calcite}$. The wollastonite-melilite-calcite reaction is stable at lower temperatures than paragenesis with spurrite and it is formed at higher μ_{CO_2} . Corresponding to a still lower temperature is the paragenesis of wollastonite and plagioclase with grossular which occurs in rocks with pyroxene-hornfels facies. Associations of helenite with grossular are not observed in the Anakit contacts but it is possible. With a further lowering of the temperature, wollastonite becomes unstable (its formation with the given μ_{CO_2} is impossible).

The foregoing demonstrates that with the successive lowering of temperature (increasing the μ_{CO_2}) there is an increase in the amount of calcite in the parageneses until it is possible to have a paragenesis of calcite and quartz, just as is true at high CO_2 pressures. The foregoing shows great similarity to the conclusions of Korzhinskiy made by him on the basis of studies of parageneses of abyssal facies, i.e., with the successive increase of μ_{CO_2} with depth [22]. The phenomenon of change in the mineral parageneses in carbonization (or decarbonization) is determined only by the chemical μ_{CO_2} in which the temperature and pressure changes are reflected.

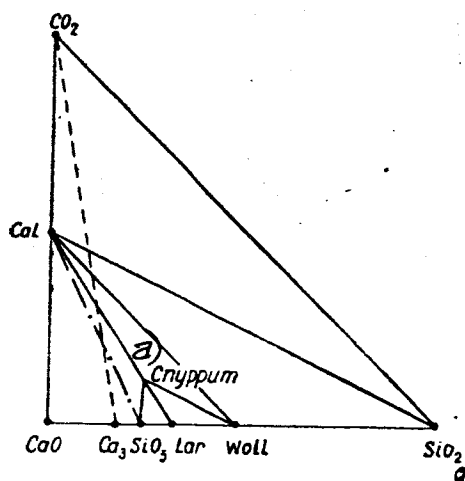


Fig. 30. Legend: a) spurrite.

Shown in Fig. 30 is a diagram of the composition and paragenesis of the $\text{CaO} - \text{SiO}_2 - \text{CO}_2$ system for high metamorphism temperatures according to Korzhinskiy. Making use, to establish the order of carbonization of calcium silicates, of a beam passing through the CO_2 vertex -- the beam is characterized by the constant ratio of $\text{CaO} : \text{SiO}_2$ -- we can note the following change of three mineral parageneses in the increase of CO_2 pressure of lime- Ca_3SiO_5 -calcite, calcite-spurrite- Ca_3SiO_5 , spurrite-wollastonite-calcite, calcite-wollastonite-quartz, and finally quartz-calcite [22]. This diagram in its overall form can also be used to analyze changes in mineral associations with temperature in the case of progressive metamorphism because it reflects the tendency of carbonization in lowering the temperature of exocontacts. However, it does not fully illustrate the change in the parageneses in a temperature drop in the case of regressive metamorphism. Sufficiently well described in Fig. 31 are the associations which appear generally in the regressive replacement of spurrite-containing marbles. In the lowering of temperature which accompanies an increase in the chemical potential of CO_2 there is a replacement of the spurrite-wollastonite-calcite paragenesis by an association of tilleyite-wollastonite-calcite (tilleyite replaces spurrite in conformance with the reaction: $\text{spurrite} + \text{CO}_2 \rightleftharpoons \text{tilleyite}$) and further -- the replacement of the paragenesis with tilleyite by the association with scawtite ($\text{Ca}_4\text{Si}_3\text{O}_8(\text{CO}_3)_2$) which, apparently is in equilibrium, under the given conditions, with calcite and wollastonite [78, 80, 89]. In associations with scawtite such high temperature minerals of the larnite-merwinite-spurrite subfacies like larnite, rankinite ($\text{Ca}_3\text{Si}_2\text{O}_7$) and others are presumably unstable, i.e., it does not belong to the sanidinite facies.

Thus, from the foregoing, it appears that associations of sanidinite facies are formed at maximum temperatures of metamorphosis and minimal values of the chemical potential of CO_2 for the given conditions, whereas associations

of pyroxene-hornfels facies appear at lower temperatures of contact metamorphism and higher values of P_{CO_2} .

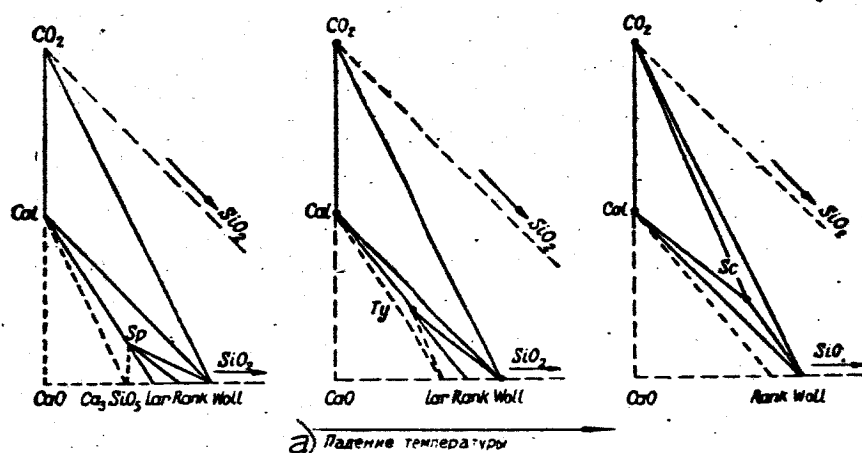


Fig. 31. Legend: a) temperature drop.

We shall briefly consider the kinetics of metamorphic reactions leading to the formation of the above-mentioned associations. Metamorphogenic minerals of high temperature parageneses are formed as a result of a series of consecutive reactions with the presence of clay, free silica, calcite and dolomite components. The reactions occur mainly in the solid phases, but possibly with a certain amount in the gaseous reactions. In consequence of very low pressures "water and other substances with high vapor pressure which ordinarily are important in crystallization and serve as catalyzers of a reaction, are easily removed from a system and do not perform their function" [56, page 455] in the metamorphism of a sanidinite facies. Hence, the chemical conversion of substances accompanied by the appearance of new mineral phases occurs as a result of direct reactions of the hard silicates and carbonate phases, as demonstrated by numerous experiments carried out during the past three decades [6-8, 59].

The most characteristic peculiarity in the reactions between hard substances is the clearly manifested scalariform condition, and the appearance

of numerous intermediate, metastable phases reacting with one another and the original substances even in the more simple situations. For example, in heating a mixture of CaCO_3 and SiO_2 in a 1:1 ratio, there is first formed a double calcium silicate which later combines with the metastable phases $\text{Ca}_3\text{Si}_2\text{O}_7$ and Ca_3SiO_5 ; not until then does CaSiO_3 which appears due to earlier compounds, begin to form [7,59]. Further, in accordance with studies by Berezhnyy, before monticellite and merwinite is formed in the system CaO-MgO-SiO_2 , there is obtained a whole series of intermediate products. Upon synthesizing these minerals, which serve an essential intermediate phase, we get Ca_2SiO_4 . Monticellite, according to Berezhnyy, forms much more quickly than merwinite. If diopside is used as the original product for the synthesis of monticellite, then apparently akermanite [6,7] is formed as the intermediate phase. In the formation of helenite or anortite from appropriate components the original products of the reaction are binary compounds whose action with a third oxide or with one another results in the formation of terminal products [59].

Multiple phases in metamorphic reactions are apparent also in the series of 13 reactions (stages of progressive metamorphism) of Bowen; he established these on the basis of analysis of natural parageneses and the order of their appearance in zonal aureoles of intrusive bodies [63].

Another characteristic of the reactions between the hard phases is the very limited mobility of substances taking part in the metamorphism, and this explains the extraordinarily changeability of the composition of rocks being formed; these fully inherit the chemical composition and peculiarities of distribution of components in the original non-metamorphosed rocks. The speed and completeness of reactions between solid substances is determined: 1) by the speed of the diffusion of particles; 2) the speed of processes on the boundaries of phases which leads to the destruction of the crystalline

lattices of the original substances [59].

Along with this, in the formation of metamorphic products gaseous reactions also play an important part (with CO_2), especially in some instances. It is difficult to estimate how great is the role of the gaseous reactions in each case, but there is no question that in the formation of carbonate-containing silicates of calcium (spurrite, tilleyite), as well as in the recrystallization or formation due to the exchange reaction of calcite (in the absence of water) CO_2 can play a role of primary importance. In the formation of tilleyite from spurrite there is apparently a reaction between the solid and gaseous phases with the appearance of a new solid phase.

We shall consider the metasomatic processes occurring in the contacts of the Anakit trappean massif.

The earliest and highest temperature metasomatic mineral is cuspidine; we place it in this stage on the basis of its close association with garnet and the subsequent universal formation of minerals of contact metamorphism. The temperature for the formation of cuspidine in the Anakit contact was probably about $500 - 700^\circ\text{C}$, because it was at these temperatures that the mineral was recently synthesized, though at somewhat greater pressures -- 1360 atm [93]. If the stability curve of cuspidine is inclined positively toward lower pressures then at a pressure of 350 atm the temperature of its synthesis should not exceed 700°C . The temperature existing at the time of formation of the garnet-pyroxene skarns were below the temperature of formation of cuspidine, but judging from the close space and time factors of andradite and cuspidine they should not differ too much.

In the process of metasomatism there was an addition to the exocontact from the Anakit massif of such components like fluorine, water, iron, silica, and clay. Calcium and magnesium were probably borrowed from the intruding

rocks, as is apparently true of a portion of the SiO_2 , Al_2O_3 , and others.

In the formation of magnesio-ferrite the solutions removed from the trappean massif iron only. This is evidenced by the fact that magnetite with a high content of magnesium cannot become crystallized from basaltic melts even in the first stages of its crystallization because such a magnetite should be in equilibrium with high magnesium content olivine -- practically pure forsterite -- and this is never attained in traps. The highest content magnesium type of olivine which forms from the magma before the other minerals contains 22% of fayalite molecules [49]. Further, "in the initial magma the magnetite molecule is virtually absent and is formed due to a subsequent oxidizing process" [49, page 115]. The crystallizing basaltic melt evolves toward an increase in the relative content of iron over magnesium. This peculiarity has been noted by several Soviet and foreign petrographers; in the Siberian traps it was first found and explained by Sololev [49]. Thus, the terminal differentiates of basalts cannot contain any noticeable amounts of magnesium, a fact which impedes the formation of magnesian magnetite. Magnetite containing an increased amount of magnesio-ferrite molecules usually appears close to the surface [4] from hydrothermal solutions separating from trappean intrusives and having a relatively high concentration of magnesium and iron. It is assumed that the separation of hydrothermal solutions occurred during the lifting of the basaltic magma from the depths to the upper portion of the platform due to the marked drop in external pressure [2]. Without contradicting such a possibility for the Angaro-Ilimsk, Ilimpeysk and certain other deposits of the Siberian platform, we will note that the intrusive source is not the only one from which solutions with a high concentration of magnesium are possible. Apparently, the magnesio-ferrite ores formed in the exocontacts of the Anakit massif by displacing forsterite calciphyres, diopside hornfels, etc., under conditions

of oxidation and sufficiently high temperatures appeared during the process of replacing magnesium from the enveloping rocks. The oxidation conditions make it favorable to oxidize FeO into Fe_2O_3 with the simultaneous replacement of the deficient amount of iron oxide by magnesium oxide [4, 38], which is a part of the lattice of magnetite. The formation of hematite occurs simultaneously with magnesio-ferrite.

The abundant development of serpentine in magnesio-ferrite ores also points to the high quantity of magnesium in the replacement rocks. Serpentine is formed in situ because of forsterite and other magnesium-containing minerals; in the formation of diopside-serpentine metasomatic veins it replaces dolomite.

The most interesting products of hydrothermal activity are epidote and the aqueous silicates of calcium. The presence of epidote testifies to the relatively great depth of formation of the Anakit massif compared with the traps of the surrounding region [49]. However, such abyssophobic minerals like spurrite, cuspidine, hellebrandite, gyrolite and others undoubtedly point to the fact that the formation of metamorphic rocks in the exocontacts of the Anakit massif has occurred at a shallow depth. Apparently, the contact zones of this mass, if are one of several instances where it was possible from the standpoint of pressure for a complex of rocks to form of the sanidinite facies of metamorphism and epidote. This circumstance is supported by the previously cited computations to the effect that the formation of rocks in the exocontact massif occurred at depths of 1200-1300 meters and not in the immediate vicinity of the earth's surface. Apparently these contact rocks are the representatives of those rare cases where the high temperature metamorphism led to the appearance of mineral associations of the sanidinite facies under conditions of relatively great depth (for this facies).

C O N C L U S I O N

Rocks of the exocontact zones of the Anakit-differentiated trappean massif are characterized by their variety of minerals formed over a wide interval of temperatures due to the processes of metamorphism, metasomatism and post-metasomatic hydrothermal activity (temperature in the contacts of the massif changed from 1000 to 100-200°C, i.e., to temperatures at which hillebrandite and hyrolite were formed according to Toropova, Nikogosyan, Mchedlov-Petrosyan, and others [33,57,96 and others]). In the contacts there appears a whole series of interesting mineral associations, but the most important from the theoretical point of view is the complex of calcium minerals of the larnite-merwinite-spurrite subfacies of metamorphism. In connection with this it is interesting to consider the question under what conditions on the Siberian platform in the contact limestones with traps can this subfacies appear. The first condition is the composition of the enveloping rocks; this should generally correspond to marl which apparently contains a certain amount of free silica (limestone rocks low in silica sometimes contain an admixture of dolomite)¹⁾. A second necessary condition is a high temperature in the exocontacts -- a condition produced by the proximity of the incurrent channel of the trappean body. Meeting the first condition in the Siberian platform, apparently, are the lithological peculiarities of the Kochumdeks formation of the Lower Silurian because in the metamorphism of the rocks it was this formation that produced the spurrite marbles in the contacts of the Anakit massif and, probably the mineral associations of the larnite-merwinite-spurrite subfacies found in the Podkamennaya Tunguska

1) The admixture of dolomite is necessary in the formation of magnesium containing high temperature metamorphogenic minerals such as merwinite, akermanite, and others.

River basin [29]. The high temperature of the exocontacts cannot be regionally distributed at shallow depths, hence the mineral complexes of the sanidine facies should appear only in the vicinity of the incurrent channels of trappean bodies where there is a maximum heating of the enveloping rocks at the moment of intrusion. Thus, the most probable region for the distribution of marbles of the larnite-merwinite-spurrite subfacies includes the western edge of the Tunguska syncline (regions of the lower flow of the Podkamennaya Tunguska, Bakhta, Lower Tunguska Rivers) where the Kochumdeks deposits are widely developed. Not excluded, however, is the possibility of finding similar metamorphic rocks in other parts of the surrounding region of the Tunguska syncline in a similar geological situation.

Of course, rocks of the larnite-merwinite-spurrite subfacies can appear in the metamorphism of non-carbonaceous rocks also, such as the clay shales. In that case, in order that they may properly be classed as the sanidine facies they should contain parageneses with tridymite, mullite, etc. The possibility of finding such high temperature hornfels in the vicinity of the incurrent channels of trappean bodies, apparently is quite good, and the Anakit region, in this sense, is no exception because the sedimentary non-carbonaceous rocks in the Siberian platform are very widely developed.

The author wishes to express his deep gratitude to Academician V. S. Sobolev for his guidance in this work.

B I B L I O G R A P H Y

1. Abushik, A.F. O zhivetskikh izvestnyskakh na zapadnoi okraine Sibirskoy platformy. Mat-ly po geologii i polezn. izkop. Sib. platformy, nov. seriya, vyp. 23 VSEGEI. L. 1959.
2. Angaro-Ilimskiy zhelezorudnyy mestorozhdeniy trappovoy formatsii yuzhnoy chasti Sibirskoy platformy. Sb. M., Gosgeoltekhizdat, 1960.
3. Bazhenova, T. K., Chzykovskaya, E. V. K metodike lyuminestentno-bituminologicheskikh issledovaniy porod. Mat-ly po geol., gidrol, geofiz. i polezn. izkop Zapadnoy Sibiri. Tr. SNIIGGIMSa, No. 1, 1959.
4. Betekhtin, A. G. Gidrotermal'nyye rastvory, ikh priroda i processy rudobrazovaniya, Sb. Osnovnyye problemy v uchenii o magmatogennykh rudnykh mestorozhdeniyakh, izd. 2 M., Izd-vo AN SSSR, 1955.
5. Bozin, A. V. O novykh vykhodakh ordovika v yuzhnoy chasti Tungusskoy sinekrizy. Mat-ly po polezn. iskop. Krasnoyarskogo kraya, vyp. 1, KGU. Krasnoyarsk, 1961.
6. Budnikov, P. P., Berezhnoy A. S. Reaktsii v tverdoy faze v silikatnykh sistemakh. Uspekhi khimii, t. 40, No. 5, 1946.
7. Budnikov, P. P. and Berezhnoy, D. S. Reaktsii v tverdykh fazakh. M., Promostroyizdat, 1949.
8. Budnikov, Bobrovnik, D. P. Reaktsii v tverdom sostoyanii mezhdru SiO_2 i CaO , kaolinom i yego produktami obzhiga. Ukr. khim. zhurn., t. 12. 4, 1937.
9. Vinchell, A. N., Vinchell G. Opticheskaya mineralogiya. Izd-vo inostr. lit., 1953.
10. Dav, V. N. O vykhode siluriyskikh porod v tsentral'noy chasti Tungusskoy sineklizy (basseyne r. Eyki). Mat-ly po geol. Sob. platformy, nov. seriya, vyp. 7, VESEGEI, 1955.
11. Dragunov, V. I. Geologicheskoye stroeniya yuzhnoy chasti zapadnogo obramleniya Tungusskoy sineklizy. Mat-ly po geol. Sib. platformy, nov. seriya, vyp. 23, VESEGEY. L., 1959.

12. Yelisseyev, E. N. Denisov, A. P. Rentgenometricheskoye issledovaniye pirrotina. Vestn. LGU, No. 18, ser. geol. i geogr., vyp. 3, 1957.
13. Yermakov, N. P. Issledovaniya mineraloobrazuyshchikh rastvorov. Izd. Khar'k. gost. un-ta. Khar'kov, 1950.
14. Zavaritskiy, A. N. Sobolev, V.S., Kvasha, L. G., Kostyuk, V. P. and Bobriyevich, A. P. Novyye diagrammi dlya opredeleniya sostava vysokotemperaturnykh plageoklazov. Zap. Vses. mineral. o-va, ch. 87, Vyp. 5, 1958.
15. Zavaritskiy, A. N., Sobolev, V. S. Fiziko-khimicheskiy osnovy petrografii izverzhennykh gornykh porod. M., Gosgeoltekhizdat, 1961.
16. Zaytsev, N. S. O tektonike yuzhnoy chasti Sibirskoy platformy. Voprosy geologii Azii, T. I. Izd-vo AN SSSR, 1954.
17. Zaleskiy, M. D. Paleozoyskaya flora Angarskoy serii. Atlas. Tr. Geol. kom., vyp. 174, 1918.
18. Zolotukhin, V. V. Primeneniye mikrostrukturnogo analiza k izvershennym porodam effuzivnogo oblika Inform. Byull. NIIGA vyp 19, L. 1960.
19. Zolotukhin, V. V. Pervyye rezultaty primeneniya mikrostrukturnogo analiza k issledovaniyu differentsirovannoy intruzii. Noril'sk 1. Sb. Mat-ly po genet. i eksperim. mineralogii, No. 1, Novosibirsk, 1962.
20. Kasatkin, P. I. Zhelezorudnyy baseyn r. Nizhney Tunguski. Byull. tekhn. inform. Komb. No. 1-2. Noril'sk, 1949.
21. Korzhinskiy, D. S. Zavisimost' mineraloobrazovaniya ot gulbiny. Zap. Vses. Mineral. ob-va, t. 66, vyp 1, 1937.
22. Korzhinskiy, D. S. Faktory mineral'nykh ravnovesiy i mineralogicheskiye fatsii glubinnosti. Tr. In-ta geol. nauk AN SSSR, vyp. 12, petrogr. ser. No. 5, 1940.
23. Korzhinskiy, D. S. Ocherk metasomaticheskikh protsessov. Sb. Osnovnyye problemy v uchenii o magmatogennykh rudnykh mestorozhdeniyakh, izd. 2. Izd-vo AN SSSR, 1955.

24. Kornilov, N. A. K mineralogii serpentinov. Zap. Vses. Mine al. ob-va, ch. 90, vyp. 5, 1961.
25. Kushev, S. L. Geomorfologiya doliny nizhnego techeniya r. Nizhney Tunguski, Tr. geomorfol, In-ta AN SSSR, vyp 11, 1934.
26. Lebedev, A. P. Differentsirovannyye trappovyye intruzii "Vilyuyskikh gor". Tr. In-ta geol, rudnykh mestorozhd., petrografii, mineralogii i geokhimii AN SSSR, vyp. 29, 1959.
27. Levinson-Lessing, F. Yu., Struve, E. A. Petrograficheskiy slovar' izd. 2. ONTI, 1937.
28. Malich, N. S. Paleozoyskiye struktury basseyna srednego i nizhnego techeniya r. Podkamennoy Tunguski. Mat-ly po geol. i polezn. iskop. Sib. platformy. VSEGEI, nov. ser. vyp. 23, 1. 1959.
29. Malich, N.S. Grigor'yev, V. V. O svyazi magmatizma s tektonikoy v basseynakh nizhnikh techeniy rek Podkamennoy Tunguski i Bakhty. Mat-ly po geol. i polezn. iskop. Sib. Platformy, VESEGEI, nov. ser. vyp. 31, 1960.
30. Masaytis, V. L. Petrologiya Alandzhakhskoy trappovoy intruzii. Tr. VSEGEI, nov. ser., t. 22. L., 1958.
31. Mikheyev, V. I. Rentgenometricheskiy opredelitel' mineralov. M., Gosgeol-tekhizdat, 1957.
32. Moiseyev, I. V., Teben'kov, V. P., Mikhaylov, A. F. Geologiya i poleznyye iskopayemye basseyna R. Nizhney Tunguski. Tr. Arkt. in-ta, t. 139, 1939.
33. Mchedlov-Petrosyan, O. P., Babushkin, V. I. Ob ispol'zovanii kristallokhimicheskikh dannyykh dlya termodinamicheskogo analiza protsessov gidrotermalnogo sinteza gidrosilikatov kal'tsiya. Dokl. AN SSSR, t. 128, No. 2, 1959.
34. Neyburg, M. F. Opyt fitostratigraficheskogo sopostavleniya verknepaleozoyskikh otlozheniy Antarkidy i Gondvani (Indiya). Vopr. geol. Azii. T.1, M., Izd-vo AN SSSR, 1954.
35. Nikiforova, O. I., Andreyeva, O. N. Stratigrafiya ordovika i silura

Sibirskoy platformy i yeye paleontologicheskoye obosnovaniya (Brakhiopody).

Tr. VSEGEI, nov. ser., T. 56, vyp. 1. L., 1961.

36. Nikolayev, V. A., Dolivo-Dobrovol'skiy, V. V. Osnovy teorii protsessov magmatizma i metamorfizma. M., Gosgeoltekhizdat, 1961.

37. Ostrovskiy, I. A., Mishina, G. P., Povilaytis, V. M. PT-proyektsiya sistemy kremnezemvoda Dokl. AN SSSR T. 126, No. 3, 1959.

38. Pavlov, N. V. Magnomagnetitovyie mestorozhdeniya rayona Tungusskoy sineklizy Sibirskoy platformy. Tr. In-ta geol. rudnykh mestorozhd., petrografii, mineralogii i geokhimii AN SSSR, vyp. 52, 1961.

39. Pavlov, N. V., Yanchenko, M. T. Nekotoryie novyye dannyye o magnomagnetitakh. Geol. rudnykh mestorozhd., No. 2, 1959.

40. Polunina, L. A., Afanas'yeva, M. A. Trappy nizhnego techeniya r. Nizhney Tunguski Mat-aly po geol. i polezn. iskop. Sib. platformy, VSEGEI, nov. ser., vyp. 44, 1960.

41. Radchenko, G. P., Shvedov, N. A. Verkhnepaleozoyskaya flora uglenosnykh otlozheniy zapadnoy chasti basseyna r. Nizhney Tunguski. Tr. Arkt. in-ta, t. 157, 1940.

42. Rankin, D. A., Wright, F. E. Troynaya sistema CaO-MgO-SiO_2 . L., 1935.

43. Rasskozya, E. S. Kontinental'nyie kamnougol'nyie otlozheniya Tunguskogo basseyna. Dokl. AN SSSR, t. 122, No. 3, 1958.

44. Reverdatto, V. V. O nakhodke tilliita v konaktovoy zone Anakitskogo trappovogo intruziva na Nizhney Tunguske. Dokl. AN SSSR, T. 142, No. 5, 1962.

45. Semenov, L. S. Nekotoryie zakonomernosti razmeshcheniya postmagmaticheskikh rudoproyavleniy mezhdurech'ya rr. Nizhney i Podkamennoy Tungusok. Mat-ly po geol. i polezn. iskop. Sib. platformy, VSEGEI, nov. ser. vyp. 31, 1960.

46. Semenov, L. S. O svyazi postmagmaticheskogo orudeneniya s intruziyami trappov povyshennoy shchelochnosti. Inform. sb. VSEGEI, No. 40, 1960.

47. Serdyuchenko, D. P. Khlорity, ikh khimicheskaya konstruktsiya i klassifikatsiya. tr. In-ta geol. nauk AN SSSR, vyp. 140, 1953.

48. Sobolev, V. S. Redkiy tip kontaktovogo metamorfizma izvestnyakov. Zap. Vseross. mineral, ob-va, T. 64, No. 1, 1935.
49. Sobolev, V. S. Petrologiya trappov Sibirskoy platformy. Tr. Arkt. in-ta, T. 43, 1936.
50. Sobolev, V. S. Fedorovskiy metod. M., Gosgeoltekhizdat, 1954.
51. Sobolev, V. S. O davlenii pri protsessakh metamorfizma. Sb. Fiziko-khimicheskiye problemy formirovaniya gornyykh porod i rud., T.1, M., Izd-vo AN SSSR, 1961.
52. Teben'kov, V. P. Predvaritel'noye soobshcheniye o rabote Nizhne-Tungusskoy ugol'noy ekspeditsii v 1936 godu. Byull. ANII, No.10-11, 1936.
53. Teben'kov, V. P. Raboty Nizhnetungusskoy geologicheskoy ekspeditsii v 1937 godu. Problemy Arktiki, No. 1, 1938.
54. Teben'kov, V. P. Gaytman, D. S., Eynor O. L. Geologicheskoye stroeniye i ugleunosnost' r. Nizhney Tunguski ot r. Severnoy do r. Chapkokto. Tr. Arkt. in-ta, t. 126, vyp. 1, 1939.
55. Turner, F. J. Evolyutsiya metamorficheskikh porod. Izd-vo inostr. lit., 1951.
56. Turner, F., Ferhugen, Dz. Petrologiya izverzhennykh i metamorficheskikh porod. Izd-vo inostr. lit. 1961.
57. Toropov, N. A., Nikogosyan, Kh. S., Boykova, I. I. Sintez i issledovaniye nekotorykh svoystv gillebrandita i drugikh gidrosilikatov kal'tsiya. Tr. 5-go soveshcheniya po eksperim. i tekhn. mineralogii i petrografii. M., Izd-vo AN SSSR, 1958.
58. Treger, V. E. Tablitsy dlya opticheskogo opredeleniya popodoobrazuyushchikh mineralov. M. Gosgeoltekhizdat, 1958.
59. Uelsh, A. Reaktsii mezhdru trverdymi telami. Sb. Khimiya tverdogo sostoyaniya. Izd-vo inostr. lit., 1961.
60. Khakhlov, V. A. O raschlenenii permo-karbonatevykh otlozheniy Severo-Zapadnoy

chasti Azii. Vestn. ZSGRT, No. 1, 1937.

61. Chekanovskiy, A. A. Dnevnik ekspeditsii A. A. Chekanovskogo po rr.

Nizhney Tunguske, Oleneku i Lene v 1873-1875 gg. Zap. Rus. Geogr. ob-va, T. 20, No. 1, 1896.

62. Barth, T. F. W., Correns, C. W., Eskola, P. Die Entstehung der Gesteine, Springer, Berlin, 1939.

63. Bowen, N. L. Progressive metamorphism of siliceous limestone and dolomite. The Journal of Geology, v. 44, No. 3, 1940.

64. Clabaugh, S. E. Contact metamorphism in the Christmas Mountains, Brewster County, Texas. Bull. Geol. Soc. of America, v. 64, No. 12, pt. 2, 1953.

65. Danielsson, A. Das Calcit-Wollastonitgleichgewichte. Geochim. et Cosmochim. Acta. No. 1, 1950.

66. Eskola, P. On mineral facies. Geol. Föreningens Förhandlingar, 51, No. 2, 1929, Ref. N. Jahrb., 1931, 1, 2.

67. Fyfe, W. S., Turner, F. J., Verhoogen, J. Metamorphic reaction and metamorphic facies. Geol. Soc. Amer. Mem., 72, 1958.

68. Glass, I. I., Jahns, R. H., Stevens, R. E. Helvite and danalite from New Mexico and the Helvite group. The Amer. Min., v. 29, No. 5-6, 1949.

69. Goldschmidt, H. J., Rait, J. R. Silicates of the perovskite type of structure. Nature, v. 152, 1943.

70. Goldschmidt, V. Die Gesetze der Gesteinsmetamorphose, mit Beispielen aus der Geologie des Südlichen Norwegens. Videnskapssel. Skr. I, Math.-Nat. - KI., 22, 1912.

71. Harker, R. I. The synthesis and stability of tilleyite. $\text{Ca}_5\text{Si}_2\text{O}_7(\text{CO}_3)_2$. Am. Journ. of Sci., v. 257, No. 9, 1959.

72. Harker, R. I. Formation of tilleyite, $\text{Ca}_5\text{Si}_2\text{O}_7(\text{CO}_3)_2$ in the contact metamorphism of siliceous limestones. Bull. Geol. Soc. Amer., v. 69, N 12, pt. 2, 1959.

73. Harker, R. I., Tuttle, O. F. The lower limit of stability of akermanite. *Amer. Journ. of Sci.*, v. 254, No. 8, 1956.
74. Homme, F. S., Rosenzweig, A. Spurrite and monticellite skarns in the Tres Hermanas Mountains, Luna County, New Mexico. *Bull. Geol. Soc. of Amer.*, v. 69, No. 12, pt. 2, 1958.
75. Hughes, C. I. An occurrence of tilleyite-bearing limestones in the Isle Rhum, Inner Hebrides. *Geol. Mag.*, v. 97, No. 5, 1960.
76. Larsen, E. S., Dunham, K. S. Tilleyite, a new mineral from the contact zone at Crestmore, California. *Amer. Mineralogist*, v. 18, No. 11, 1933.
77. Larsen, E. S., Foshag, W. F. Merwinite, a new calcium-magnesium orthosilicate from Crestmore, California. *Amer. Mineral.*, v. 6, No. 10, 1921.
78. Mason, B. Larnite, scawtite and hydrogrossular from Tokatoka, New Zealand. *Amer. Mineralogist*, v. 42, N 5-6, 1957.
79. Muir, I. D. The clinopyroxenes of the Skaergaard intrusion, eastern Greenland. *Min. Mag.*, v. 29, N 214, 1951.
80. Murdoch, G. Scawtite from Crestmore, California. *Am. Min.*, v. 40, N 5-6, 1955.
81. Naidu, M. G., Covindarajulu, B. V. Occurrence of calciphyres near Malarajanahundi Nanjangud (Mysore state). *Current Science*, v. 23, N 10, 1954.
82. Nockolds, S. R., Vincent, H. G. C. On tilleyite and its associated minerals from Carlingford, Ireland. *Min. Mag.*, v. 28, N 198, 1947.
83. Osborn, G. D. On the occurrence of custerite and monticellite in metamorphosed limestone from Carlingford., *Geol. Mag.*, v 69, N 812, 1932.
84. Osborn, G. D. The metamorphic limestones and associated contaminated igneous rocks of the Carlingford district Co. Louth. *Geol. Mag.*, v. 69, No. 815, 1932.
85. Schmalhausen, J. Beiträge zur Jura-Flora Russland. *Mém. Ac. Imp. des Sc. St. Pet.*, 7 ser, v. 27, No. 4, 1879.

86. Taylor, J. H. A contact metamorphic zone from the Little Belt Mountains. Montana. Am. Min., v. 20, No. 2, 1935.
87. Temple, A. K., Heinrich, E. Wm., Spurrite from Coahuila, Mexico. Bull. Geol. Soc. of Amer., v. 71, No. 12, pt. 2, 1960.
88. Tilley, C. E. On larnite (calcium orthosilicate, a new mineral) and its associated minerals from the limestone contact-zone of Scawt Hill, Co. Antrim. Miner. Mag., v. 22, No. 125, 1929.
89. Tilley, C. E. Scawtite, a new mineral from Scawt Hill. Min. Mag., v. 22, No. 128, 1930.
90. Tilley, C. E., Hardwood, H. F. The dolerite-chalk contact at Scawt Hill, County Antrim. Min. Mag., v. 22, No. 132, 1931.
91. Tilley, C. E. The gabbro-limestone contact-zone of Camas Mör, Muck, Inverness-Shire. Bull. de la Commission geolog. de Finlande, No. 140; Suomen Geol. Seura No. 20, 1947. Pentti Eskola 65 - vocotisjuhlajulkaisu.
92. Tuttle, O. F., Harker R. I. Synthesis of spurrite and the reaction; wollastonite + calcite \rightleftharpoons spurrite + carbon dioxide. Am. Journ. of Sci., v. 255, No. 3, 1957.
93. Valkenburg, A., Rynders G. F. Synthetic cuspidine. Am. Min., v. 43, No. 11-12, 1958.
94. Van der Kaaden, G. High-temperature albite and contiguous feldspars. Journ. Geol., v. 58, 1951.
95. Wager, L. R., Deer, W. A. The petrology of Skaergaard intrusion. Medd om Grønland. Bd. 105, No. 4, 1939.
96. Weeks, W. F. Heats of formation of metamorphic minerals in the system $\text{CaO} - \text{MgO} - \text{SiO}_2 - \text{H}_2\text{O}$ and their petrologic significance. Journ. Geol., v. 64, No. 5, 1956.
97. Wright, F. E. On the contact minerals from Velardena, Durango, Mexico. (Gehlenite, spurrite, hillebrandite). Am. Journ. of Sci., v. 26, No. 156, 1908.

98. Wyatt, M. The Camasunary (Skye) gabbro-limestone contact; part 2 of Ph. D. Thesis. Cambridge University, 1953.
99. Yoder, H. S. (Ir.) Effect of water on the melting of silicates. Ann. Rep. of the Director of the Geoph. Lab. 1957-1958. Carnegie Inst. Washington, Year Book, 57.

V. V. Reverdatto

METAMORPHISM IN THE CONTACTS OF ANAKIT TRAPPEAN MASSIF
IN THE LOW TUNGUSKA RIVER

Three stages of mineral-formation are found: metamorphic, metasomatic and postscarn, hydrothermal stages. At the first stage the forming of two contact-metamorphic facies takes place: sanidinite and pyroxene-hornfels ones. The deposition of facies in the aureole of the Anakit trappean massif is different and is conditioned by temperature and reserves quantity of heat of magmatic melt, which in its turn depends on the distance from incurrent canal, through which magma entered the chamber, occupied now by the intrusive. The sanidinite facies is represented by larnite-mervinite-spurrite sub-facies. At the further stage the formation of cuspidine, pyroxene - garnet scarns and iron ore formation appears. At the third stage the different hydrothermal minerals, namely, gillebrandite and others are formed. The conclusion is made about dependence of carbonate decarbonatization (decarbonatization) reactions on the temperature at the constant pressure.
